NASA CR-141404

WATER COLOR AND CIRCULATION SOUTHERN CHESAPEAKE BAY

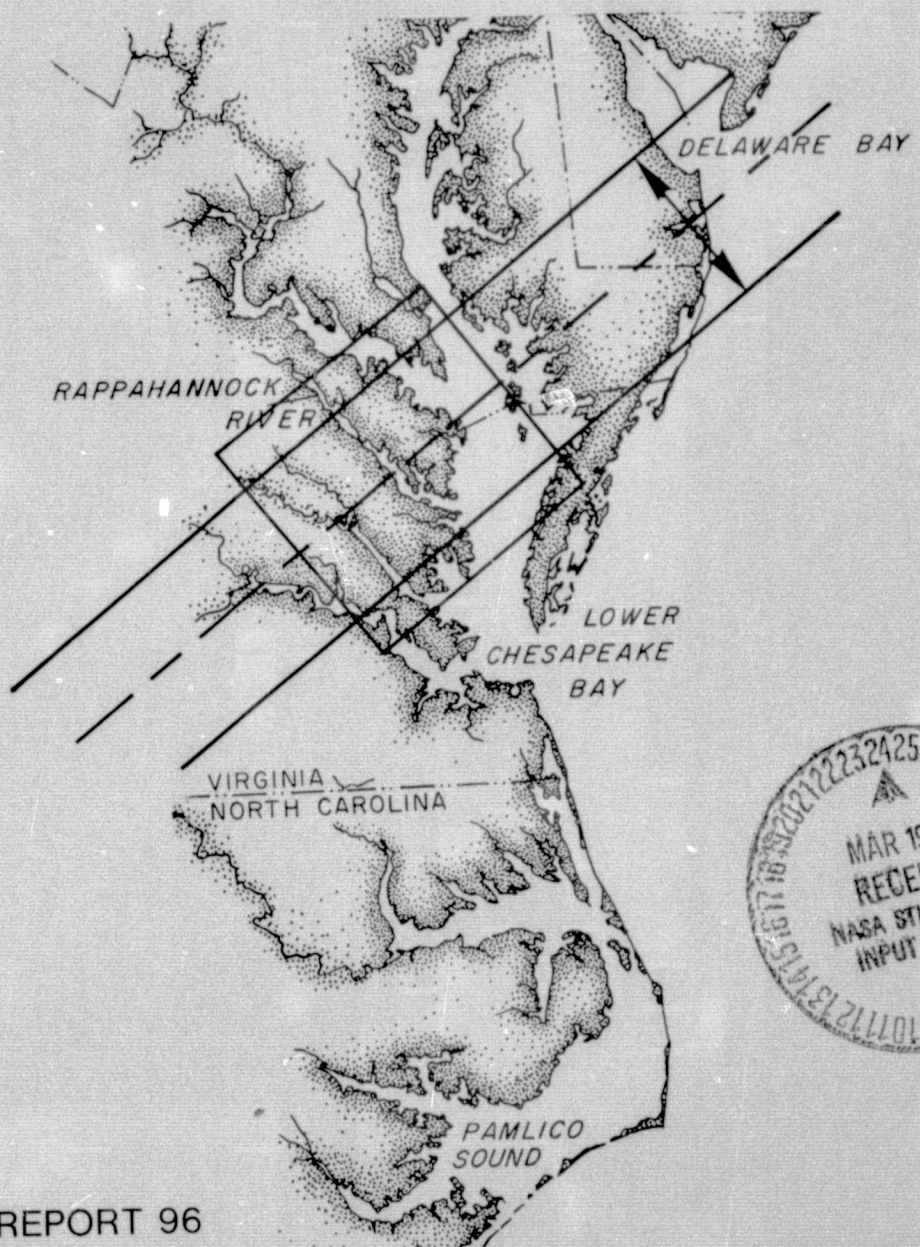

SPECIAL REPORT 96

in Applied Marine Science and Ocean Engineering of the

Virginia Institute of Marine Science, Gloucester Point, Virginia 23062.

October 1975

VIRGINIA INSTITUTE OF MARINE SCIENCE

Gloucester Point, Virginia 23062

SOUTHERN CHESAPEAKE BAY WATER COLOR AND CIRCULATION ANALYSIS

PART I

Final Report for NASA Contract NAS 6-2327

Skylab EREP Number 602647(517)

Virginia Institute of Marine Science

William J. Hargis, Director

David Oberholtzer, Ph.D.
NASA-Wallops Station
Technical Monitor

Report Prepared By
Maynard M. Nichols, Ph.D.
Va. Inst. of Marine Science

Executive Summary of Significant Results

Satellite imagery from two EREP passes over the Rappahannock Estuary of the Chesapeake region are analyzed to chart colored water types, to delineate color boundaries and define circulatory patterns.

Surface observations from boats and helicopters concurrently with Skylab overpass, define the distributions of suspended sediment, transparency, temperature, salinity, phytoplankton, color of suspended material and optical ratio. Important features recorded by the imagery are a large-scale turbidity maximum and massive red tide blooms. Water movement is revealed by small-scale mixing patterns and tidal plumes of apparent sediment-laden water. The color patterns broadly reflect the bottom topography and the seaward gradient of suspended material between the river and the Bay. Analyses of red, green and natural color photos by microdensitometry demonstrates the utility of charting water color types of potential use for managing estuarine water quality. The Skylab imagery is superior to aerial photography and surface observations for charting water color. The imagery acquired is a valuable contribution to the study of coastal zone processes and management.

FORWARD

This report is submitted in accordance with NASA contract NAS6-2327, of April 16, 1973. It includes results of research and field experiments accomplished through support of the contract in the form of charts, photographs, calculations and written documentation. Content embraces detailed results from studies of principal organisms, circulation, suspended sediment, and water pollution; an evaluation of the relative importance of surface, aircraft, and satellite data in preparation of the results; assessment of the utility of EREP imagery as an aid to research and management of the marine environment and resources of Chesapeake Bay; an assessment of the operational utility of results obtained an estimate of the associated cost benefits; and a discussion of the accuracy of the results and the problem of extending the referred analysis technique to wide areas of the United States or world.

Results are based on analysis of visible region Skylab Earth Resources Experiment Package (EREP) including the S-190A multispectral photographic facility and the S-190B earth terrain camera. Results of the S-192 multispectral scanner computerized output obtained concurrently with the photography, will be presented separately in a forthcoming report.

ACKNOWLEDGEMENTS

Like most scientific endeavors in space the results reported herein are a product of a collective effort of many persons.

Mission planning and coordination of surface observations was performed by M.M. Nichols assisted by H. Gordon.

Collection of field data and surface observations was accomplished by:

J. DuPuy
D. Doumlele
V. Gibson
H. Gordon
E. Lawrence
M. Nichols
W. Odelman (NASA-Wallops)
M. Penney
P. Stofan
G. Thompson
A. Zwirko

One spectroradiometer was supplied by NASA-Wallops Station and another by American University, Dr. R. Anderson.

Helicopter support was provided by the U.S. Coast Guard, Elizabeth City, North Carolina and by NASA-Wallops Station, Virginia.

Film analyses were accomplished on equipment made available by the U.S. Geological Survey, EROS Program, Topographic Division, Reston, Virginia; by the NASA-Langley Research Center, Hampton, Virginia; and by the NASA-Wallops Station. Mr. Walter Montgomery of NASA-LRC helped with isodensity tracing, Mrs. Meredith McKelway drafted the figures and Mrs. Cindy Otey typed the report. Photographs and draftings were reproduced by Ken Thornberry and William Jenkins.

Besides on-the-scene team members the study benefited by technical advice and consultations from VIMS interdisciplinary professional staff. Administrative support was rendered by Dr. R. Byrne, Dr. J. Zeigler and Mr. Roy Washer of VIMS.

C O N T E N T S

1. INTRODUCTION

Coastal waters display marked color variations resulting from variations in suspended and dissolved loads. Such variations show distinct patterns that often change in response to waves, tides and man-made stress. Because color patterns are so dynamic they are difficult to characterize and monitor over large areas. The coastal oceanographer is faced with the problem of differentiating water masses of different color. The planktologist is faced with the interrelationship between the spectral distribution of discolored water and the species composition. The sedimentologist needs to know how the various colors relate to sediment sources and in turn to dispersal routes. The coastal engineer is faced with the problem of detecting source inputs produced by pollution or construction; he is concerned with the areal extent of such impacts. Inasmuch as color variations are so striking in space photographs it is generally believed that many such problems can be solved by remote sensing techniques. But in practice the "promise of space" remains to be realized.

1.1 Objectives:

- The objectives of this research are:
- To investigate the utility of Skylab (EREP) imagery for sensing the environment of southern Chesapeake Bay and its changes.
- To use EREP imagery to map water color and circulation at the mouth of Chesapeake Bay.
- To relate the color analysis to Bay pollution, circulation, productivity, suspended sediment and water pollution.

Objectives, Cont'd.

- To evaluate the utility of Skylab imagery to assist in research and management of the marine environments and resources of Chesapeake Bay.
- To determine the operational feasibility of using space imagery to wide areas of the world.

2. BACKGROUND AND PREVIOUS WORK

Early explorers used water color to find their way about the countless bays and channels of coastal areas and the trackless expanses of the ocean. As a result of their travels they left us a legacy of such names as the Black Sea, the Red Sea, and the Yellow Sea, Black River, and Vermillion Bay. Although the art of "color tracking" has been superceded by modern navigation, the need to "track" colored water has become of interest to solve present-day oceanographic problems.

By means of multispectral imagery and enhancement techniques Ross (1971) assessed water depths around the Bahama Islands. Ewing (1971), demonstrated that color measurements from an airborne spectrophotometer are a useful index to biological productivity around Georges Bank. Burgess (1971) used multispectral photography to measure sewage concentrations and dispersal patterns around an ocean outfall off the Oregon coast. Strandberg (1966, 1967) has published numerous examples of color photographs for water quality analysis. And Piech and Walker (1971) present a method for quantitizing water quality from aerial surveys. The use of color imagery for study of benthic vegetation is reviewed by Conrad, Kelly and Boersma (1968). Surface currents have been measured successfully by Keller (1963) in

Charleston Harbor and by Waldichuk (1966) in the Fraser River mouth. Ichiye and Plutchak (1966) used color photography to analyze dye concentrations.

Large areas of water color change are obvious in many space images. There has been much speculation as to the interpretation and meaning of these color patterns, but few measurements have been made at the same time the photographs were taken. If the color patterns can be mapped and related to coastal water masses and circulation, future space imagery should be made more useful and provide a better understanding of coastal processes.

3. RATIONALE FOR SENSING WATER COLOR

The color of water is derived from absorption and scattering of both the water as well as dissolved and suspended material. Figure 1 shows microphotographs of different types of particles contributing to color in the Rappahannock Estuary. These particles include inorganic sediment as well as organic sediment plus organic detritus, plankton and debris all of which are in various states of aggregation. Such particles cause light to be scattered and thus render the water turbid and discolored. Spectral definition depends not only on the composition of the suspended material but also on its concentration (load) and particle size.

Besides these in situ variations, water color changes with changes in lighting sources, ie. with time of day and with changes in cloudiness. Additionally, there are effects

of reflection due to the discontinuity in refractive index at the air-water interface. Rippling and ruffling of the surface enhance color because of reduced reflection. In shallow water the color is often determined by light backscattered from the bottom. Water color also changes with changes in atmospheric parameters; i.e. with changes in spectral and energy distributions of skylight. In an image each of these peripheral effects may be recorded as an apparent change in color. Color of water caused by absorption of dissolved material is accompanied by a shift in peak transmittance toward longer wavelengths. In the Rappahannock this is a consequence of selective absorption by humic materials which locally drain backwaters and swamps. Therefore, when an image is obtained, the spectral reflectance recorded on the image is a product of many variations and modifications in light energy from the water column, the surface and the atmosphere.

The colored water masses, interfaces and circulation patterns that are commonly observed in coastal waters are determined not only by the light absorbed and backscattered, but by the history of the water. If modifications of light energy can be accounted for, the color changes should indicate water mass distributions in a way similar to the distributions of the particle content. Similarly the color interfaces should be a boundary between different populations of particles. And variations of other water characteristics, as temperature and salinity, may also be associated with the change in water color. If these premises are correct, color patterns can be used for differentiating water masses and for interpreting circulation.

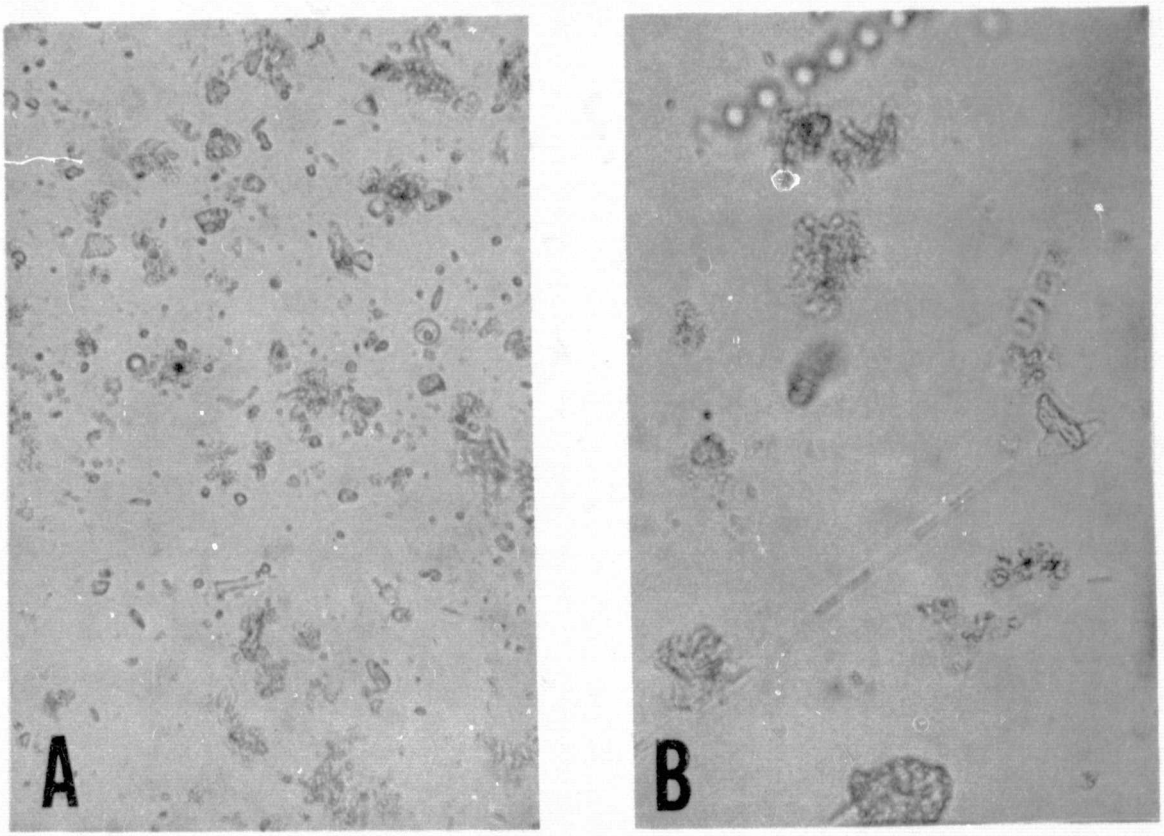

Figure 1. Microphotographs of light scattering suspended material common to the Rappahannock Estuary; A, mainly sediment particles and debris from the upper estuary; B, mainly phytoplankton from the lower estuary.

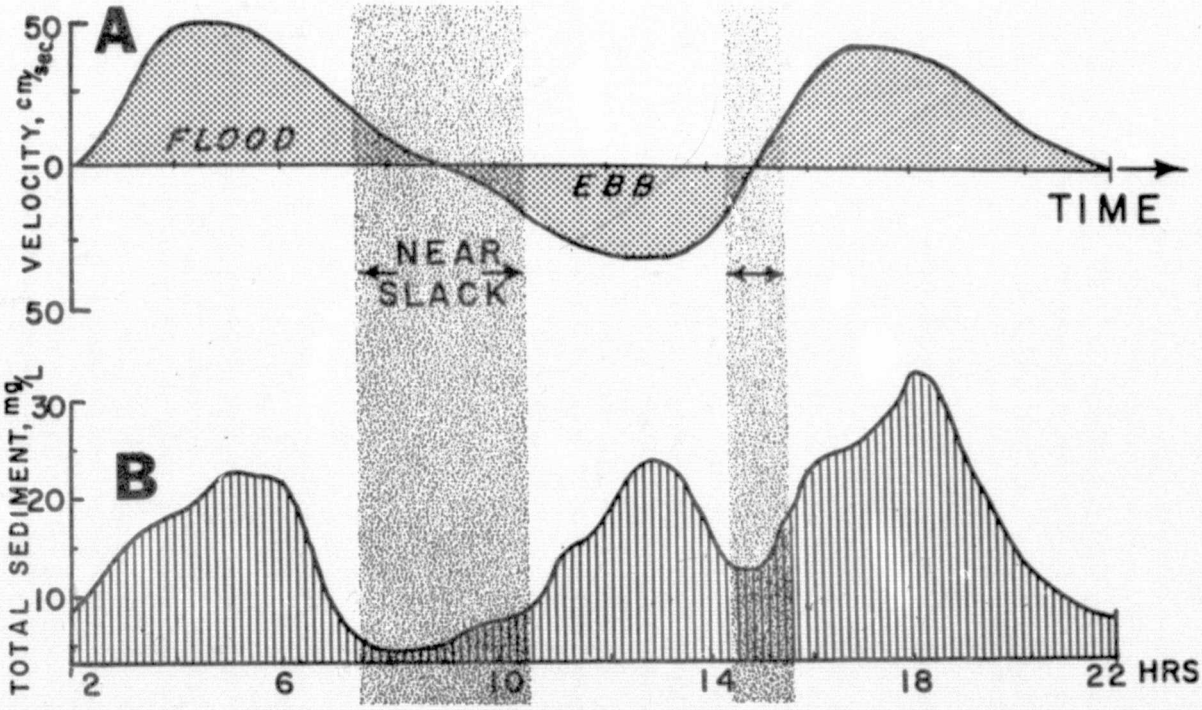

Figure 2. Time variations of current velocity (A) in relation to corresponding variations of total suspended material (B) in the upper Rappahannock Estuary.

Rationale, Cont'd.

Our ability to sense different types of colored water rests on the fact that each water type reflects radiant energy in distinctive amounts at certain specified wavelengths. Therefore, when multiband photography is acquired simultaneously in several wavelength bands, each type of color water ideally can be identified by virtue of its multiband "signature" or spectral response pattern. But because coastal waters are so dynamic, constantly changing in response to tides, waves and currents, the resulting signatures and color patterns are also constantly changing. Therefore, signatures identified at a single time or place must accommodate this fact.

4. PROFILE OF THE TEST SITES

The lower Chesapeake Bay is part of a large estuarine system which drains the James and York Rivers and numerous small tributaries. Because of its multiple water sources, which include the Atlantic Ocean as well as inland drainage, water masses are complicated. Since the configuration is complex the circulation is also complicated. Moreover, water depths are relatively shallow, averaging less than 9 meters deep. The bathymetry consists of a series of shoals cut by several large channels that are continually swept by the tide. Because the lower Bay is relatively large it is ideally suited to the broad view of the space camera. It displays varicolored water masses and pronounced interfaces that are readily recorded on multiband film. The area touches on the urban areas of Norfolk and Hampton, it is partly fed by sewage outfalls and in-

dustrial wastes, but at the same time it is a productive fishing area.

The Rappahannock Estuary is one of nine major estuarine tributaries to Chesapeake Bay. Like the Potomac and the James Estuaries, it is narrowly funnel-shaped and relatively shallow, less than 5 meters deep on the average except for the axial channel which is 8 to 23 meters deep. A submerged sill at the mouth, 9 meters deep, partly deters inflowing water from the Bay so that the estuary is dominated by the river.

The Rappahannock offered several advantages for study of EREP imagery. Its configuration is relatively straight and bottom geometry is simple. Water properties, namely salinity and suspended sediment concentrations, gradually change seaward along the estuary length as part of a broad gradient. Local tributaries that drain into the estuary supply freshened water from different sources. However, the estuary is relatively undisturbed by major engineering works and it is relatively free from pollution except for the duck farm effluent near Urbanna which is largely contained in ponds. The estuary is renowned for its oyster production. The chief advantage of this estuary as a test site is that its turbid waters and circulation are well known from previous field studies (Nelson, 1959, 1960 and Nichols, 1972) as well as from numerous NASA photographic overflights since 1968 (e.g. Nichols, 1971). Such information provided substantial baseline control and a predictive understanding of use for analyzing the surface truth. Figure 3

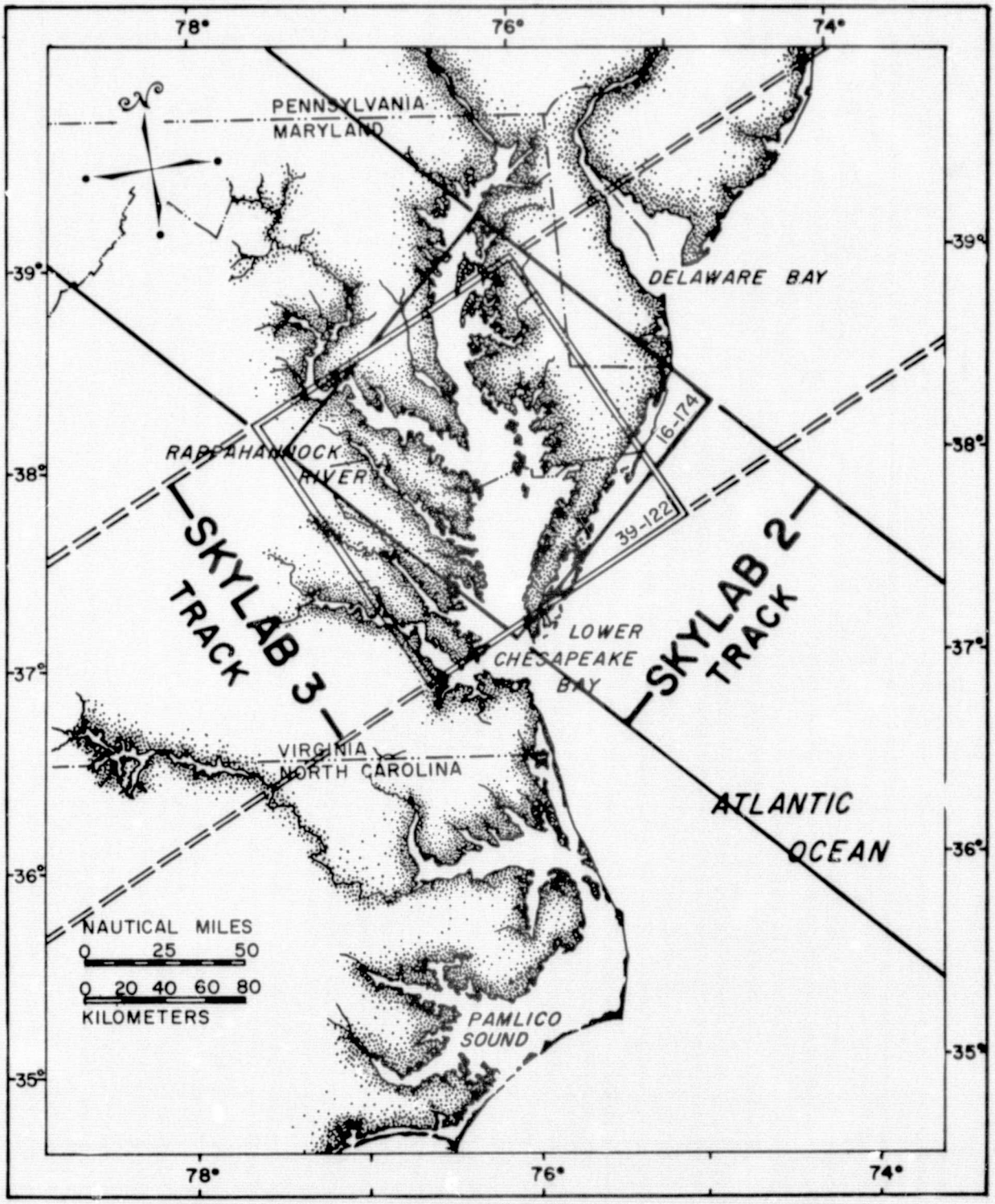

Figure 3. Location of test sites, the Lower Chesapeake Bay and the Rappahannock River estuary in relation to Skylab 2 and Skylab 3 orbit tracks and S-190A images acquired.

shows the Rappahannock Estuary in its geographic setting of the Chesapeake region.

The chief movement of water in the estuary is produced by the tide. Waves are important on shoals during short periods of high wind. The tide range is 70 cm on the average and currents vary from nearly zero at slack water to more than 30 cm per sec at maximum current over a period of 3 hours. Such currents cause intensive mixing of fresh and salty water. Velocities are capable of scouring soft bottom muds and supporting particulate material in suspension more than 50 percent of the time.

The mean tidal current diminishes with distance seaward from 35 cm per second in middle reaches to 14 cm per sec near the mouth. This trend follows the seaward increase in cross-sectional areas as the estuary deepens and widens toward the mouth. But in the upper estuary mean velocities are relatively uniform along the estuary channel from 30-35 cm per sec. Consequently, the transporting capacity of the current is also relatively constant through the upper estuary between 48 and 80 km above the mouth. Because the time of slack waters varies along the estuary length the current speed at any one time, such as captured by an instantaneous photograph, also varies. When the current is slack at the mouth it is maximal in the upper estuary near Tappahannock.

River inflow averages 45 m^3 per sec on the average at Fredericksburg. At the time of EREP photography in early June 1973 a small freshet of about 336 m^3 per sec flowed through the estuary,

whereas at the time of photography Sept. 1973, inflow was very low, less than 14 m^3 per sec. Consequently, the sediment load at this time was supplied mainly from the floor and shores of the estuary proper rather than from the river, as was the case in early June.

Concentrations of suspended material typically vary with tidal current speed at one point over one-half a tidal cycle. As shown in Figure 2, the concentrations rise and fall with the strength of the current whereby concentrations are higher near maximum current than near slack water. The variations are most pronounced near the bottom but they also occur near the surface, especially over the shoals. Only about 10 to 20 percent of the load remains in suspension at slack water; whereas the rest is alternately resuspended from the bottom and settled out.

Superimposed on the back and forth motion of the tide there is a small net or residual current generated by density differences between fresh and salty water. Speeds are only 2 to 4 cm per sec but over many tidal cycles the current is significant in transporting material in suspension over the long term. Thus, material suspended in the lower layer below about 6 meters is gradually carried landward whereas material in the upper layer and in freshwater reaches, is carried seaward.

Estuary water is partly-mixed most of the time. Vertical mixing of salt and fresh water is incomplete throughout the salt intrusion and therefore the transition from fresh to salty water is relatively broad. The Rappahannock lacks a sharp interface and turbid front characteristic of salt wedge systems except during

short periods of extreme flooding. However, a partly-mixed system like the Rappahannock is the most common type in the Chesapeake region and along the U.S. East Coast.

In summary, the Rappahannock Estuary test site has relatively mild hydrographic conditions of tide and river inflow. Its geometry is relatively simple consisting of an axial channel bordered by submerged shoals; its shoreline is relatively straight. Rapid changes in tidal currents produce marked changes in suspended material with time. The estuary is undisturbed by major engineering works and is relatively free of pollution.

5. SURFACE TRUTH STUDIES

The approach to evaluating Skylab imagery called for extensive correlative surface observations. These consist of a number of parameters characteristic of water masses and estuarine gradients: e.g., temperature, salinity, turbidity and phytoplankton community composition. Additionally, parameters affecting the quality and quantity of reflectance are included; e.g. total suspended load, chlorophyll-a, secchi disc depth, color of suspended material, irradiance and optical ratio (ratio of scatterance to transmittance), and particle size.

5.1 Mission planning and operations:

Surface truth observations were planned to coincide with the time of the Skylab pass and with supportive Skylab aircraft flights. Additionally, observations were planned at two 2-hour intervals before and after Skylab orbit-over concurrent with high altitude (60,000 foot) aircraft overflights. These additional observations were required to account for rapid tidal changes of current velocity and water color and to determine the local time history of the water masses.

Stations and transects were laid out to cover areas of water defined by the S190A field of view. Additional stations were positioned to account for local spatial variations across color boundaries and narrow gradient zones. Stations were laid out on a basic grid at 7 km intervals (Fig. 4A) for southern Chesapeake Bay, and at 2 to 4 km intervals along the Rappahannock length (Fig. 11A).

Although Skylab surface observations were initially planned to interface with observations of the NSF-RANN Bay-mouth flux study, these plans did not materialize because of clouded skies and delays in Skylab-2 schedules. An alternate site, the Rapphannock River estuary was selected after it was learned that Skylab-3 tracks drifted eastward. Although the track cut transverse to the estuary axis, and thus transverse to the dominate water movement direction, the site offered many color features common to coastal environments--plankton blooms, sediment plumes, grass beds, turbid patterns--and a range of colored water in a broad gradient from the river toward the sea.

5.2 Field observations and methods:

The surface observations consist of:

- Pre-Skylab reconnaissance transects across the lower Chesapeake Bay, May 12, 1973.
- Skylab sampling and measurements in the lower Chesapeake Bay, May 31, 1973 and in the Rappahannock Estuary, September 12, 1973.
- Follow-up water color boundary studies in the lower Bay and spectro-radiometer measurements in the Rappahannock Estuary, June 13, 1974.

Of the nine candidate passes and nine field preparations to meet Skylab passes, only one set of surface observations were obtained coincident with Skylab imagery. The other observation series were aborted because of clouded sky conditions.

Surface measurements were made and water samples were collected either from several runabouts or from helicopters hovering at 1 to 2 m altitude or landing on the water surface. The helicopters not only had the advantage of covering a large area within

a short time, but also provided a platform from which observers could view transient surface features and color boundaries from the same view-angle as the space cameras. The visual observations were recorded along the line of flight by a hand-held camera and by plotting on a chart.

Stations were positioned over water areas by sighting on landmarks or ranging on buoys. Many stations were located close to buoys to afford tight horizontal control. The stations were then plotted directly on a work chart at the time of observation and later transferred to a small-scale master such as reproduced in Figures 4A and 11A.

Surface water was sampled with a bucket and with a Kemmerer water bottle at selected depth intervals beneath the surface. The sample water was poured into precleaned mason jars and/or nalgene containers and returned to the laboratory for analysis. All the samples were processed within 8 hours after recovery to avoid decomposition during storage. Plankton samples were fixed with preservative so as to allow processing and microscopial examination over a period of several months.

A brief description of the parameters measured, their purpose and analyses methods is given below:

- Temperature is a measure of water thermal characteristics expressed in degrees Celcius. For offshore oceanography, temperature is an indicator of water mass types but in estuaries where mixing is rapid it reflects the admixture of surface and bottom waters as well as thermal exchange with the atmosphere and characteristics of different source waters. Measurements were made with a stem thermometer brought into equilibrium in a bucket within 30 seconds after recovery.

- Salinity is a measure of dissolved salts expressed in parts per thousand. In estuaries salinity indicates the degree of dilution and mixing of fresh and salty water from different sources. Depth profiles often define the upper and lower estuarine layers. Salinity of water samples returned to the lab was determined to ±0.05‰ on a Beckman model RS-7A inductive salinometer.

- Suspended "sediment" is the total concentration of solid suspended material. This includes sediment as well as plankton and organic detritus. The concentrations characterize the total suspended load in the water. Suspended sediment was measured gravimetrically by filtering an aliquot of water through a tared AA Millipore filter of 0.8 μ pore size. Procedural details are given in Nichols (1971).

- Optical ratio is the logarithmic ratio of scatterance to transmittance as measured in an optical cell of a Southern Analytical suspended solids analyzer. An aliquot of 300 ml of sample water was introduced into the cell through the bottom and the ratio was read after 10 seconds. Procedural details are given in Nichols (1971).

- Secchi disc depth is an additional means of estimating optical characteristics of the water. A 15 cm diameter black-white disk is lowered from the surface and the depth at which it just disappears is read on a graduated line. Disk depths give a gross measure of the extinction coefficient, which is a useful index for comparing the transparency of different colored water. Measurements are subject to about 10-20 percent error because of backscattered light off the water surface and because of wave motion on the surface which hampers depth readings.

- Color of suspended material is significant because suspended concentrations produce most of the scatterance and thus impart spectral qualities to the water. Color was measured by comparison of material collected on the Millipore filters with color chips in the Munsell book of color. Each color is defined by a hue, value and chroma; e.g. 10y 4/6 in which 10y is the hue, 4 is the value and 6 is the chroma. Hue refers to the primary colors of the spectrum; value refers to the property of lightness and chroma refers to the degree of saturation. Because the thickness of material on the filters varies somewhat with the amount of material filtered, value necessarily becomes darker with increased thickness of sediment on the filter.

- Chlorophyll "a" is a group of green phytoplankton pigments active in photosynthesis. Distributions of chlorophyll provide a rough index to the relative productivity of different colored water masses. Concentrations were measured by filtering a measured volume of about 400 ml of sample water through a Whatman GF/c 5.5 cm glass fiber filter. Filters were then dried and ground with a teflon homogenizer, mixed with 10 ml of 90 percent acetone and centrifuged for one minute. Fluorescence of the extracts was measured in a Turner fluorometer with the scale "zeroed" against 90 percent acetone and the fluorescence was converted to concentration of chlorophyll "a" in the original sample.

- Particle size partly determines the quantity of light scattered from suspended material as well as the rate that settling removes material from near-surface water. Particle size was measured by an electronic Coulter Counter Model TA after the material was removed from Millipore filters. Samples were prepared by digesting in acetone to remove excess filter fibers, centrifuged to remove acetone, and intensely shaken to disaggregate the material. Particle size was measured over the range from 0.6 μ to 64 μ which covers the bulk of the size range in the Rappahannock. Two aperture tubes were used, 30 μ and 140 μ to cover the range and data were combined into a single size distribution.

- Current speed and direction was not measured in the Rappahannock because these parameters are relatively well known from extensive measurements of the U.S. Coast and Geodetic Survey (NOS) and the Virginia Institute of Marine Science. The predicted tidal current tables of NOS were considered satisfactory for surface truth. The times of slack water given in the predicted tables were verified visually in the field and found to be accurate to ±20 minutes. For the lower Chesapeake Bay current speed and direction was determined both from the predicted tables and from drogues tracked by NASA-Wallops radar system.

- Irradiance is defined as the radiant flux of light energy on an infinitesimal element of surface divided by the area of that element. The values are expressed as microwatts per square centimeter per nanometer. The radiometric measurements ascertain the spectral characteristics of both the incident and the returned irradiance which affects image color and intensity.

5.3 Experimental techniques for spectroradiometer measurements:

Spectroradiometer measurements were made concurrently with other surface truth measurements at the time of Skylab III pass-over as well as several hours before and after EREP data acquisition. Measurements made with an ISCO model SR spectroradiometer in the range from 500 nm to 700 nm. The measurements were directed first at the sun and then normal to the water embracing both reflected and upwelling light energy. Because cloud cover varied during the measurement period, correspondence between readings was very poor and the derived upwelling measurements were variable and uncertain. The limited number of readings obtained are given in Appendix 12.4.

In order to determine the estuarine-wide reflectance variations and trends for the Rappahannock Estuary, a special spectroradiometer run was made on June 13 and 14, 1974 over a 50 mile length of the estuary. Additionally, measurements of salinity and secchi disc depth were made concurrently with radiometer measurements and water samples were analyzed for optical log ratio, suspended sediment concentration and particle size. Although this run was not made at the time Skylab III imagery was obtained, there was good reason to believe that the overall trend of reflectance along the estuary is of use to verify the broad isodensity zones derived from the satellite imagery.

The spectroradiometer measurements were made with an ISCO model SR spectroradiometer operated by NASA Wallops Flight Center and equipped with a field chart recorder. The chart recorder uses a special accessory which drives the spectroradiometer scanning mechanism and allows a completely automatic and continuous output

of spectral energy over a range of 380 to 750 nm, or 750-1350 nm. The spectroradiometer is fitted with a remote probe consisting of a three-foot section of fiber optics which transmits the light to a detector inside the radiometer. The fiber optic probe can be fitted with a series of non-reflective black cones (15^{o}, 30^{o}, 45^{o}) designed and built by NASA Wallops to approximate the field of view of an aerial sensor and thus eliminate unwanted reflection from the boat as well as to minimize noise from sun glint.

The configuration chosen for determining incident energy was the remote probe without a cone, but with an opel glass diffuser. Readings were taken in a vertical direction which serves to integrate both direct energy from the sun and skylight over a hemisphere. Water readings were made with a 30^{o} cone and without the diffuser disc in a direction normal to the water surface over the bow of the boat while free drifting. By removing the diffuser disc the radiometer is far more prone to large variations from sun glint, but with the cone and diffuser in place, the sensitivity of the instrument is not sufficient to allow satisfactory measurements. The measurements were made by making a full visual and IR scan on the sun and sky, then reconfiguring and repeating the measurements for water. Care was taken to insure conditions remained constant over the five minute interval needed to make one complete series of readings.

The instrument was calibrated to accommodate variations in transmission of the fiber optic probe with wavelength and variations in probe configuration for incident and reflected energy. This was done at NASA Wallops with a special tungsten calibration lamp made for this purpose. The output of the lamp in a specified forward direction is known at a given current setting (using a regulated power supply) and is tracable to

an NBS standard lamp. Calibration is performed by operating the spectroradiometer in its field configuration using the tungsten lamp as a source. With the output of the lamp known in candles at a given current setting the spectral intensity is calculated. And knowing the distance between the detector and the lamp, the incident spectral irradiance is determined. A ratio of the incident irradiance and the irradiance reading of the radiometer, allows one to calculate a spectral correction factor. This was done every 5 nm from 400-700 nm and the data were stored on a computerized look-up table.

Reflectance was determined from a computer program designed to perform numerical integration band by band on the chart output and form a simple water-sun irradiance ratio. The chart was digitized on an X-Y coordinatagraph of NASA Langley Research Center which served as input to the computer in punched card form. Before the integration was performed the program utilized the look-up table of spectral correction factors to adjust spectral irradiance values (y coordinate from the spectroradiometer charts) from the field.

5.4 Distribution of water characteristics

The data acquired from observations and measurements during the several field efforts are given in Appendix 12.1 and 12.2.

5.4.1 Lower Chesapeake Bay

Surface truth observations of May 31, 1973 were compiled into charts showing in plan view, the distribution of different water properties (Figs. 4A-4D, 5A-5D). The salient features of these distributions are:

- Bay entrance water is cooler than ocean water or estuarine water. The "cool pool", which is centered in the south-central reaches of the entrance, represents a zone of cool bottom water that is mixed upward into near-surface water (Fig. 4C) over the shoals.

- Salinity increases with distance seaward over a broad zone--from 15‰ inside the Entrance to 29‰ outside the Entrance. Salinity is greater on the north side of the Entrance than on the south side, a feature that reflects the density distribution and inward flow of ocean water along the north side (Fig. 4B).

- Chlorophyll "a" displays patchy distributions but generally decreases seaward. It is locally high along the Hampton shore and off Little Creek harbor, a distribution that may indicate nutrient enrichment accompanying a slight degree of pollution in these areas (Fig. 4D).

- Total suspended solids or sediment, also has a very patchy distribution but is generally higher inside the Entrance than outside it. Concentrations are locally high off Lynnhaven inlet as a result of ebb discharge of high sediment loads. They are also locally high in the cool "pool" where mixing carries high near-bottom concentrations toward the surface (Fig. 5A). Relatively high concentrations, greater than 15 mg/l, also occur near Thimble Shoals where sediment accumulates in a near-surface convergence zone (Fig. 5A).

- Secchi disk depths are smaller in nearshore water than in oceanic water. Waters along the north Entrance reaches are more transparent than along the south reaches. This reflects the discharge of relatively turbid Bay water along the south side whereas the inflow of ocean water intrudes along the north side (Fig. 5B).

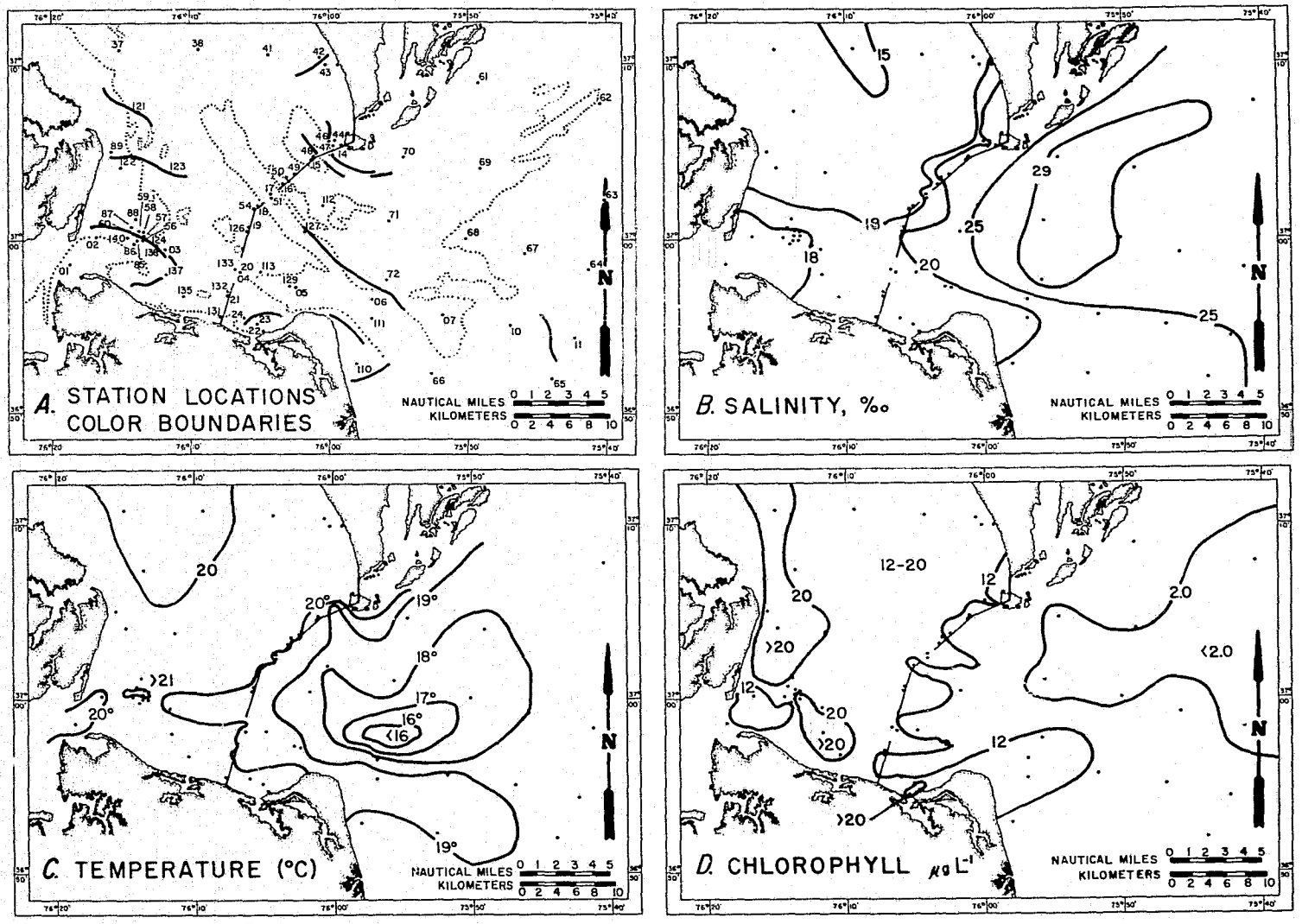

Figure 4. Locations of surface truth station locations and color boundaries in lower Chesapeake Bay (A) and distribution of water properties; (B) salinity; (C) temperature, (D) chlorophyll, May 31, 1973.

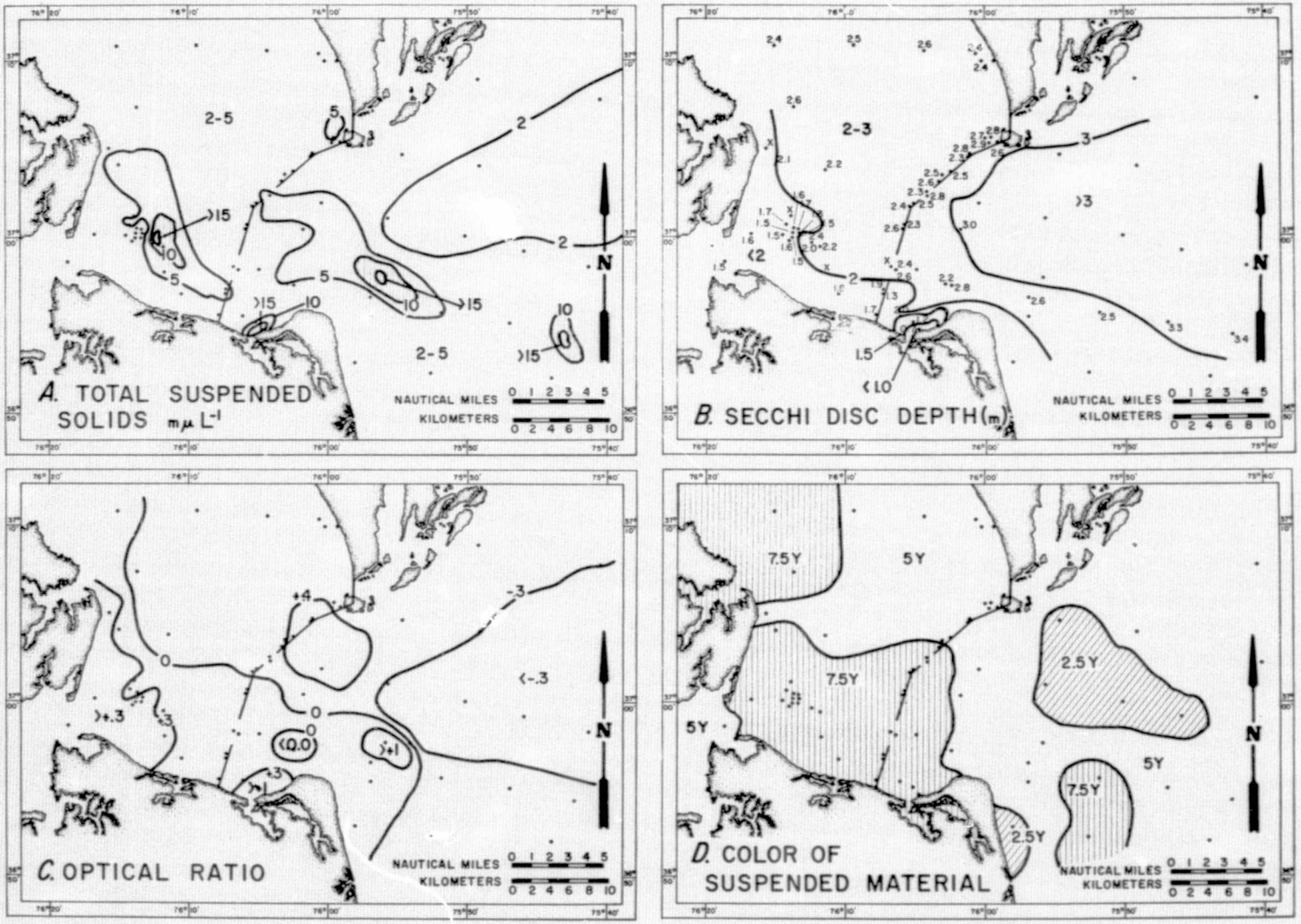

Figure 5. Distribution of water properties in lower Chesapeake Bay May 31, 1973. (A) total suspended solids (sediment), (B) secchi disk depth; (C) optical ratio and (D) color of suspended material.

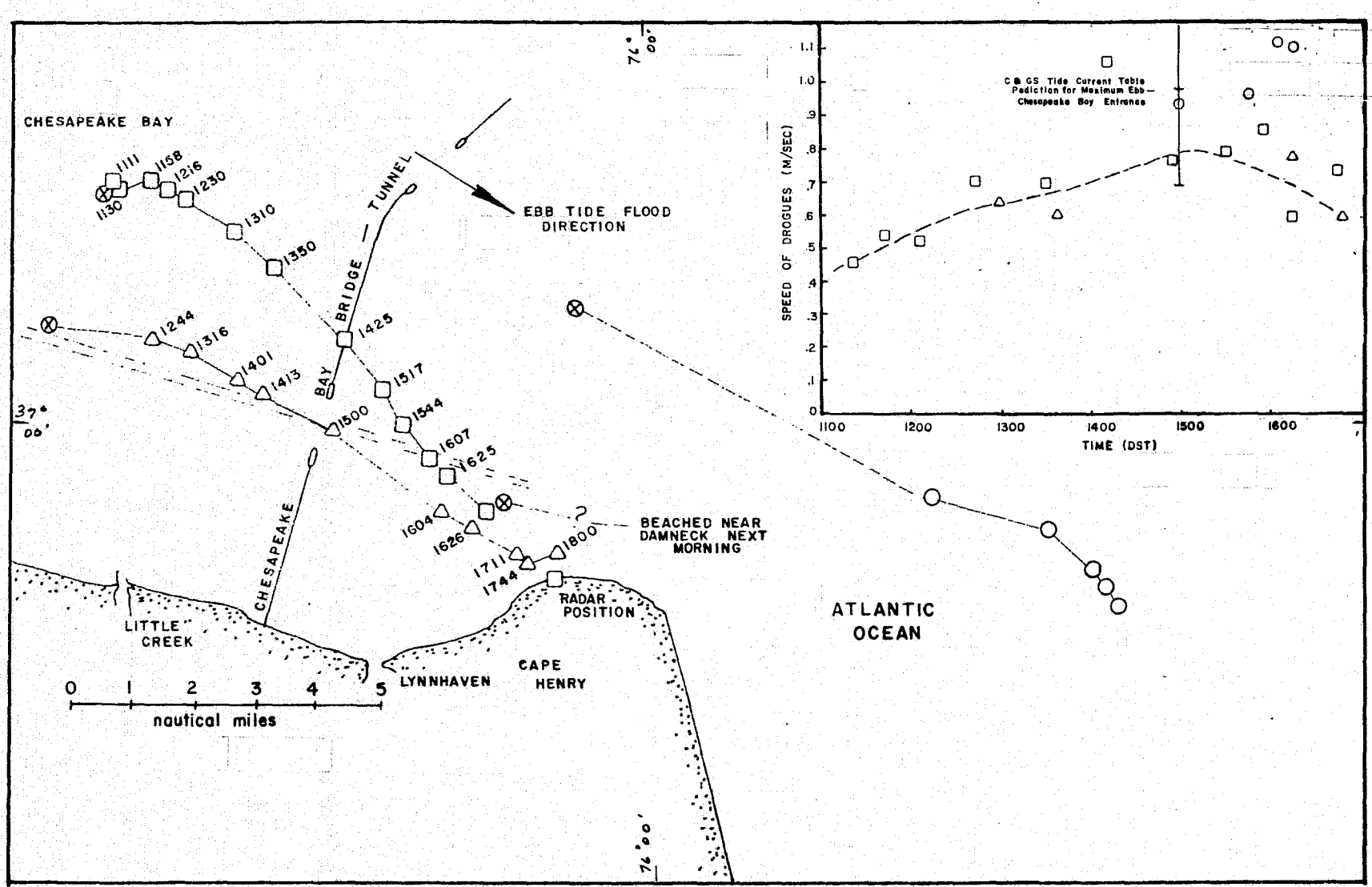

Figure 6. Paths of surface drogues in lower Chesapeake Bay, May 31, 1973. Time in EDT. Inset, upper right gives corresponding speed of drogues.

- Optical ratios generally parallel the distribution of disk depths except over the north shoals where they are locally positive indicating high turbidity. Ratios are relatively high (positive) inshore and low offshore in relatively clear ocean water (Fig. 5C).

- Color of suspended material displays hues of 7.5y, light olive brown along southwest reaches, and 2.5y light olive in the central outer reaches of the Entrance. Consequently, offshore waters which are plankton rich, are greenish whereas sediment-rich inshore waters are brownish or yellowish brown (Fig. 5D).

- Current speed and direction derived from drogue tracks (Fig. 6) show that surface water converges toward Cape Henry on the ebb tide. Speeds are greater offshore than in the Bay. The offshore track (Fig. 6) follows an extension of the Chesapeake Channel and travels beyond the Entrance shoals. Speeds (Fig. 6, inset) fall within the range of speeds predicted by the tidal current tables.

5.4.1.1 Water Color Boundaries

Water color boundaries are a prominent feature of surface waters in Lower Chesapeake Bay. Besides the contrasting color and turbidity the position of these boundaries is often indicated by lines of foam, or ruffled surface water. Often large quantities of floating debris as grass fragments, plastic debris, wood or dead fish are entrained in the lines. When the weather is calm and little foam is produced the boundaries are indicated by zones of smooth water or slicks dampened by oil.

From an aerial vantage point the boundaries appear as sinuous or arcuate lines extending 300 to 5,000 meters in length. As shown in Figure 4A, the boundaries are often broken, e.g. around Cape Charles of the northern entrance reaches where they form transient echelon patterns. Such boundaries form during both ebb and flood

current, but they are most pronounced and of greater length on the ebb current. They recur at about the same position at comparable stages of successive tides, but their intensity and length may vary with local conditions of flow and wind. Thus, the position of the boundaries is not fixed but varies within narrow limits.

An evaluation of the water properties along the color boundaries reveals no marked discontinuity of temperature and salinity such as occurs across boundaries separating oceanic water masses. Instead, there are only small changes in optical properties, ± 20 percent change in optical ratio and ± 12 percent change in disk depths. By contrast suspended sediment concentrations, phytoplankton concentrations and chlorophyll "a" distributions, vary irregularly across the boundaries. Since most parameters did not show objectively consistent differences across the boundaries it appears that the boundaries are caused by water properties or surface conditions other than those observed in this study.

Aside from the contrasts of water properties the boundary positions relate to the bathymetry and configuration of the lower Bay and its contiguous estuaries. Four types of boundaries are recognized from their distributional pattern that relates to estuarine geometry:

1. Axial boundary in which the boundary lies along the axis of tidal channels. These are common to narrowed reaches and the confluence of merging ebb tributary channels.

2. Lateral boundary which runs along the channel shoulder between shoal water and channel water.

3. Distal boundary which leads downstream from points of land and headlands and lies between channel water and "lee" water downstream of the point.

4. Concentric boundary which lies transverse to the channel axis often off an estuary entrance where water masses from different sources meet.

Figure 7 shows schematically different boundary types in relation to bottom geometry and inferred secondary currents.

Field observations together with evaluation of aerial photographs indicates the boundaries are created by a local circulation. From the accumulation of floating material in foam lines associated with the boundaries it is deduced that there is an inward flow of water toward the boundary. This flow has been confirmed by observing the movement of mimeograph paper spread out in lines 50 to 100 meters transverse to the boundary. Within a short time, 5 to 15 minutes, the paper accumulates in the boundaries often first from one side and then the other. It may be inferred that the inward flowing water descends along the boundary and there is a compensatory flow at depth away from zones of descending water. Such movements or secondary currents, have been observed by engineers in hydraulic models and flumes (Ciray, C., 1967; Vanoni, 1946). They are superimposed on the normal tidal flow and often occur in shear zones between rapidly moving channel water and slower moving shoal water or "lee" water behind headlands. In other cases, they originate in reaches where two channels merge or at the downstream "nose" of a shoal where there is a convergent flow of water. Differences in suspended load may arise from the amount of relatively clear water maintained near the surface or moved downward.

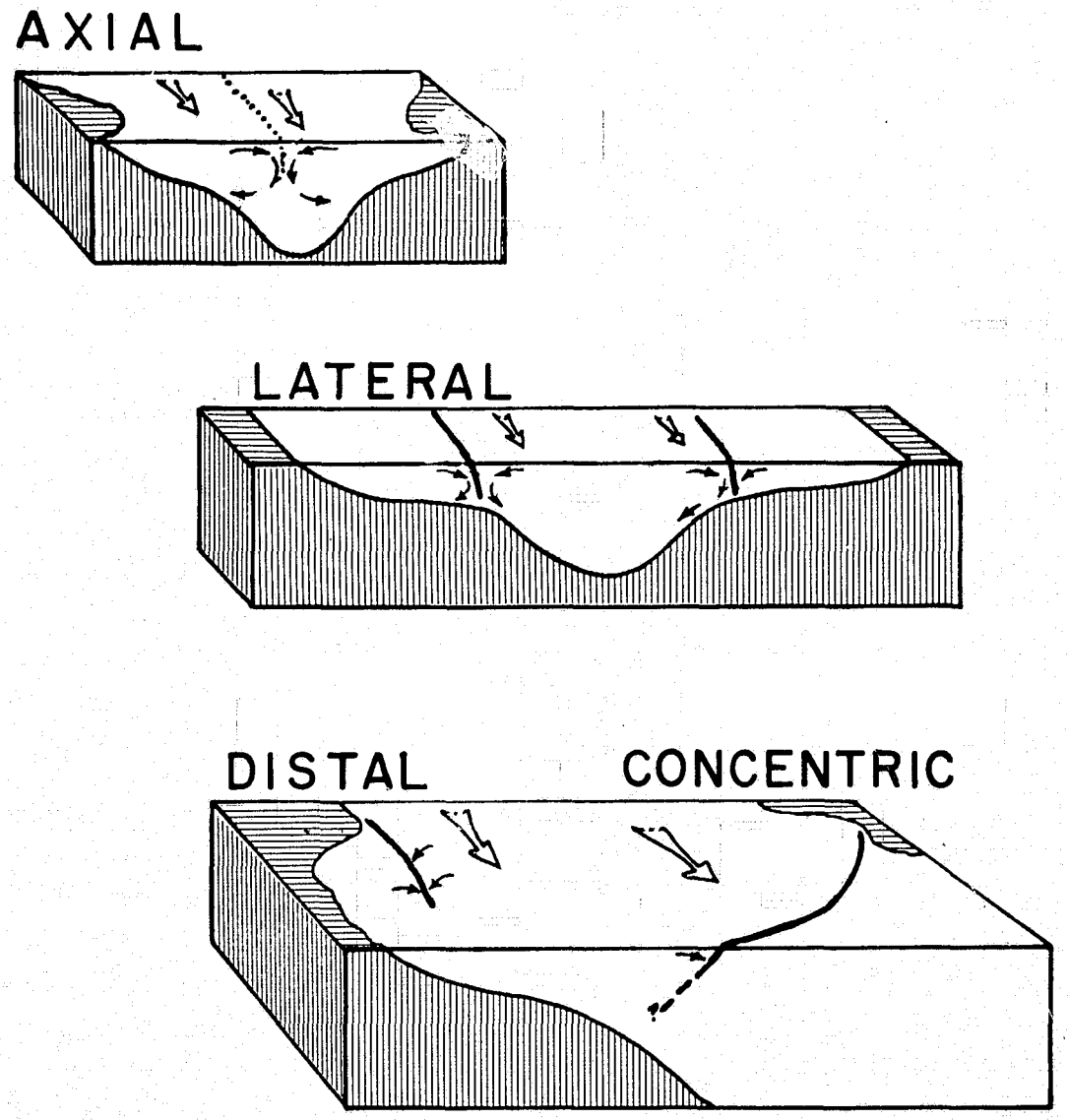

Figure 7. Schematic diagrams of different boundary types in relation to bottom geometry, configuration and secondary currents, single arrows; predominate tidal flow, double arrows.

5.4.1.2 Water property interrelationships.

When the concentrations of chlorophyll "a" are plotted against salinity values for all stations in the lower Bay there is a trend for chlorophyll to decrease with increasing salinity (Fig. 8). This relationship indicates that chlorophyll derived from production in relatively freshened water is diluted with distance seaward by mixing with salty water. If the chlorophyll were represented by photo densities in the green band a similar relationship to salinity would be expected.

Water types of different suspended load and transparency are differentiated by a scatter plot of 1/disk depth versus total suspended concentrations, Fig. 9. The graph shows that inshore waters off the James Estuary entrance and along the Norfolk shore are low in transparency whereas Bay water off central reaches is relatively clear. Disk depths distinguish the estuary water masses better than the suspended load. If disk depths relate to photo densities, water types could be charted from the imagery alone.

Figure 10 shows that disk depths also allow classification of waters of different salinity. Salty water of the central and oceanic reaches are relatively clear in contrast to freshened water of inshore reaches, north and south. Again, if disk depths relate to photo densities, water types of different salinities, could be differentiated from the imagery.

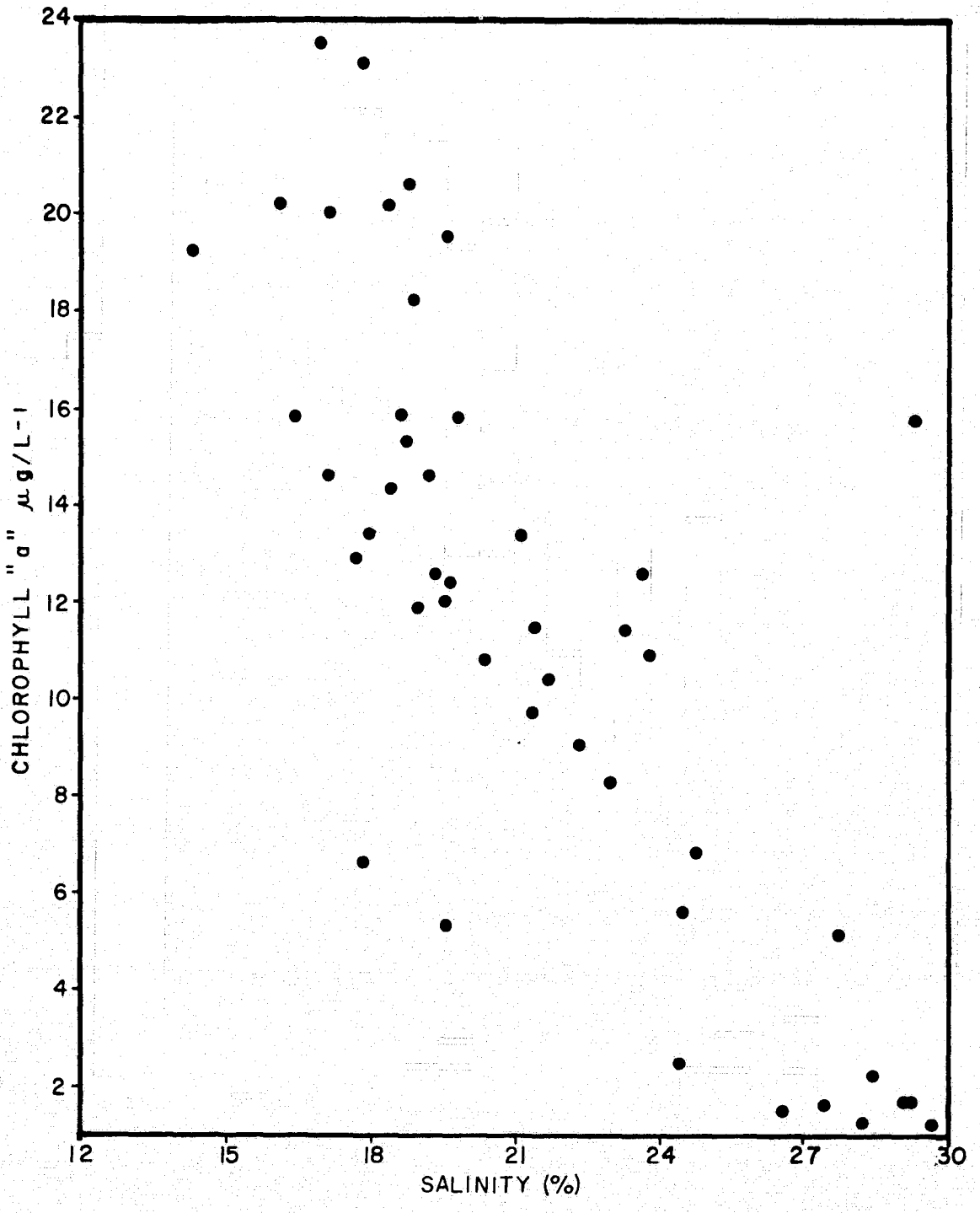

Figure 8. Scatter diagram of chlorophyll "a" concentrations versus salinity for stations in lower Chesapeake Bay, May 31, 1973.

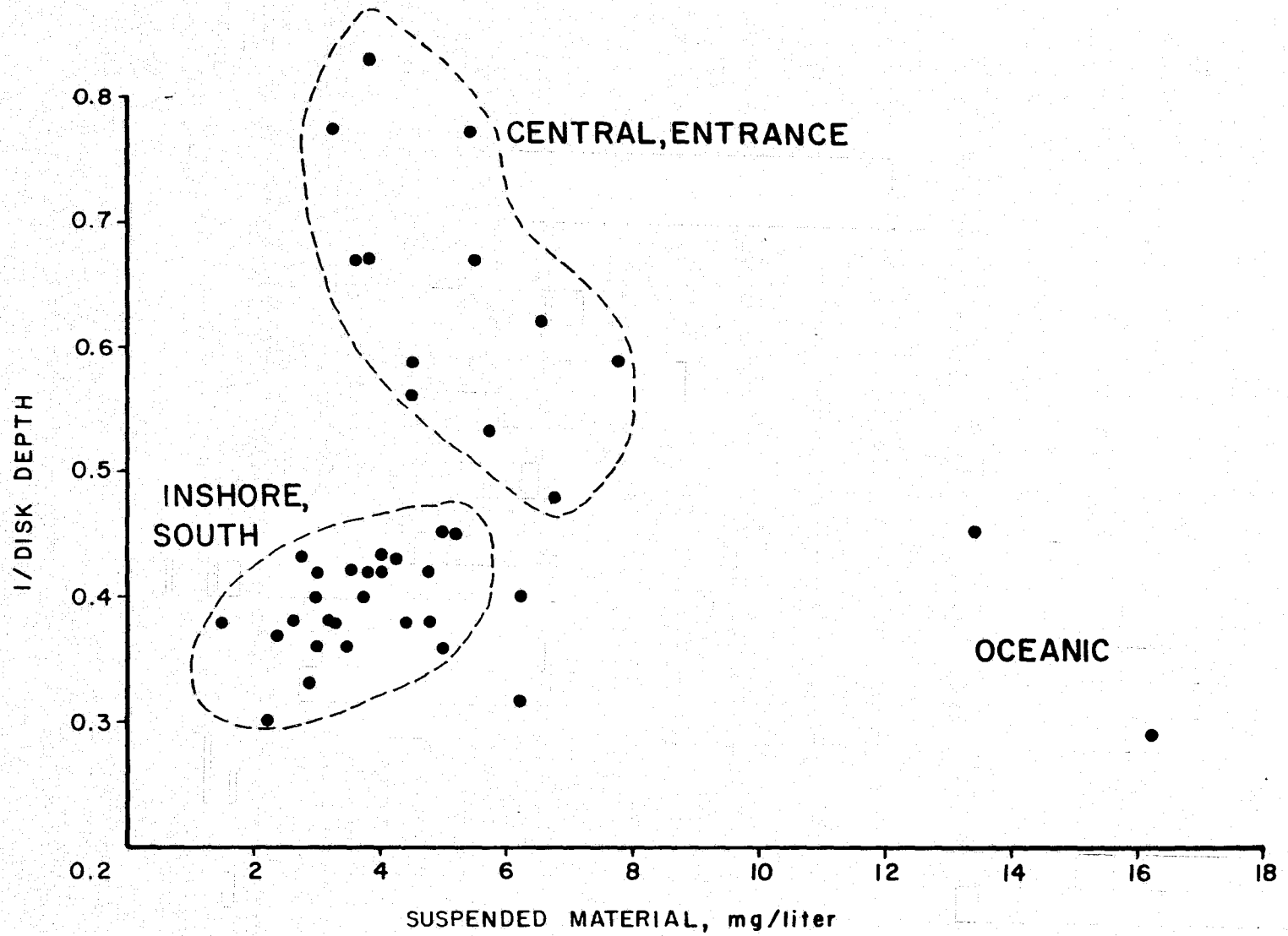

Figure 9. Scatter diagram of 1/disk depth versus concentrations of total suspended material for stations in lower Chesapeake Bay, May 31, 1973. Clusters define different water masses.

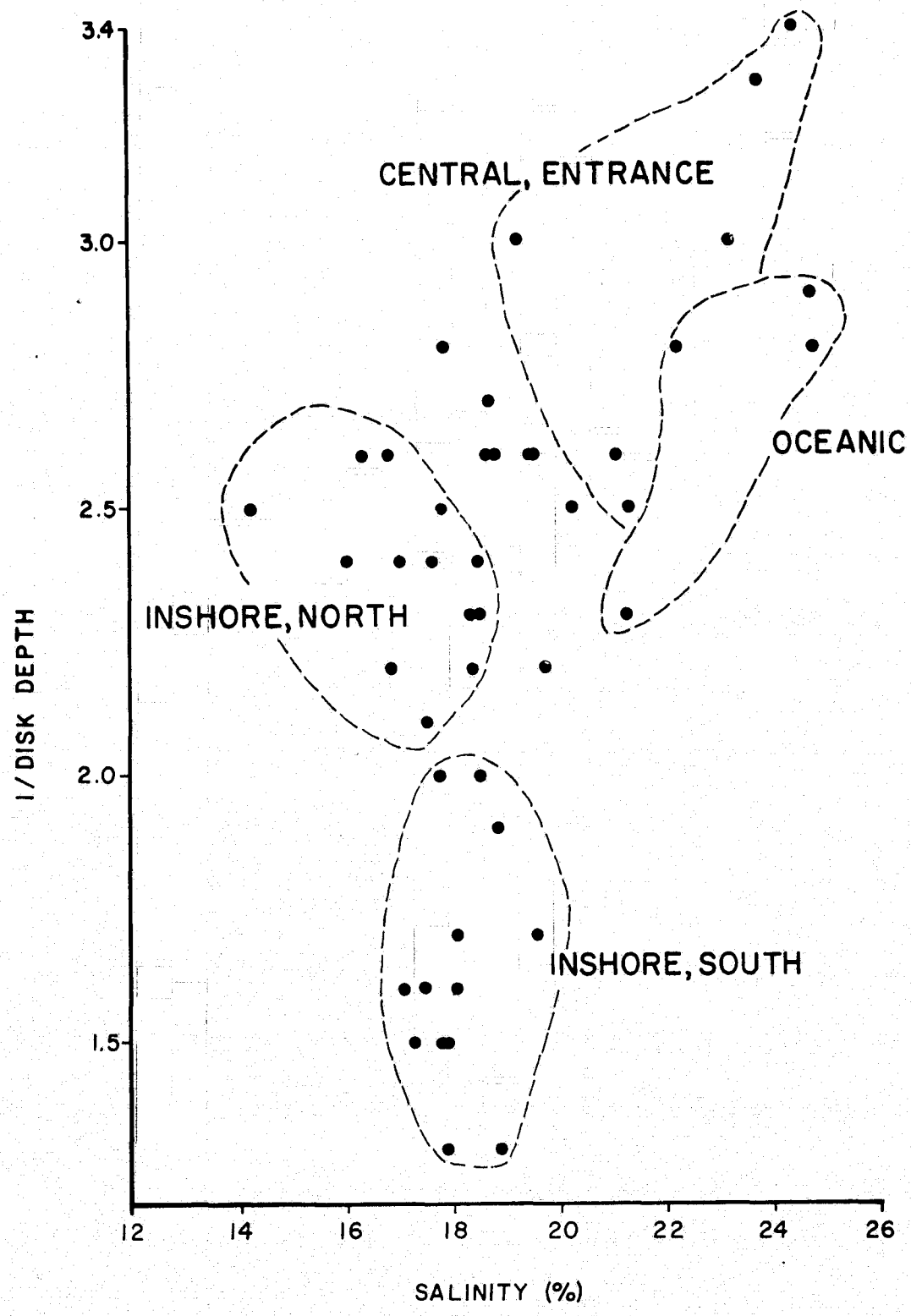

Figure 10. Scatter diagrams of 1/disk depth versus salinity for stations in lower Chesapeake Bay. May 31, 1973. Clusters define different water masses.

5.4.2 Rappahannock Estuary

An evaluation of surface truth observations of Sept. 12, 1973 (Skylab 3) displayed as distributions of water properties Figures 11, 12 and 13, reveals the following salient features:

- Color boundaries are limited to middle and lower reaches. They are relatively weak and often broken into short segments. They consist mainly of lateral and irregular concentric types (Fig. 11B).

- Water is relatively isothermal throughout the estuary. Estuary water is slightly warmer than Chesapeake Bay water by about 1°C (Fig. 11C).

- Salinity increases with distance seaward from 1‰ above Tappahannock to more than 15‰ off the estuary mouth (Fig. 11D). The highest longitudinal gradient of salinity occurs in the upper estuary, between Tappahannock and Morrattico, a change from 3 to 7‰.

- Concentrations of total suspended material are relatively high in the upper estuary and relatively low in the middle and lower estuary as well as in the Bay. The greatest seaward decrease takes place in the middle estuary near Morattico (Fig. 12A).

- Optical ratios generally decrease with distance seaward i.e. become less positive and more negative, a trend which reflects seaward decreasing turbidity (Fig. 12B).

- Secchi disk depths are greater in the upper, turbid reaches than in the lower less turbid reaches. A zone of low transparent water over the shoals on the south side of the mouth, parallels a zone of low optical ratios and high suspended concentrations (Fig. 12C).

- Chlorophyll "a" distributions are patchy but in general they are relatively high in turbid upper reaches and high at the mouth whereas they are low in middle reaches (Fig. 12D).

- Color of suspended material is light olive brown, 7.5y hue, in lower reaches and mainly light olive, 5y hue, in upper reaches. Locally the color is grayish olive (10y) in lower reaches (Fig. 13).

- Concentrations of phytoplankton decrease irregularly from upper reaches to middle reaches whereas they are more or less uniform in the lower estuary (Fig. 13).

- Mean particle size is small and varies within narrow limits, from 4.5 μ in the upper estuary to 17.9 μ in the lower estuary.

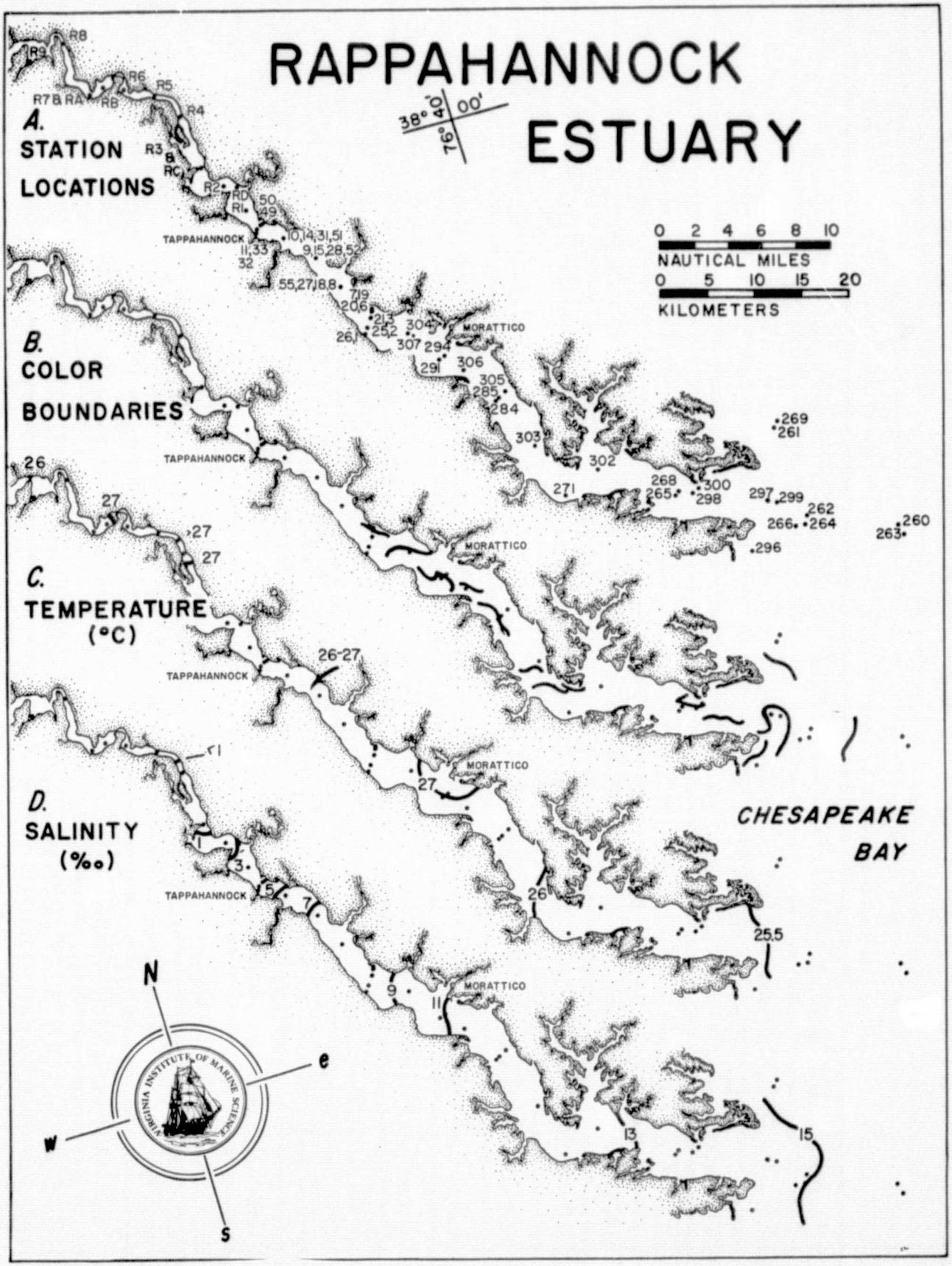

Figure 11. Location of surface truth stations in the Rappahannock Estuary, Sept. 12, 1973 (A), and distribution of color boundaries (B). Distribution of properties of surface water: (C) temperature and (D) salinity.

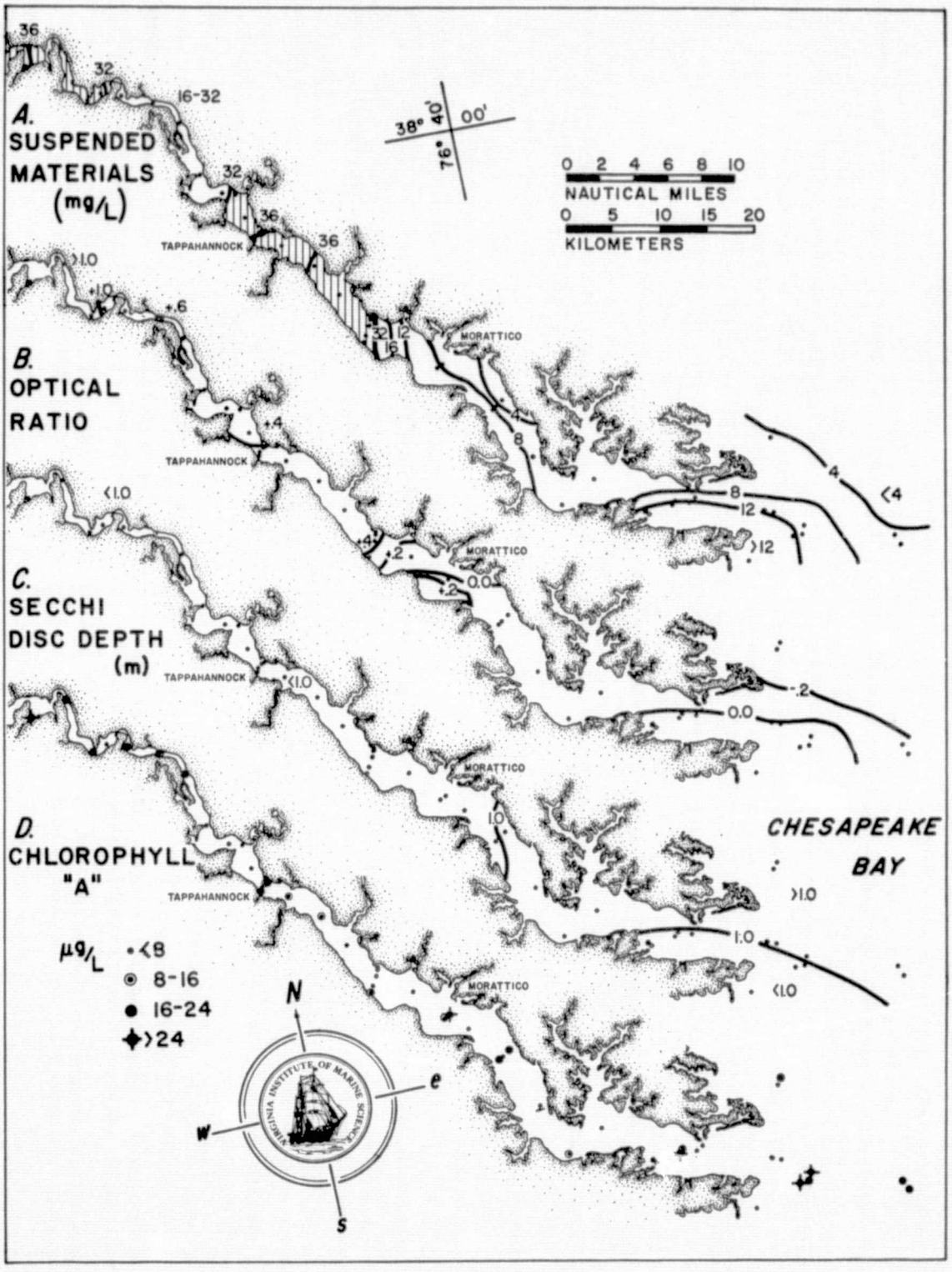

Figure 12. Distribution of properties in surface water of the Rappahannock Estuary (A) total suspended material, (B) optical ratio, (C) secchi disk depth, (D) chlorophyll "a", Sept. 12, 1973, zone of the turbidity maximum is shaded, Fig. 12A.

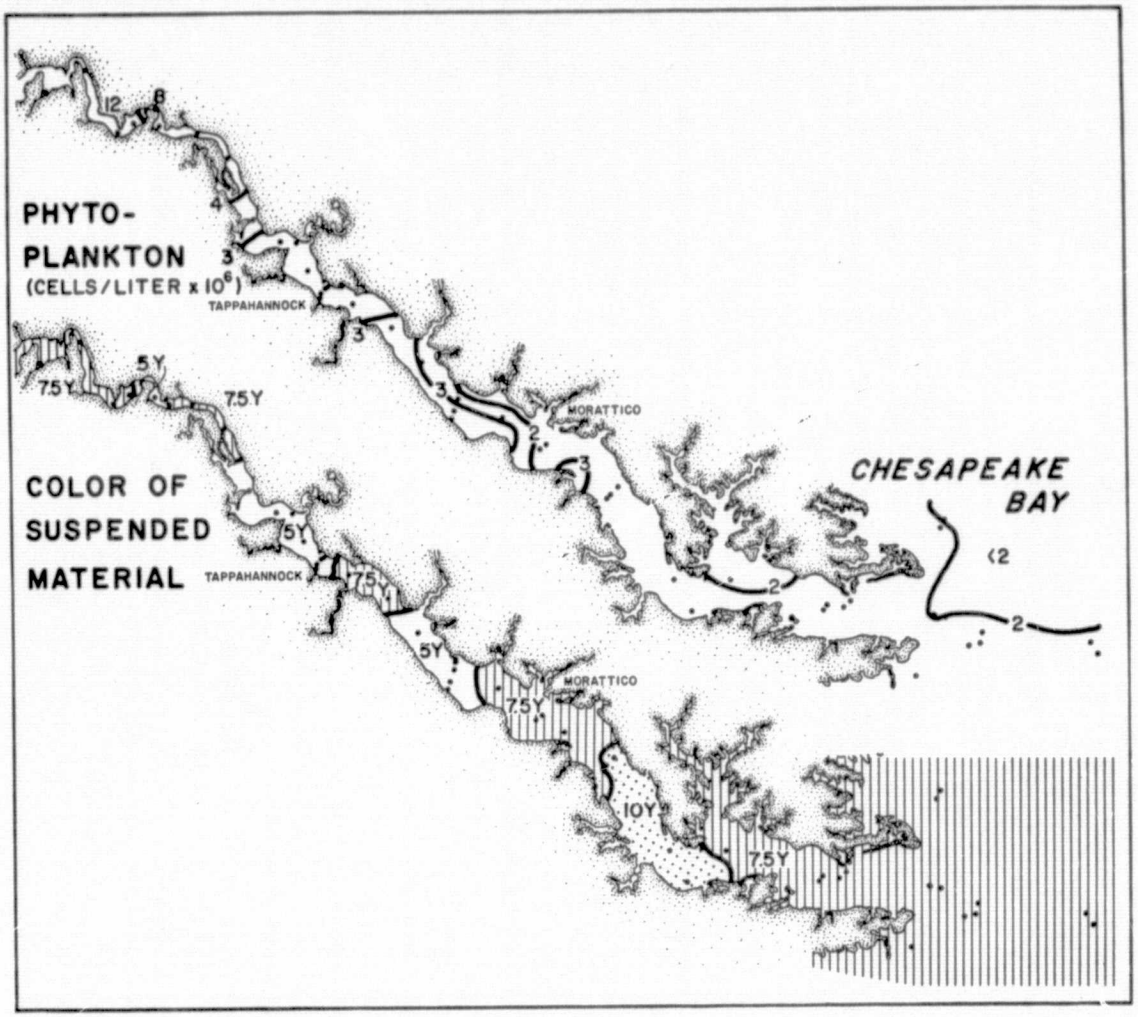

Figure 13. Distribution of phytoplankton (upper) and color of suspended material (lower) in surface water of the Rappahannock Estuary, Sept. 12, 1973.

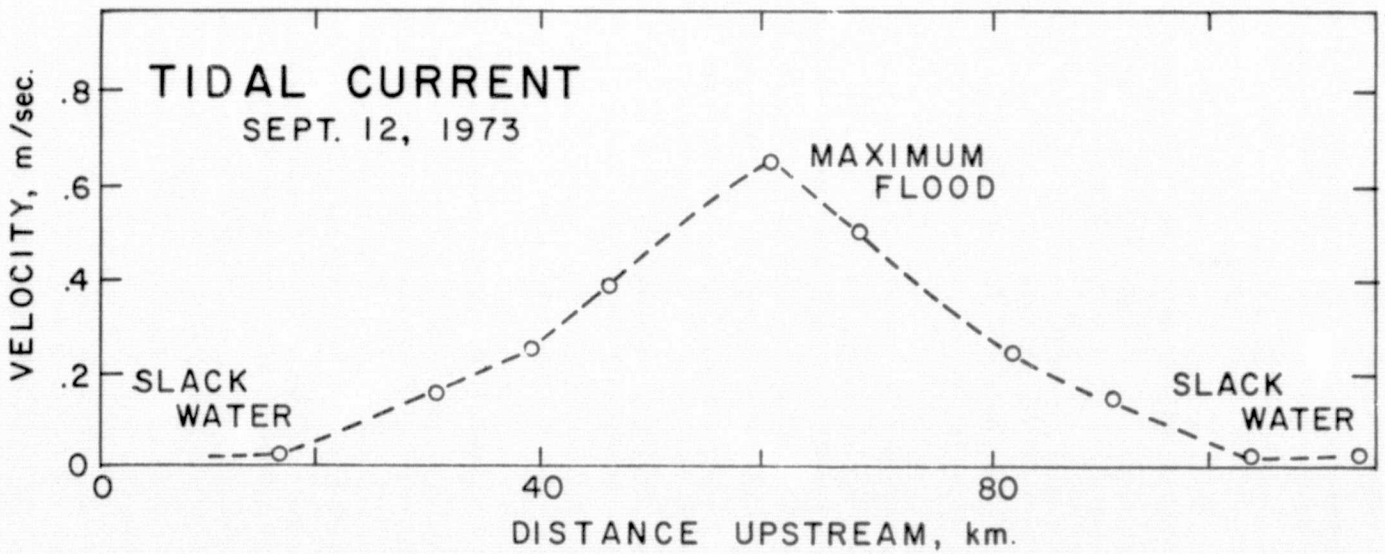

Figure 14. Distribution of current speed along the length of the Rappahannock Estuary, Sept. 12, 1973; at time of Skylab photography 1209.

- Current velocity at the time of Skylab pass-over, 1209 EDT Sept. 12, 1973 was slack near the mouth and at the head, but maximum flood at Tappahannock in the upper Estuary (Fig. 14).

A series of "follow-up" observations, made June 13, 1974 under conditions of tide and inflow similar to those of September 12, 1973 (Skylab 3), reveals similar distributions of salinity, suspended sediment distribution , disk depth, optical ratio and mean particle size (Fig. 15, Appendix 12.4). Only part of the irradiance measurements are reported herein because the values are either contaminated by cloud coverage or spurious due to instrument malfunctions.

A comparison of water property distributions along the estuary length reveals several interrelationships between optical and hydrographic parameters. For example the seaward decrease of secchi disk depth parallels a seaward decrease in optical ratios (Figs. 15 and 16). Phytoplankton, chlorophyll and suspended sediment concentrations also generally decrease from the upper estuary to the middle estuary, whereas farther seaward they rise near the mouth. The seaward decrease through the upper estuary is a result of downstream dilution of sediment supplied from the river. High suspended material near the mouth is probably caused by high levels of plankton manifest in the high chlorophyll values (Fig. 16). Similarly the downstream decrease of sediment concentrations (Fig. 16) is a result of dilution and settling out of river-borne material from near-surface water. Settling is substantiated by the decrease in mean and median particle size from the upper to the middle estuary. But farther seaward, in-

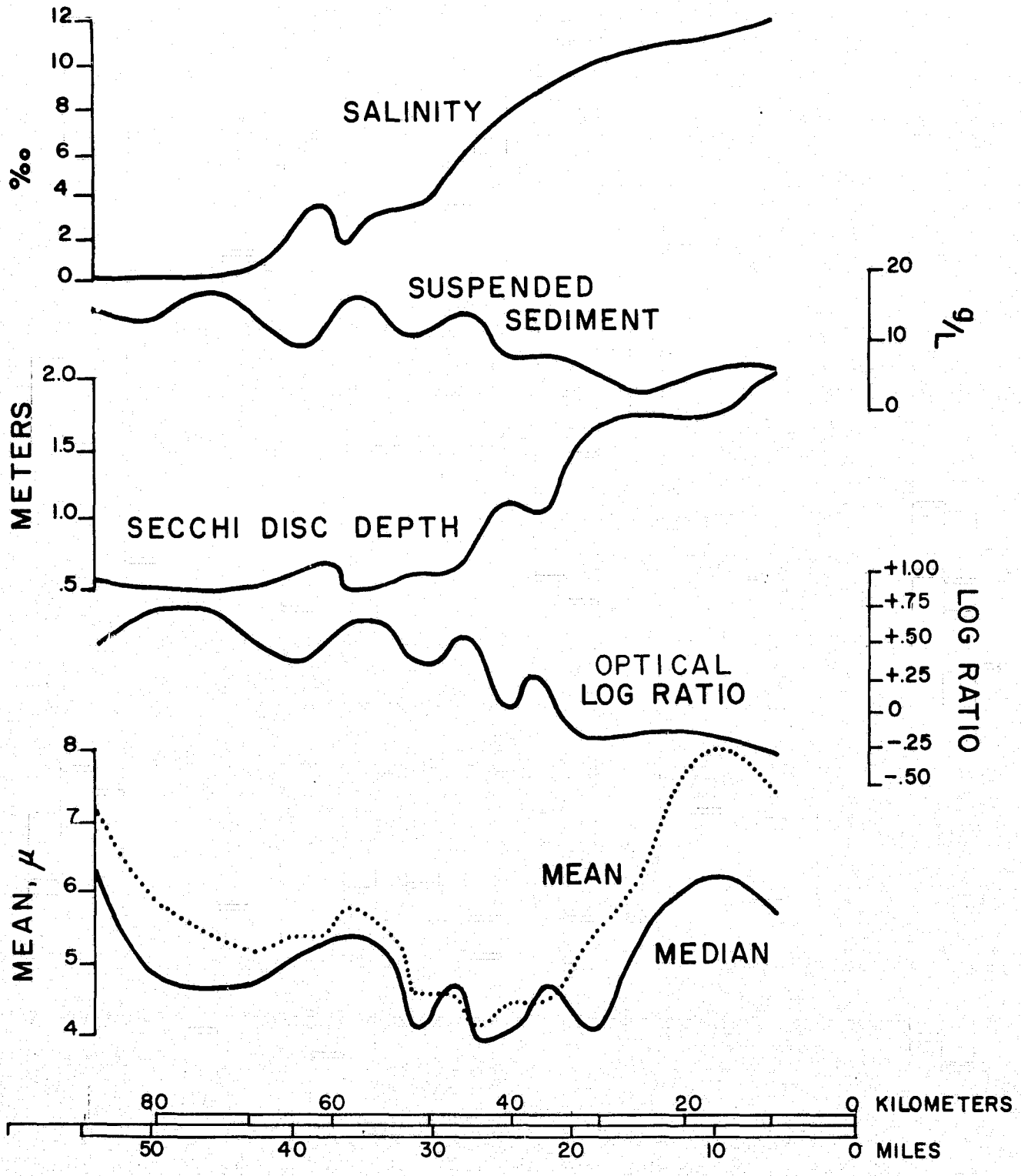

Figure 15. Distribution of water properties and particle size of suspended sediment along the length of the Rappahannock Estuary, June 13, 1974.

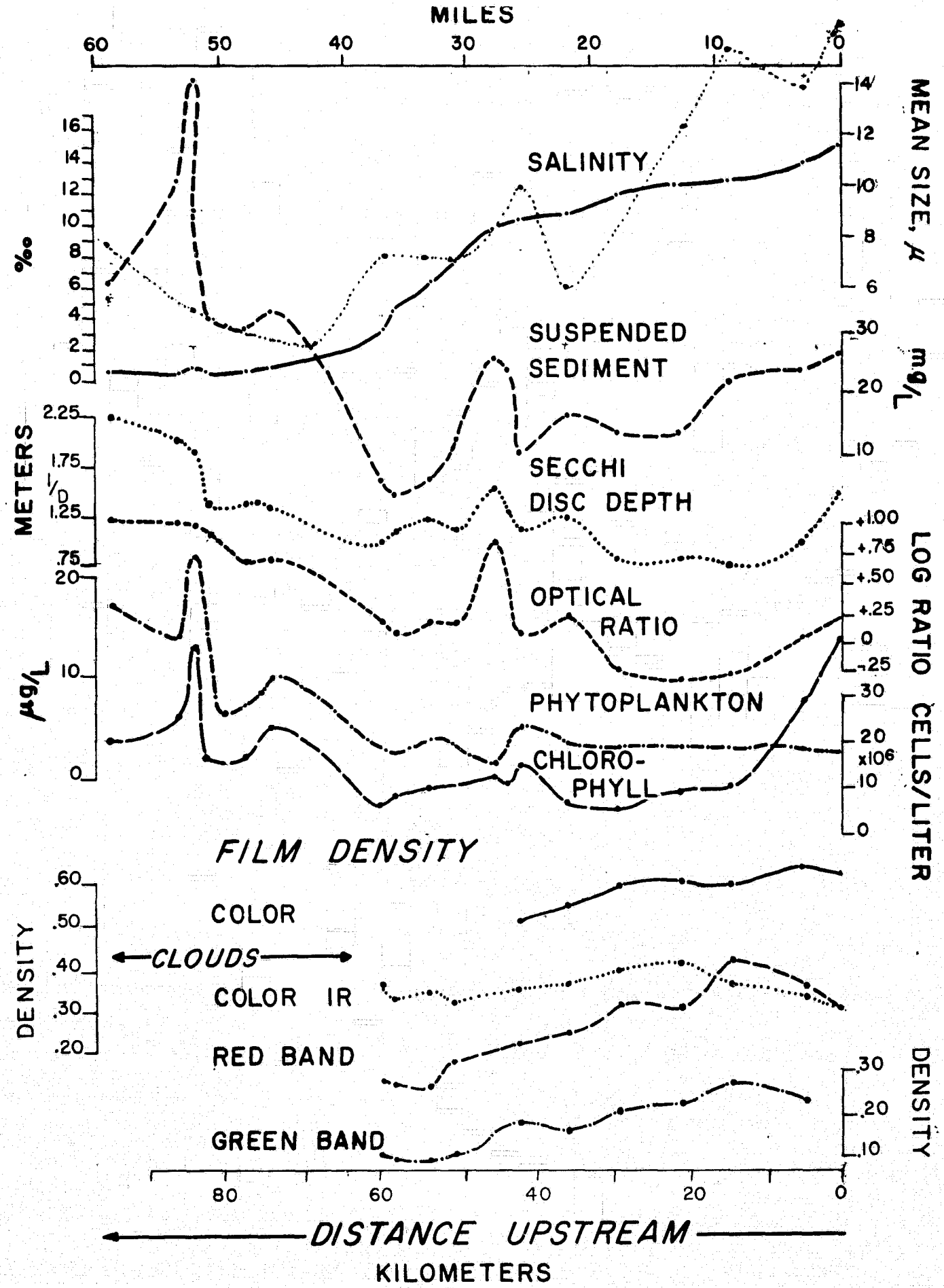

Figure 16. Distribution of water properties along the length of the Rappahannock Estuary, Sept. 12, 1973. Corresponding distribution of photo densities for multispectral imagery of Skylab 3.

creased proportions of phytoplankton contribute to the greater particle size. It is these factors that produce the broad gradient of water and optical properties along the estuary length. It remains to be seen if these properties contribute to spectral reflectance in the space imagery.

6. REMOTE SENSING STUDIES

6.1 Data acquisition

The imagery analyzed was obtained from two Skylab missions, Skylab 2 and 3, June 12, 1973 and September 12, 1973. Both missions cover an alternate test site, the Rappahannock Estuary, since the Skylab track drifted away from the prime test site, the southern (lower) Chesapeake Bay. Photography was not scheduled to meet specific conditions of the tide or to cover certain natural phenomena important to resource management. Instead, photography was attempted whenever skies were clear and at a time when Skylab orbited on track 57 during daylight hours (required for photography). Since the prime site, the Lower Chesapeake Bay, was one of the few sites on track 57, it was given relatively low priority. No photographic coverage was obtained on the prime site.

Tables 1, 2 and 3 summarize pertinent imagery data acquired on the Rappahannock Estuary, the alternate test site. The film-filter combinations were selected to provide multiband coverage at four 100 nm intervals from 500 nm to 900 nm in 70 mm format. Additional imagery was obtained in color infrared (500 to 800 nm) and natural

Table 1. Imagery data of the S190A camera for the Rappahannock test site, June 12, 1973. From NASA-Skylab data book, No. 32-25077.

S190A - MULTISPECTRAL PHOTOGRAPHIC CAMERA

PROJECT DPAR#73-179- 9
MISSION 2 ORBIT 9 SITE 0
SENSOR S190A RECORDING FORMAT 21 FLIGHT DATE 6 12 73

TRJGMT 163:13: 1:20.1863 TMID 163:12:26:55.2000 TSR 163:12:44: 4.7996 TSS 163:12: 9:49.3999
TRJGET 18: 0: 1:19.3863 ATM TIME4166:15:**:39.0078 TESR 163:12:44:22.0002 TESS 163:12: 9:32.5000
AMT 163:13: 1:19.6119 REV NO. 417.000

*** CAMERA AND EXPOSURE DATA ***

CAMERA STATION	FRAME NUMBER	FILM TYPE	FILTERS	APER. STOP	INTEG. EXPOS. TIME	EXPOSURE INITIATE TIME	EXPOSURE INITIATE DELTA-T	EXPOSURE OCCURRENCE TIME	EXPOSURE OCCUR. DELTA-T	INITIATE/ 2ND-OCCUR. INTERVAL	SECOND OCCUR. DELTA-T	BIT PERIOD COUNT
1	13-166	EK242	CC/	F/ 6.7	8.7784	163:13: 1:19.8400	8.0000					
2	14-166	EK242	DD/	F/ 6.7	8.7784			163:13: 1:19.8641				70
3	15-174	EK242	EE/	F/ 9.5	8.7172			163:13: 1:20.1863	0.3221	0.3463	7.7312	21
4	16-174	S0022	FF/	F/ 4.8	8.8686			163:13: 1:20.5085	0.3221			100
5	17-166	S0022	BB/	F/ 5.6	8.8.38			163:13: 1:20.8305	0.3221			51
6	18-166	0022	AA/	F/ 5.6	8.8106			163:13: 1:21.1526	0.3221			2

NO. OCCUR. PULSES 5 STAND. DEV. OF OCCUR. PULSES 0.00E-01
AVE. OCCUR. PULSE DELTA-T 0.3221 MAX. DEV. OF OCCUR. PULSES 0.00E-01

*** FIELD OF VIEW COORDINATES ***

	CENTER OF FRAME	UPPER LEFT CORNER OF FRAME	UPPER RIGHT CORNER OF FRAME	LOWER LEFT CORNER OF FRAME	LOWER RIGHT CORNER OF FRAME
LATITUDE (DEG:MIN)	38:12.3	38:22.4	37:10.1	39:14.4	38: 1.3
LONGITUDE (DEG:MIN)	- 76: 5.3	- 74:46.3	- 75:52.1	- 76:18.8	- 77:23.8

*** CAMERA MALFUNCTIONS ***

CAMERA STATION	CAMERA MALF. START	CAMERA MALF. STOP

Table 2. Imagery data of the S190A camera for the Rappahannock test site, Sept. 12, 1973. From NASA-Skylab data book, No.33-25023.

S190A - MULTISPECTRAL PHOTOGRAPHIC CAMERA

PROJECT S190 DPAR 0A-DPCA-03-36-22-1
MISSION 3 ORBIT 36 SITE 0
SENSOR S190A RECORDING FORMAT 21 FLIGHT DATE 9 12 73

TRJGMT 255:17: 9:31.7499 TMID 255:16:16:56.2998 TSR 255:16:34:18.5000 TSS 255:15:59:32.2000
TRJGET 46: 5:58:41.7500 ATM TIME 95: 1: 4: 0.2793 TESR 255:16:34:34.7000 TESS 255:15:59:15.7998
AMT 255:17: 9:31.2340 REV NO. *******

*** CAMERA AND EXPOSURE DATA ***

CAMERA STATION	FRAME NUMBER	FILM TYPE	FILTERS	APER. STOP	INTEG. EXPOS. TIME	EXPOSURE INITIATE TIME	EXPOSURE INITIATE DELTA-T	EXPOSURE OCCURRENCE TIME	EXPOSURE OCCUR. DELTA-T	INITIATE/ 2ND-OCCUR. INTERVAL	SECOND OCCUR. DELTA-T	BIT PERIOD COUNT
1	37-122	EK2424	CC/	F/ 9.5	8.7419	255:17: 9:31.3440	10.0000					
2	38-122	EK2424	DD/	F/ 9.5	8.7387			255:17: 9:31.4267				38
3	39-122	EK2443	EE/	F/ 9.5	8.7387			255:17: 9:31.7500	0.3231	0.4059	10.2209	125
4	40-122	SO 356	FF/	F/ 4.0	8.9518			255:17: 9:32.0727	0.3228			81
5	41-122	SO 022	BB/	F/ 5.6	8.8356			255:17: 9:32.3950	0.3224			34
6	42-122	SO 022	AA/	F/ 5.6	8.8323			255:17: 9:32.7173	0.3223			114

NO. OCCUR. PULSES 5 STAND. DEV. OF OCCUR. PULSES 3.86E-04
AVE. OCCUR. PULSE DELTA-T 0.3226 MAX. DEV. OF OCCUR. PULSES 4.88E-04

*** FIELD OF VIEW COORDINATES ***

	CENTER OF FRAME	UPPER LEFT CORNER OF FRAME	UPPER RIGHT CORNER OF FRAME	LOWER LEFT CORNER OF FRAME	LOWER RIGHT CORNER OF FRAME
LATITUDE (DEG:MIN)	37:54.5	38:55.0	37:44.2	38: 3.9	36:53.8
LONGITUDE (DEG:MIN)	- 76:18.8	- 76: 6.2	- 75: 2.5	- 77:35.4	- 76:31.0

*** CAMERA MALFUNCTIONS ***

CAMERA STATION	CAMERA MALF. START	CAMERA MALF. STOP

Table 3. Imagery data of the S190B camera for the Rappahannock test site, Sept. 12, 1973. From NASA-Skylab data book, No. 33-35223.

S190B-EARTH TERRAIN CAMERA TABULATION

PROJECT OB-DPCA-0-36-31-1
MISSION 3 ORBIT 36 SITE 0
SENSOR S190B FLIGHT DATE 9 12 73

TRJGMT 255:17: 9:27.500 TMID 255:16:16:56.300 TSR 255:16:34:18.500 TSS 255:15:59:32.200
TRJGET 46: 5:58:37.500 ATM TIME 95: 1: 3:56.087 TESR 255:16:34:34.700 TESS 255:15:59:15.800
ACC.TIME 0: 0: 0: 0.000 REV NO. *******

*** CAMERA AND EXPOSURE DATA ***

FRAME NUMBER	FILM TYPE	FILTER	EFF. F-NUMBER	EXPOSURE TIME
86-299	SO 242	5	F/ 5.6	7.1

*** FIELD OF VIEW COORDINATES ***

	CENTER OF FRAME	UPPER LEFT CORNER OF FRAME	UPPER RIGHT CORNER OF FRAME	LOWER LEFT CORNER OF FRAME	UPPER LEFT CORNER OF INSET	UPPER RIGHT CORNER OF INSET	LOWER LEFT CORNER OF INSET
LATITUDE (DEG:MIN)	37:45.9	38:26.2	37:39.1	37:52.3	37:19.0	37:11.2	37:13.4
LONGITUDE (DEG:MIN)	- 76:34.1	- 76:25.7	- 75:43.4	- 77:24.9	- 76:39.5	- 76:32.5	- 76:49.3

color film (S0242) was obtained from the 18-inch focal length, Earth Terrain camera. Altogether 13 photographs were obtained in addition to partial coverage on adjoining frames.

6.1.1 Data quality

Although the photographs adequately cover the test site, film quality varies a great deal. More than 40 percent of the site is contaminated by discrete cloud coverage on each set of photographs. Additionally, there are jet trails in the Skylab 2 photos and a high cirrus "fog" that contaminates the lower estuary in the Skylab 3 photos. Such atmospheric contamination precludes accurate records of tonal and spectral reflectance from the surface.

The imagery received consists of third generation duplicates. While the duplicates are generally of good quality, exposure varies a great deal when compared to like frames of other second and third generation duplicates held by other investigators.

Since the clocks in the S190B camera malfunctioned during Skylab 2 and 3 the exact time of photography is unknown. Moreover, errors in timing of the EREP Control and Display panel preclude accurate records of photographic time for the S190A scenes (Potter et al., 1974).

Exposure of the scenes is relatively good, within ± 0.5 f stop of optimum although the natural color film of the S190A is overexposed by 0.5 to 1.0 f stop. The marked changes in reflectance from contrasting areas of land and water do not appear to have affected the

S190A or S190B scenes. The photos are free of sunglint and excess shadows except for cloud shadows. Lighting across the scene is relatively uniform and the scenes are free of dark corners.

Spatial resolution was evaluated by visual edge matching and comparison of known objects in contact size duplicate transparencies. With 2:1 contrast the S190B camera with S 242 film resolved linear features, roads and bridges, down to 10 meters. Corresponding resolution of the S190A cameras was about 50 meters which is within the range reported for pre-flight sensor performance.

6.2 Analytical techniques

The imagery was analyzed by different techniques and instruments: (1) simple photo interpretation with aid of a magnifying viewer, surface truth observations and densitometric displays of a video Data Color unit (Spatial Data systems), (2) densitometric analysis of multi-band scenes, one scene at a time, in a Joyce-Loebl microdensitometer-isodensitracer, (3) analysis of a single scene, the S190B natural color scene, with an Optronics scanning microdensitometer. Both gray maps and single scan profiles were made of water areas throughout the test site. Use of the Joyce-Loebl and Data Color units followed conventional procedures. Procedural details and techniques for the Optronics analysis are presented below.

6.2.1 Optronics - WALDIPS analysis

Film from the Earth Terrain Camera (S190B) in the form of a 4.5 inch square positive color transparency was used to make a series of three isodensity plots. The imagery was digitized on an Optronics scanning microdensitometer located at NASA Wallops Flight Center, Virginia. A spot size and raster of 50 micrometers was chosen, and three Wratten filters were placed internally in the light path to separate the three emulsion layers on the color film. Thus, three separate records of the scene were recorded on magnetic tape corresponding to the spectral bands, 4-500 nm, energy (blue), 5-600 nm (green), and 6-700 nm (red).

The microdensitometer scans the film placed on a rotating drum, by stepping a light source head inside the drum in unison with a detection head outside, which is directed normal to the rotation of the drum. Each time the drum makes one revolution the detector views the uninterrupted light source for an optical density level (assigned 0 counts), and one 50 micrometer strip of the imagery. Relative densities are expressed in terms of counts between 0 and 255 which is equivalent to an optical density of 3; higher numbers represent optically denser images corresponding to lower surface reflectance. It was decided not to express the data in terms of absolute units of radiance from the water surface or irradiance at the sensor, since the important information is better expressed in terms of changes in physical parameters and optical film density.

Isodensity plots were derived from the computer gray maps made from the microdensitometer tapes. Computer programs from a part of the Wallops Digital Information Processing System (WALDIPS) were chosen to

compile a histogram of relative densities of all 50 micrometer points digitized from the estuary and surrounding land area. The program forms thirteen density bins (within the relative density range of 0-256). Each bin contains an equal number of points which corresponds to a range of relative density; each bin is assigned a print symbol on a computer line printer, which in turn forms a 13 level gray map.

The problem of locating the land-water interface or estuary shoreline on the gray map was solved by digitizing an overlay made from the original image of the estuary on which only the land-water interface is drawn. The corresponding gray map made in this manner, with symbols excluded, outlines only the estuary shoreline and can be used to transfer an exact scale boundary to the gray maps made of the original imagery.

An examination of the 13 levels on each gray map, consisting of one for each color band, revealed a complex density structure for the land areas, but a rather simple presentation of densities representing the estuary water surface. There were generally three to five distinct symbols representing a like number of density bins with well defined boundaries for red and blue bands.

In order to increase the contrast of the water density classes, as well as the land-water contrast, the programs were rerun with density bins chosen manually. Water densities were grouped into four classes, land into two, and clouds into one. Overlays made from these gray maps form the basis for the isodensity plots presented. As stated previously, darker areas, and areas with higher numbers of relative density, correspond to regions of lower broad band spectral reflectance.

6.3 Interpretation of water color and circulation features

6.3.1 Skylab 2, Rappahannock test site, (frames SL2-15-174 and SL2-16-166)

At the time the photos were taken, reportedly at 0801 June 12, 1973, the tidal current was slack near the mouth and also near the head above Tappahannock; maximum flood dominated middle reaches. A high cirrus haze (h, Fig. 17A, B) covered the upper estuary as a cold front approached from the west; whereas altocumulus clouds blanketed parts of the lower estuary. Winds blew 5-10 knots from the southwest. River discharge was relatively high, greater than 336 m^3 per sec at Fredericksburg two days prior to photography. Therefore, sediment influx from the river was higher than normal and salinity of estuary water was depressed.

The imagery displays the present-day shoreline, tributary creeks and bordering marshes as well as sandy beaches around the mouth. Shoals 1-2 meters deep are represented by light tone patterns off Windmill Point, Greys Point and Towles Point (s, Fig. 17B). Elsewhere, dark toned areas close to shore represent eel grass beds, e.g., g, Figure 17B. The Greys Point bridge and superstructure which carries a two lane road about 22 meters wide, is clearly resolved by the camera despite successive duplications and scattered cloud coverage.

The most prominent feature in the scene is a broad zone of brownish colored water in the upper estuary. This feature (tm, Fig. 17A) is called a turbidity maximum. The reflectance in this zone is higher than is source river water farther upstream or in the estuary farther seaward. Close examination shows that the maximum is asymmetrical. Tonal gradients are sharper on its upstream side than on the downstream side. Then too, the highest brightness is centered on the southwest side of the estuary.

Intensive observations prior to photography show that the maximum develops in a convergence zone where seaward flowing river water and landward flowing estuarine water along the bottom, meet. Such currents commonly converge near the inner limit of salty water. Where the turbidity maximum is recorded in the photo it indicates the position of inner limit of salty water or on the other hand, the seaward limit of fresh river water. The zone is also a site of rapid shoaling in many estuaries. Consequently, the maximum is indicative of decreasing water depths although the film-filter "penetration" is very limited. Turbidity maxima are also recorded on the same scene in other estuaries, the Patuxent Estuary, Maryland and the Chester River estuary, Maryland.

The photograph shows that the turbidity maximum extends farther downstream over the bordering shoals than in the central channel. This pattern (e, Fig. 17A) reflects the gross aspect of the bottom geometry since the turbidity distributions form a "rolling carpet" over the bottom. Therefore, near-surface turbidity is higher over submerged shoals than in the axial channel. Such a pattern is common to the Chesapeake and its tributaries.

Locally, light-toned filaments and perturbations extend off shoreline points and headlands. At one point (m, Fig. 17A) they extend into the central channel forming a giant gyre whirling counterclockwise. Such a feature indicates that large scale lateral mixing is active in distributing suspended material.

Tonal patterns of the middle estuary indicate the tidal current was ebbing at the time of photography. This is in contrast to flood

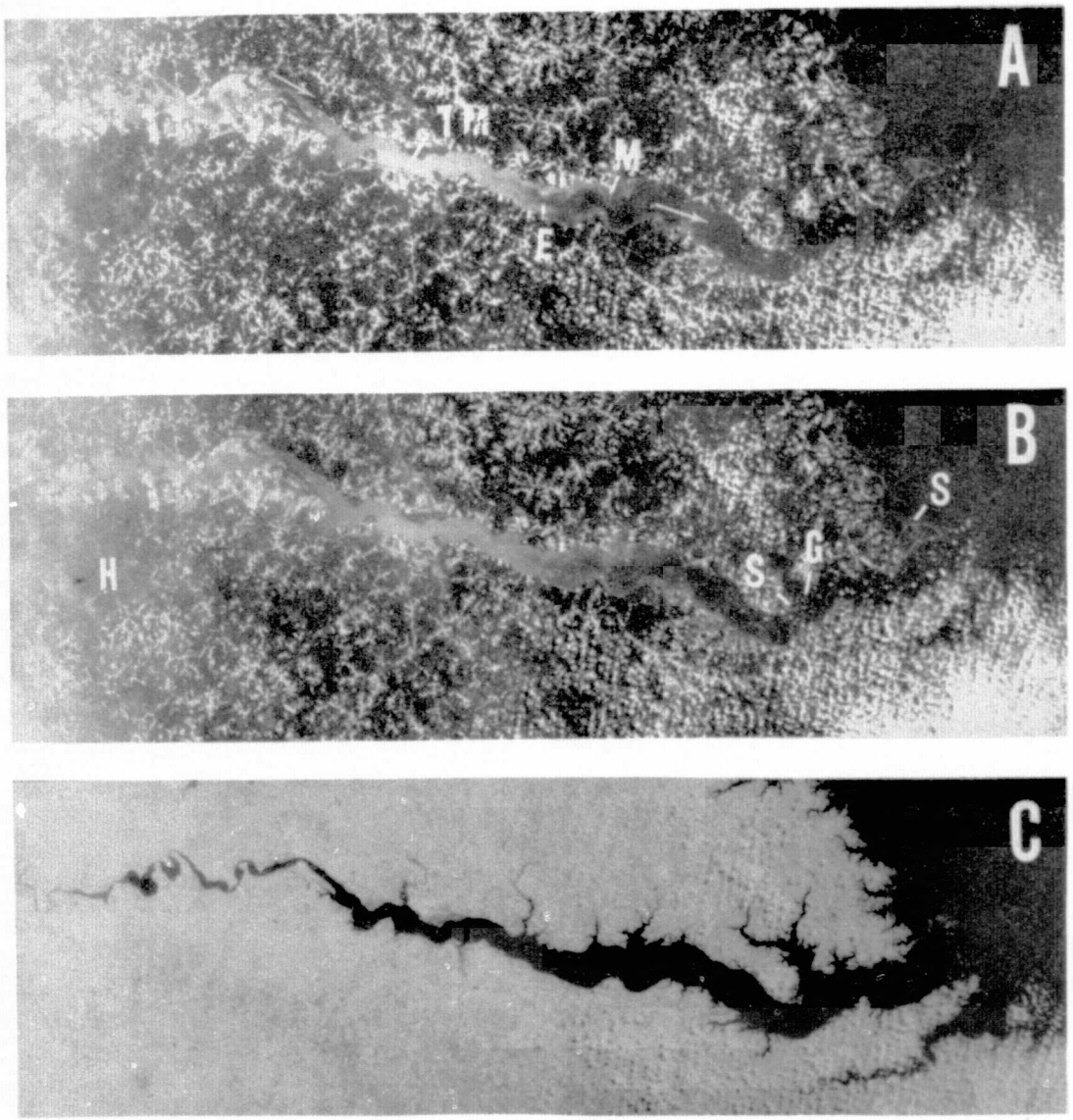

Figure 17. Reproductions of Skylab 2 imagery of the Rappahannock test site, June 12, 1973. A - red band; B - green band and C - black and white infrared. For explanation of letters, see text.

current given by the tide tables and based on the time recorded by the camera. This suggests that the recorded camera time is more than 6 hours in error. The photograph was most likely taken between 1400-1500 rather than 0801 local time (EDT).

6.3.2 Skylab 3, Rappahannock test site, (frames SL3-39-122, SL3-40-122 and SL3-86-299)

At the time these photos were taken, reportedly at 1209 EST, Sept. 12, 1973, a mild cold front was moving through the area from the west. Skies were partly cloudy and winds were light and variable. Large areas of surface water were flat calm. Tide currents were flooding fast at Tappahannock in the upper estuary whereas at the mouth and at the head (Port Royal) they were slack. River discharge at Fredericksburg was very low, less than 14 m^3 per sec. Consequently, sediment influx from the river was also very low and salinity of estuary water was higher than normal. Surface water of the lower estuary was colored dark red by a massive bloom of red tide.

The imagery records the shoreline configuration as well as tributary creeks, bordering marshes, sandy beaches and nearshore shoals around the mouth. The shoals, which are 1-2 m deep, are represented by light toned patterns off Windmill Point, Greys Point and Towles Point (s, Fig. 18). Elsewhere dark-toned patches in nearshore areas represent eel grass beds (g, Fig. 18). Spatial resolution is indicated by the Greys Point Bridge and superstructure which carries a two lane road about 22 meters wide (b, Fig. 18).

Water color is displayed by (1) dark red patches of red tide (rt, Fig. 18) throughout the lower estuary, (2) brownish-green

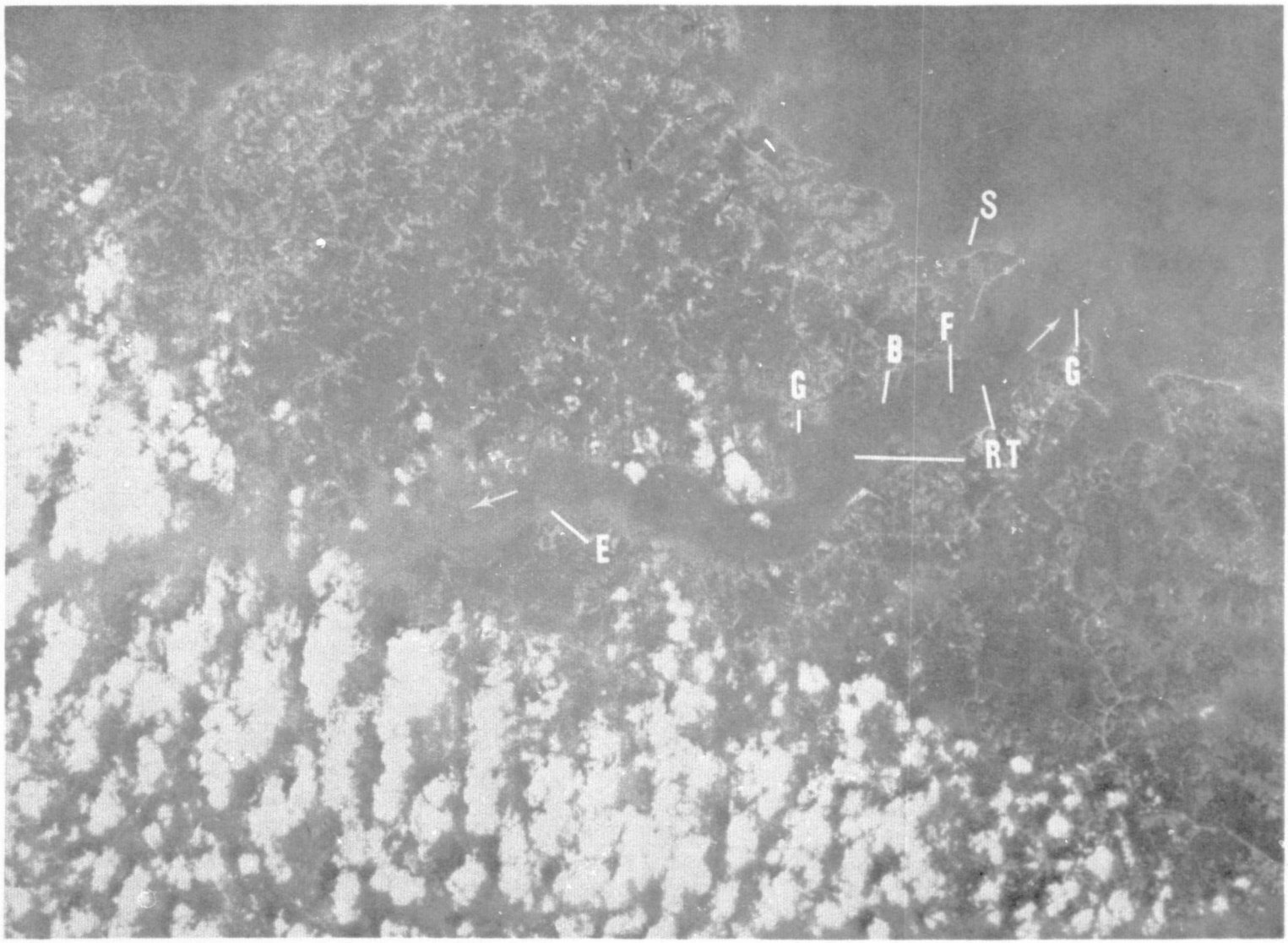

Figure 18. Skylab 3 natural color photograph of the Rappahannock Estuary, Sept. 12, 1973. For explanation of letter annotations, see text.

and bluish-gray bands in the upper estuary. The turbidity maximum is not visible. Instead the upper estuary is streaked by light and dark-toned bands with light bands over shoals and dark bands in the channel. The light-toned bands become wider and more predominate than the dark-toned bands with distance upstream. This is part of a broad tonal gradient from the river through the estuary.

In the lower estuary the red tides are represented by dark (red)-toned patches which intermingle with light-toned patches extending channelward as giant eddies from points of land (e, Fig. 18). At the mouth red tides occupy the center of a large counterclockwise gyre (g, Fig. 18). Such a spin indicates the tidal current is directed seaward (ebb) over the shoals faster than in the channel. Visual observations indicate the tide was slack close to the time of photography. Therefore, the gyre is most likely a relict feature generated by ebb tidal currents several hours prior to photography. Nonetheless, the feature indicates that large-scale lateral mixing is active in redistributing red tide plankton and other suspended materials.

At the time of photography more than ten menhaden fishing vessels 25-35 m long were operating in the lower estuary (f, Fig. 18). They were netting large schools of fish and at the same time discharging large volumes of fish oil, a pollutant, on the surface (Fig. 20). The oil spread over a broad area as a slick 4-6 km across and displaced upstream in the late flood current. However, neither the slick nor the fish schools and vessels are recorded by the photography.

The color boundaries observed on the water surface between bands of light and dark-toned water are largely recorded on the photos. They

are best displayed by the natural color film (Fig. 18) but also are recorded well on the red band film (Fig. 19A). They do not represent boundaries of water masses, but instead they display the fine-scale structure and transient mixing patterns of tidal currents that are active in the upper estuarine layer. The main boundary between water masses, the upper and lower estuarine layers, lies at mid-depth in the Rappahannock.

Of the four imagery bands displaying color patterns representing suspended material, the red band gives the best contrast. Most major patterns of suspended material are also recorded in the green band, but they are less distinct. This apparent degradation is probably caused by the masking effect of atmospheric haze. The difference in apparent water "penetration" between red and green band is very small since Secchi disk depths are largely less than 1.2 meters. The infrared band, 7-800 nm , displays suspended material only in zones of extreme turbidity in the Skylab 2 imagery (Fig. 17C).

By comparing the color and tone of estuarine water recorded in the June 12th imagery with color and tone in the September 12th imagery, changes in seasonal aspects are evident. For example, the turbidity maximum is displayed in the June imagery, a time of high inflow, sediment influx and strong river-estuarine convergence. By contrast in the same zone, the September imagery displays a broad gradient of seaward decreasing brightness broken by elongate bands. A red tide covers the lower estuary in September, but the same area is relatively clear in June. The tidal circulation is similar at each time, predominately flood in the middle and upper estuary. Despite the like conditions of current,

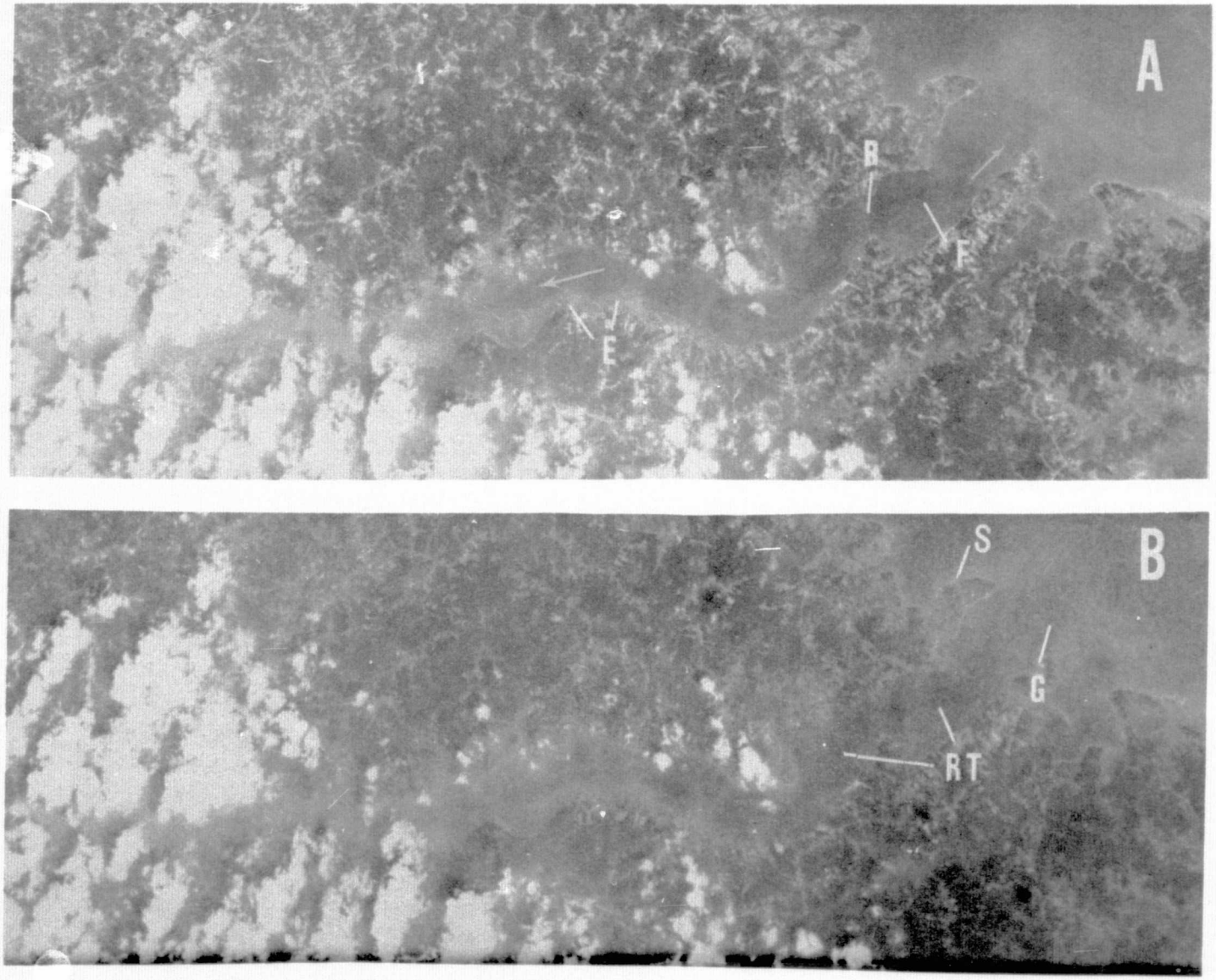

Figure 19. Reproductions of Skylab 3 imagery of the Rappahannock test site, Sept. 12, 1973. A. Red band, B. Green band. For explanation see text.

the dispersal patterns of suspended material vary widely. This may reflect different mixing conditions in the estuary, i.e. partly-stratified and well-mixed, but it most likely indicates errors in the time of photography. Nonetheless, the main seasonal phenomena, the turbidity maximum and red tide, are recorded quite well.

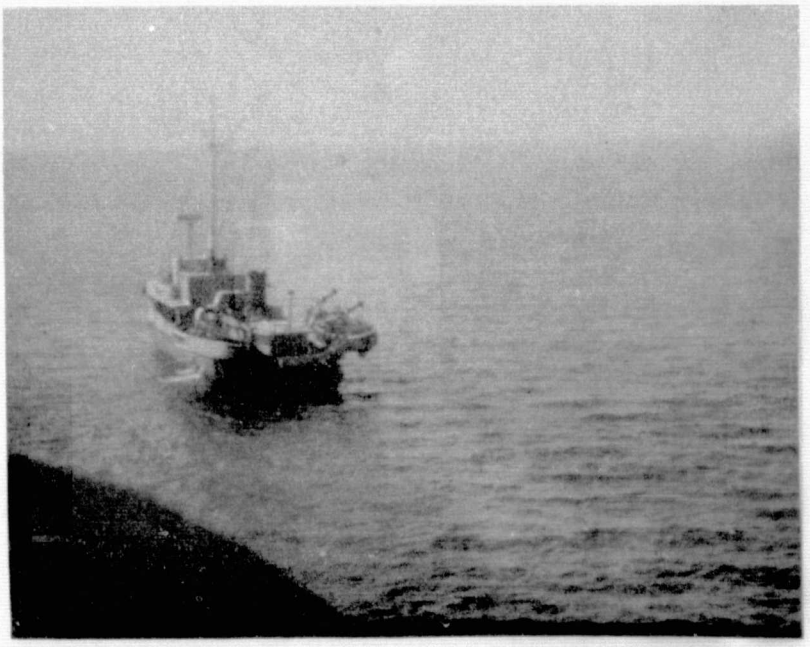

Figure 20. Near-surface view of menhaden fishing vessel the "Elenore M", discharging fish wastes that created large oil slicks, Sept. 12, 1973; view eastward in the lower Rappahannock Estuary.

6.4 Color mapping, delineation and analysis

The results of color slicing the S190B natural color image (SL3-86-299) into red, green and blue bands by an Optronics unit, are shown in Figure 21. Because of the character of the analysis and the wide slicing interval used, the charts delineate relative broad areas of colored water. All the charts show a trend of decreasing reflectance with distance seaward. The green band displays the greatest boundary detail in the lower estuary while the red band displays the greatest detail in the middle and upper estuary. The blue and green bands display an intertonging pattern in middle reaches whereby a band of relatively high density appears to intrude upstream along the northeast bank. This contrasts to a band of relatively low density that extends seaward along the southwest bank. This asymmetrical pattern grossly relates to the broad change in bottom geometry in this reach which consists of a channel (high density) and shoals (low density). This relationship is also apparent in red and green bands of the lower estuary whereby a relatively high density band occupies deeper waters of the channel and a low density band covers the shoals. The bands do not represent the bathymetry *per se* but are merely a surface reflection of turbidity patterns that generally follow the bottom topography like a

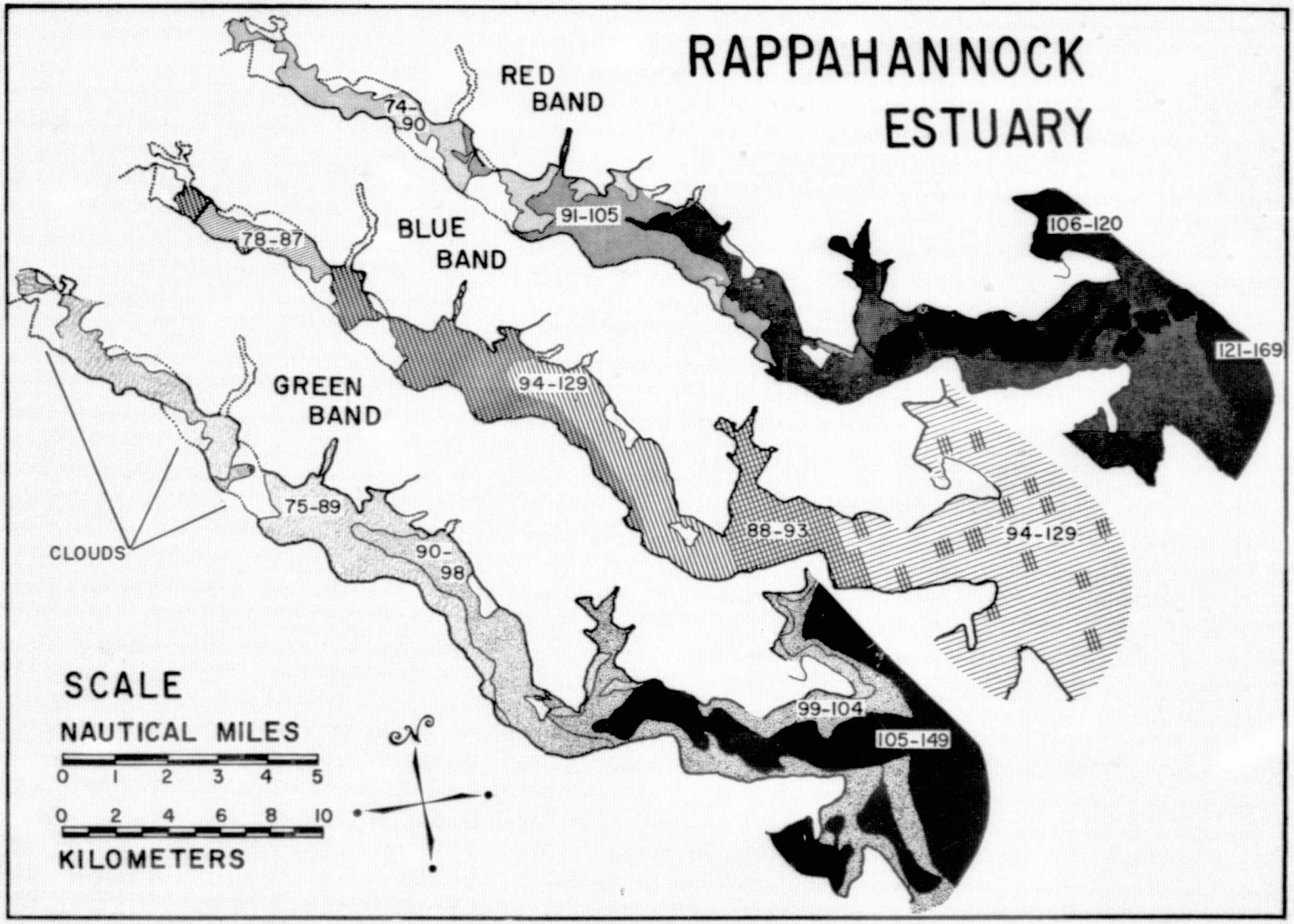

Figure 21. Water color charts of the Rappahannock Estuary, Sept. 12, 1973 developed from an Optronics gray map output of Skylab 3 imagery in 3 bands, red, green and blue. Values are relative Optronics density units.

"rolling carpet". The film density analyses fail to delineate patches of red tide although the patterns are readily visible in natural color transparencies (Fig. 18). This is because the red tide occurs as a mixture with sediment and other plankton and thus must have broad band spectral characteristics.

Results of scanning red, green and color infrared bands of the S190A imagery in Joyce-Loebl microdensitometer are shown in Figures 22, 23 and 24. All the color charts display more detailed patterns than the Optronics gray maps. The detail is also displayed in the cross profiles (insets of Figures 22, 23, and 24) which transect the charted patterns. Again, the broad trends of the profiles parallel the gross trends of the bottom topography. Both the broad trends, and many of the details, are often similar in each band though the magnitude of the fluctuation differs from band to band. The fluctuations are most pronounced in the red band. They represent a synoptic distribution of the turbid fine-structure and mixing patterns in near-surface water. Such patterns are shown in greater detail from results of scanning the natural color S190B image (SL3-86-299) at narrow density and spatial intervals in a Joyce-Loebl microdensitometer (Fig. 25).

Of the different densitometric units employed, the Data Color, Joyce-Loebl and Optronics, the Optronics gave the best results overall. The Data Color makes an excellent exploratory tool for visual displays of density patterns, but lacks spatial resolution and density control. The lack of precision in the Data Color is offset by the Joyce-Loebl microdensitometer which has good repeatability and affords accurate measurements of density. The film display and mounting table offer little

flexibility for aligning surface-truth station positions. The Joyce-Loebl generates density patterns in more detail than one can use for their evaluation in terms of surface truth. Its output displays a wealth of fine-structure in the water caused by rapid-changing conditions that are difficult to verify over broad areas by ground truth. By contrast the Optronics-WALDIPS system generates relatively "coarse" density patterns displaying major distributions of water color. By color slicing a single frame it offers registration, color and tonal control as well as repeatability.

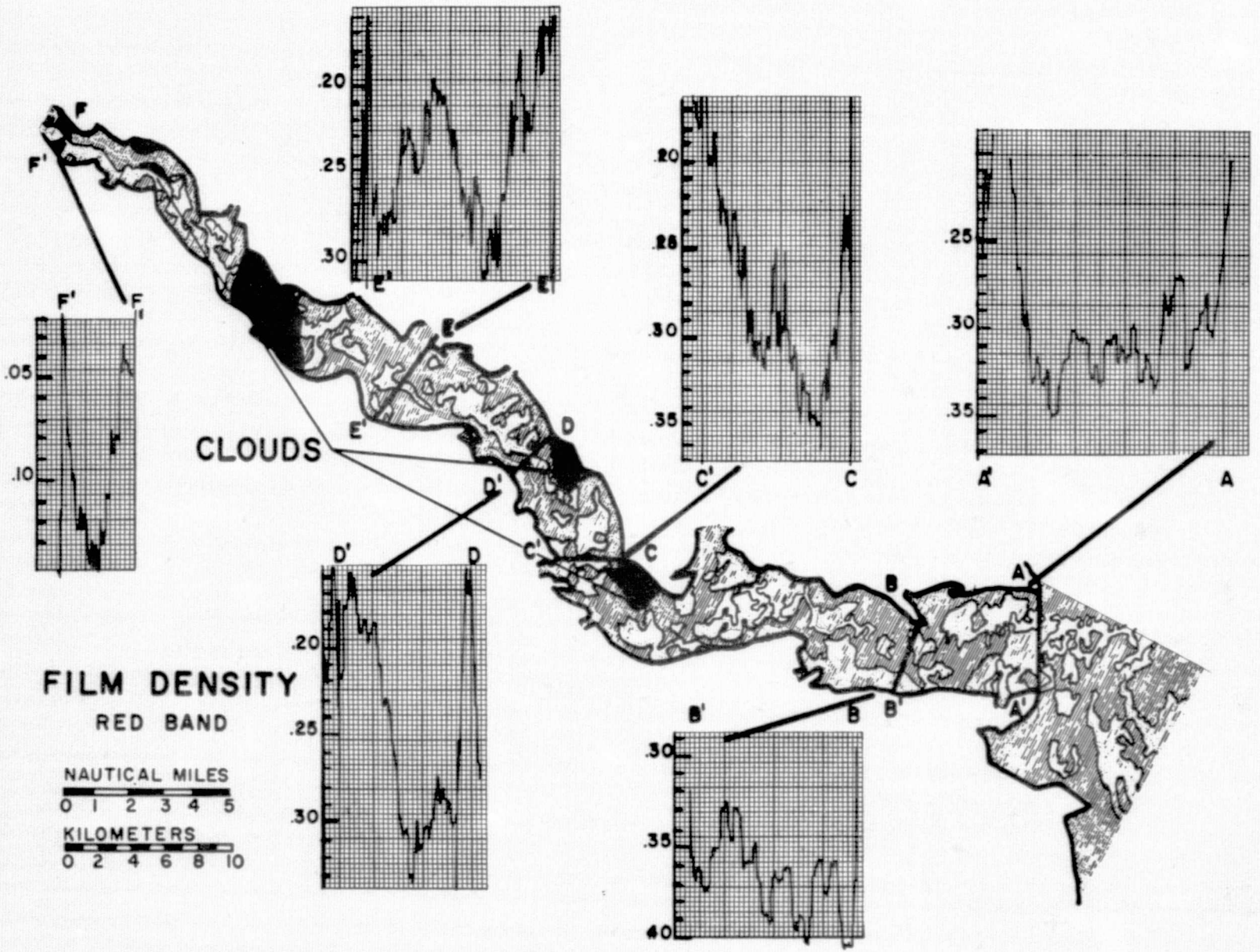

Figure 22. Water color distributions and cross profiles of the Rappahannock Estuary, Sept. 12, 1973, derived from red band film density plots of a Joyce-Loebl microdensitometer.

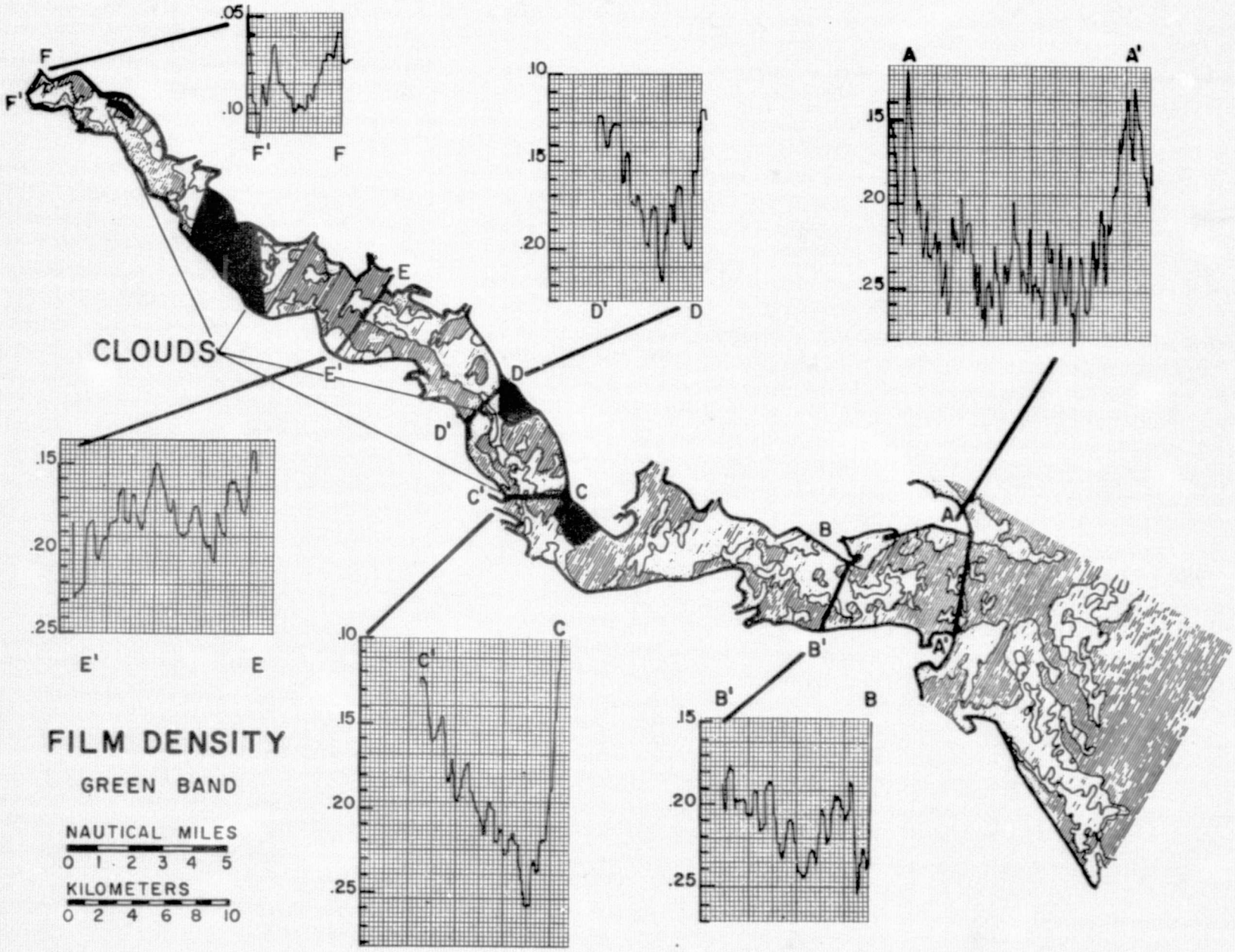

Figure 23. Water color distributions and cross profiles of the Rappahannock Estuary, Sept. 12, 1973, derived from green band film density plots of a Joyce-Loebl microdensitometer.

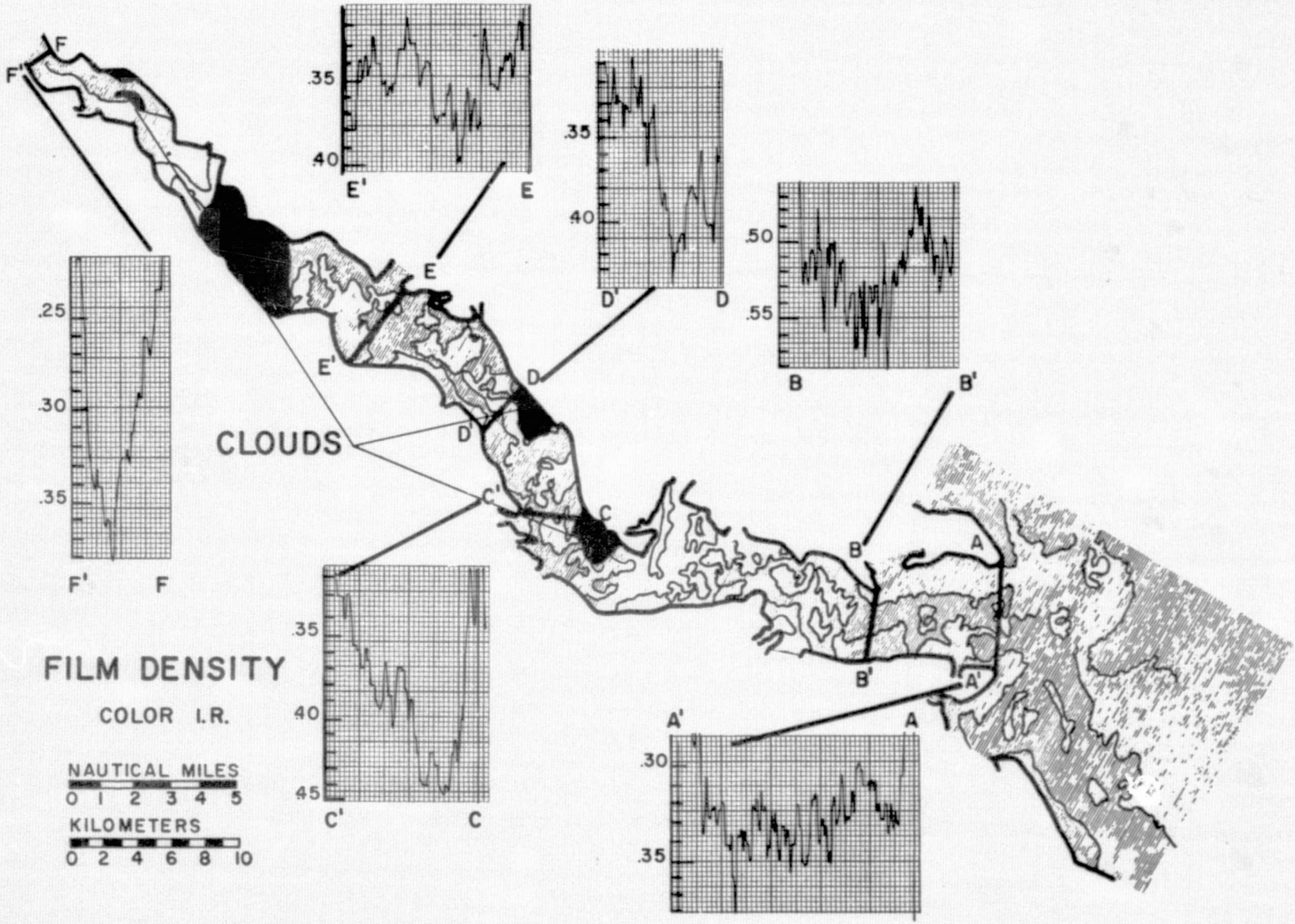

Figure 24. Water color distributions and cross profiles of the Rappahannock Estuary, Sept. 12, 1973, derived from color infrared film density plots of a Joyce-Loebl microdensitometer.

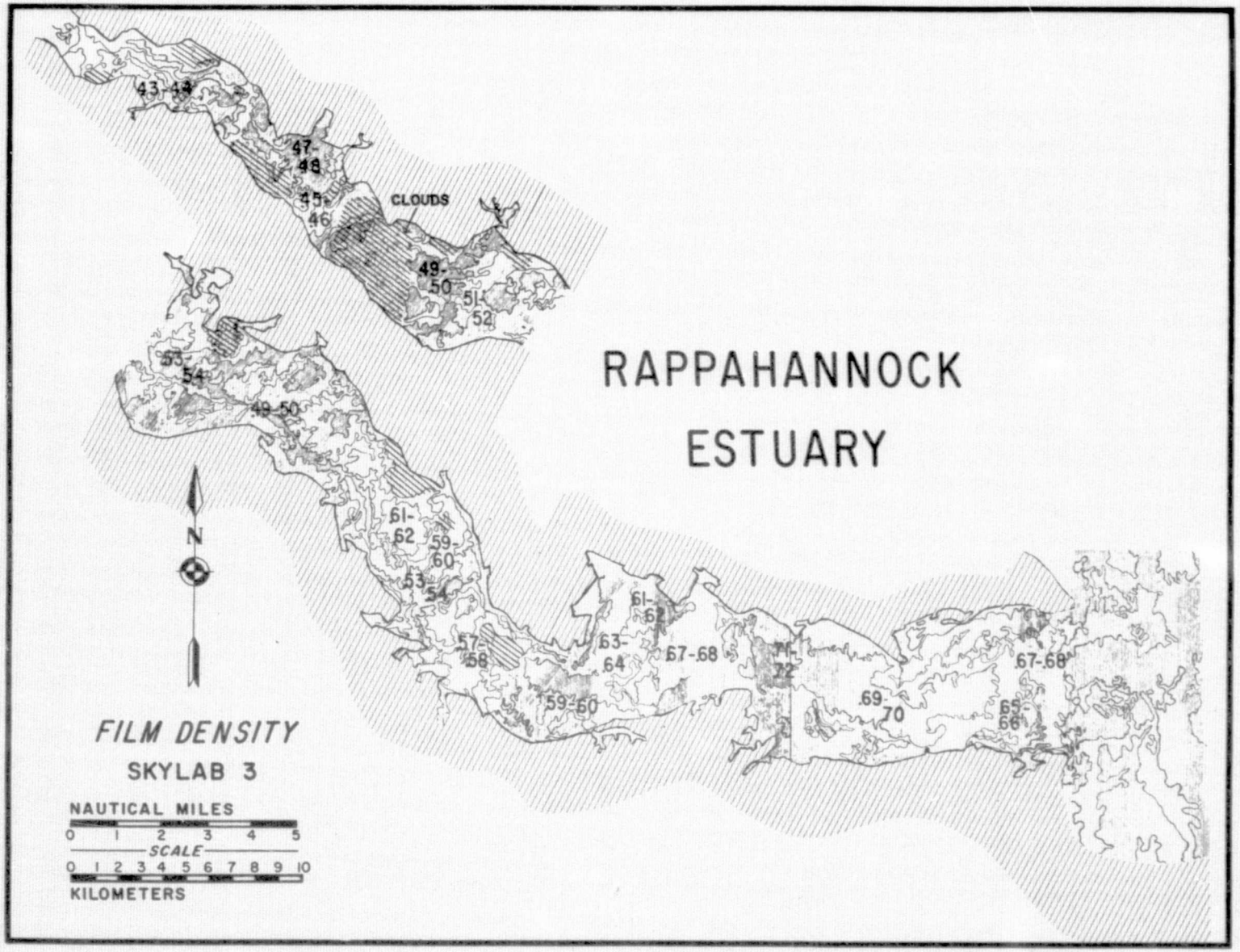

Figure 25. Water color distributions of the Rappahannock Estuary Sept. 12, 1973 derived from film density plots of natural color film in a Joyce-Leobl microdensitometer. Values are film density units.

7. IMAGERY - SURFACE TRUTH RELATIONSHIPS

The seaward gradient of suspended material is broadly reflected in a plot of total suspended concentrations versus salinity (Fig. 26). However, the relationship is not sufficiently close to be useful. The scatter is caused by suspended material supplied from the bottom, from the shores and the water itself (plankton) rather than from the river, which is the chief source of freshwater affecting salinity. Therefore, concentrations of suspended material do not relate to their source and dilution along the estuary length according to salinity.

When the optical log ratio (turbidity) is plotted against total suspended concentrations and disk depth (1/**D**) a very gross relationship is displayed (Fig. 27). The scatter is mainly due to the varying composition and particle size of the suspended material from place to place. Because of these variations, optical measurements indicate the suspended load only with broad limits (±25%).

In order to relate the film characteristics to the surface observations, film densities were determined for each surface station and the corresponding values were plotted. More than 50 scatter-plots were constructed, involving 5 measured surface parameters, 3 to 4 spectral bands and 3 different time intervals, i.e. before, after and during Skylab pass-over. The graphs suggest there is some degree of interrelationship between film characteristics and measured surface values, e.g. Figure 29.

Red band film densities derived from the Optronics gray map densities relate to optical ratios in the lower estuary during a period 30 minutes after Skylab pass-over, 1209-1239 EST (Fig. 29A). Elsewhere in the upper

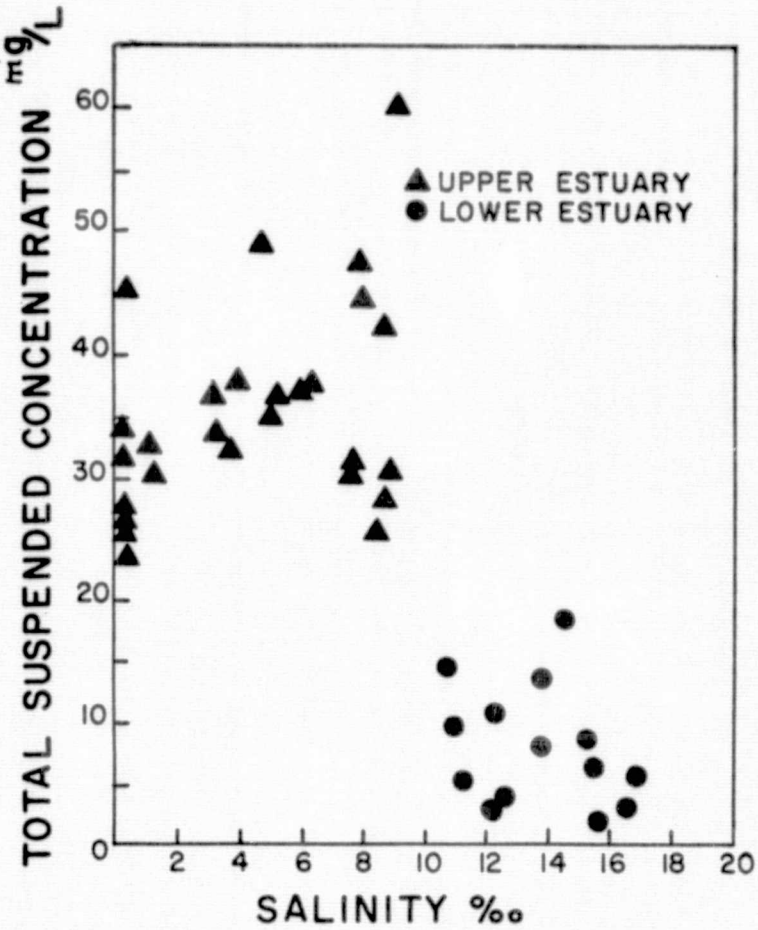

Figure 26. Scatter plot of total suspended material (sediment) versus salinity. From surface truth observations, Sept. 12, 1973 (Rappahannock Estuary).

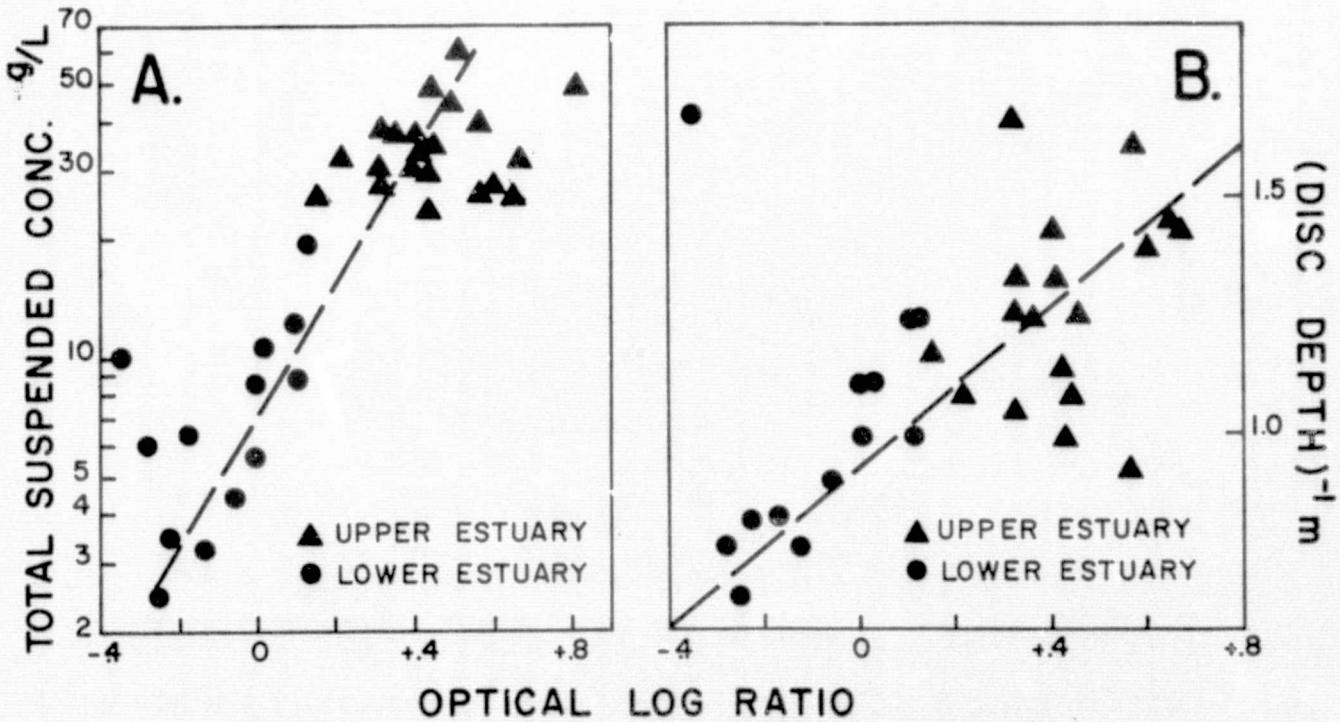

Figure 27. Relationship of optical log ratio (turbidity) to total suspended material (sediment) and disc depth (1/D); Rappahannock Estuary, Sept. 12, 1973.

estuary, and 30 minutes prior to passover (1139-1209 EST), there is a wide degree of scatter. Green band film densities also relate to phytoplankton cells per liter for a few stations in the lower estuary (Fig. 29C) but elsewhere and at different times, there is a wide degree of scatter. Figure 28 is a sample graph showing the results of an attempt to reduce the scatter plots, red band film densities derived from the Joyce-Loebl microdensitometer, were plotted against optical ratio (Fig. 29). This graph (Fig. 29) shows some promising results. At least a few points fall in line. However, the relation differs from one time to the next, ± 30 minutes of Skylab pass-over, though the slopes are similar. This demonstrates that film-surface truth relationships in the estuary are strongly time-dependent.

The wide degree of scatter is accounted for by several factors: (1) the time difference (30 minutes) between the time of surface observations and the time of photography, a time during which water characteristics change. Even with rapid sampling from helicopters it was not possible to cover the entire site simultaneously with photography. (2) possible differences between the position of the sampling point on the water and the corresponding position in the film. In a film with marked spatial variation, a slight error in positioning on the film can make a large change in the density values measured. (3) the difference between the size of sampling point on the water (.4 - .6 m^2) and the size of the sampling point in the film (which covers a ground area of 3-800 m^2 depending on spatial resolution). (4) The spectral bands are insensitive to the measured spectral qualities of the water. (5) Atmospheric haze affects the spectral distribution of light from the surface and thus distorted the true spectral quality of the water.

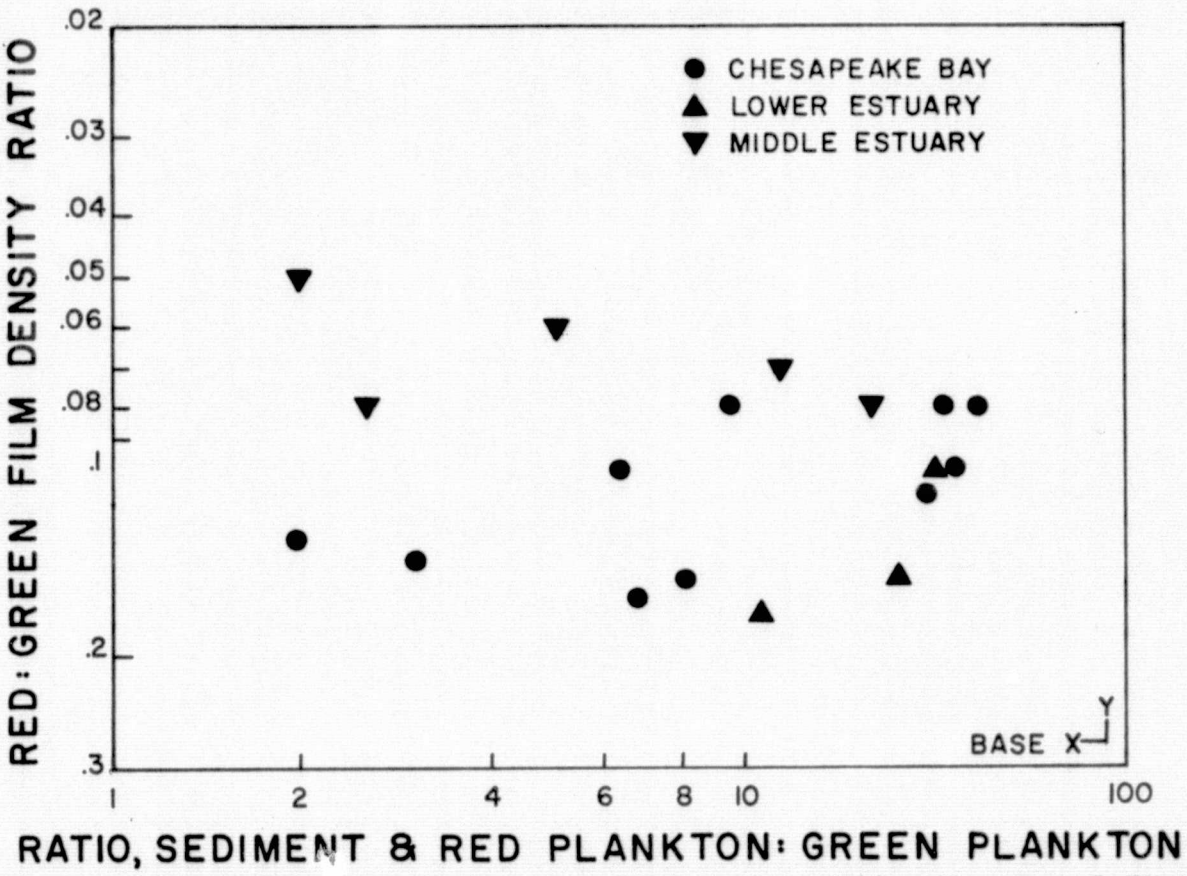

Figure 28. Scatter plot of red:green density ratio versus the ratio of sediment plus red plankton to green plankton. From Skylab 3 film and surface observations in the Rappahannock Estuary, Sept. 12, 1973.

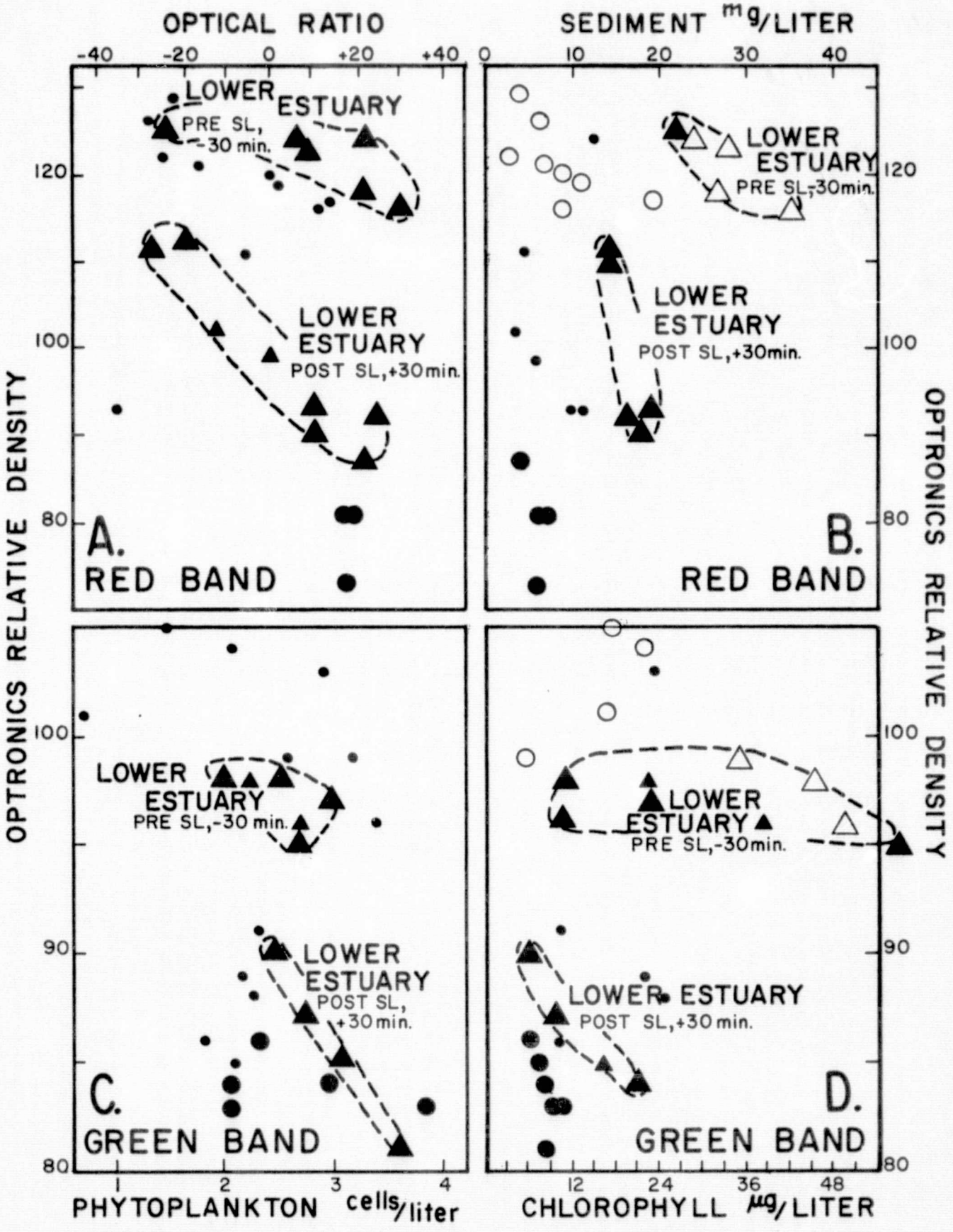

Figure 29. Relationships of Optronics relative density units in red and green band film to A. Optical ratio; B. Sediment (total suspended material); C. Phytoplankton and D. Chlorophyll. From Skylab 3 observations, Sept. 12, 1973.

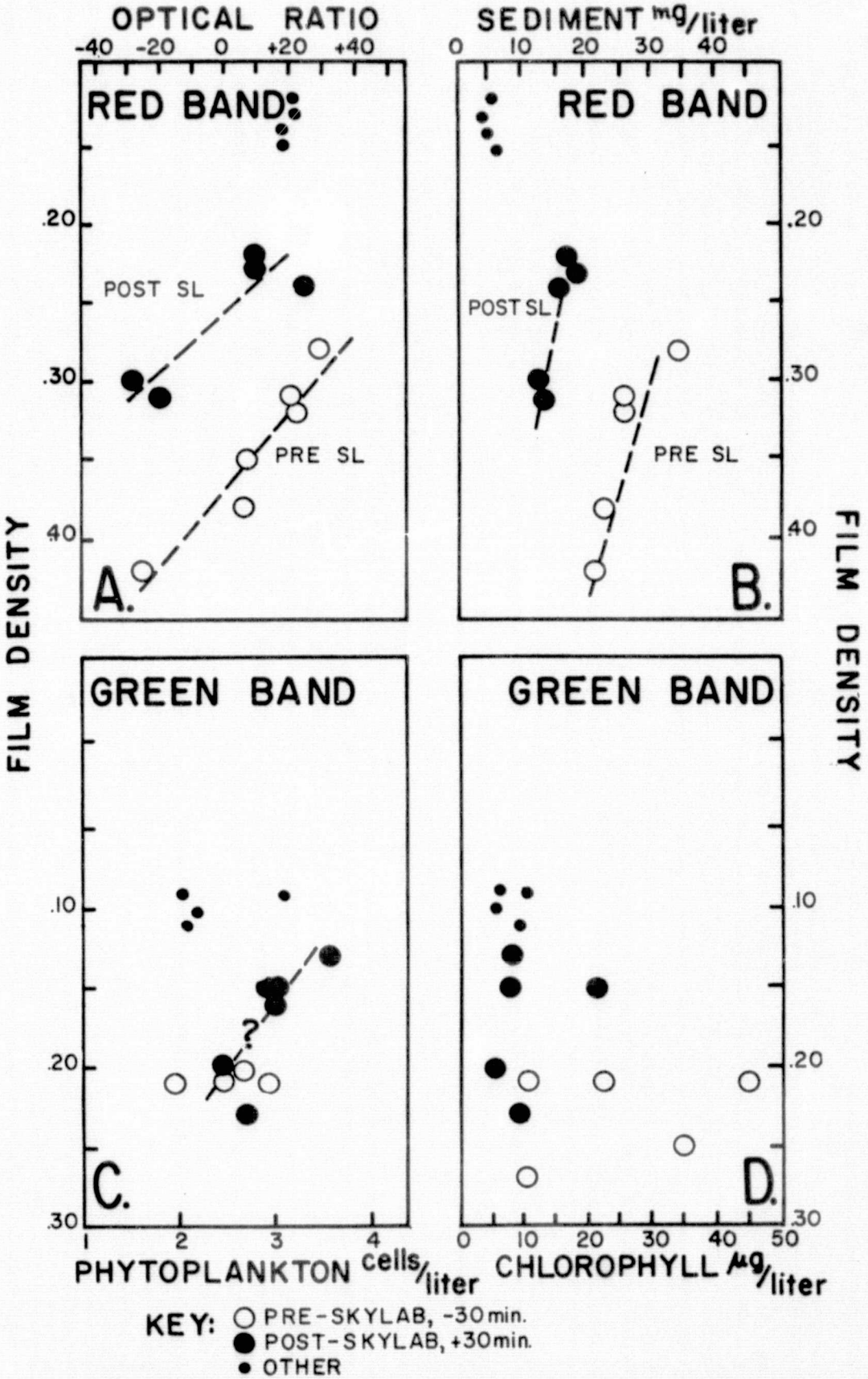

Figure 30. Relationships of film density derived from the Joyce-Loebl microdensitometer in red and green bands to A. Optical ratio, B. Sediment (total suspended material), C. Phytoplankton, D. Chlorophyll. From Skylab 3 observations, Sept. 12, 1973.

8. Surface, aircraft, satellite data evaluation

Aircraft and satellites both have characteristics that lend themselves to resource management. A comparison of Skylab multiband imagery with NASA high altitude (60,000 ft.) aircraft imagery of the Rappahannock test site taken between 1970-1974, shows the following advantages and limitations:

- Recurrent and sequential coverage at intervals of hours is desirable to record rapidly changing features of tidal environments. The Skylab orbit permitted coverage on a seasonal basis (3-4 months), however under cloud-free conditions coverage every 4-6 days may have been possible. On the other hand with aircraft flights, coverage intervals are easily linked to the temporal variations of the natural phenomena under study. It was not possible to exploit the intrinsic feature of satellites for acquisition of repetitive imagery in the present study.

- The high vantage point offered by Skylab cameras provided broad views of the entire site in a single frame. Thus, scenes are evenly lighted and well exposed so that water color could be mapped directly without corrections for color or tone distortions across the scenes. Aircraft coverage on the other hand, commonly contains dark corners and large changes of exposure in a run passing from land to water.

- The high satellite vantage point also provides a near orthographic view so that the imagery may be treated directly as a map without the need for rectification to minimize relief displacements. This is a great advantage over aircraft imagery which required rectifying many photos required to cover the same area. Thus, space imagery saves the cost of extensive data reduction and mosaicing. It provides a good base for comparative studies, frame to frame.

- Although the scale of space imagery is relatively small, it provides sufficient detail and resolution for mapping major water types and circulatory features. Until the fine-structural details of turbidity in estuarine water are understood in terms of resource management, there is no need for greater resolution such as provided by aircraft imagery. Boundary delineation of color water types on space imagery is satisfactory.

- The satellite imagery did not permit use of the stereo time-lapse technique to measure tidal currents, such as is commonly used with aircraft coverage.

- The savings which can be effected through use of space imagery in making resource evaluations is difficult to estimate. The cost of high altitude photos varies from about $5 to $15 or more per square mile. Once obtained, these photos can be used in a variety of ways including preparation of several different kinds of maps. Consequently the indirect savings may be much greater than the direct ones. Until it is known how many uses the photos or imagery will be put to, it is difficult to know how to prorate the cost of procuring them and of making maps of them. Then too, the larger and less accessible the area the greater the savings effected per unit area. Considering the global coverage of Skylab and its repetitive function, the cost per square mile prorated over a vast area would undoubtedly be much smaller for the satellite imagery than for aircraft imagery.

Surface observations and aerial-satellite imagery both have limitations and advantages for resource management. The following are among the important features:

- Aerial and space photographs do not eliminate the need for field work. Surface observations are required to determine the important third dimension of estuarine waters, depth. Vertical distributions are needed to determine salinity stratification, boundaries between major water masses, i.e. upper and lower layers, sediment profiles in relation to their bottom source and benthic habitats. Near-bottom observations are particularly important for sediment transport because sediment concentrations are typically high near the bottom. This is where the bulk of the load is carried.

  Nonetheless, photography is often very useful for planning surface observations. It is more useful in broad, well-mixed lagoons and bays than in stratified estuaries.

- The resolution of space photos is insufficient to accurately delineate many important features as grass beds, fish schools and oyster grounds. Until sensor to object relationships can be reliably established to consistently record natural phenomena, surface observations will be required.

- Whereas water color charts drawn from surface observations are necessarily based on a network of sampling points from which boundaries must be interpolated, the Skylab imagery allows direct delineation from a full field of color values.

- Space and aerial photos may rapidly become out of date. Natural phenomena are not static but everchanging. An image acquired at an earlier date may lead to fallacious conclusions as to the present nature or state of an area or phenomena.

9. UTILITY OF SKYLAB IMAGERY AS AN AID TO RESEARCH AND MANAGEMENT

The color of water such as represented in the green and blue bands, is often an index to productivity because of the coloration of phytoplankton pigments, namely chlorophyll, Ewing (1971). Lack of correlation between chlorophyll "a" measurements and corresponding film densities (e.g., Figs. 30C and D) precludes use of the present imagery as an index to production.

A variety of pollutants threaten the biological and recreational resources of the Chesapeake region. Pollutants like sewage, industrial discharges and heated effluents, affect the color or thermal characteristics of the water. However, large and illegal spills of fish oil and wastes discharged at the time of Skylab passover, could not be detected in the imagery. Evidently, the wavelength bands used were insensitive to the spectral characteristics of the oil. Major pollution sources were not detected in the Rappahannock imagery; none are known from surface observations.

Circulation in the Rappahannock, both tidal and net non-tidal circulation, is fairly well known and the flux of suspended sediment has been measured at more than 18 stations throughout the estuary.

Current observations and Skylab circulatory pattern are incomparable. Whereas the surface observations record the Eulerian flow, the imagery records the short-term line or direction of movement as displayed by optical characteristics. The imagery indicates where material may be going and it grossly indicates the load but it does not indicate how fast. The imagery patterns mainly represent short-term transient features of small-scale mixing. If steady state flow existed, an instantaneous photo would display circulatory patterns representative of the long-term predominate flow. Since water color is affected by many factors it cannot be used alone to define the circulation. Measurements by surface drogues, stereo-time lapse photography, dye patches and particle composition are also needed.

The imagery has good potential for classifying estuarine water quality according to color, turbidity or suspended load. These parameters are of importance to resource management in lakes and freshwater rivers where they determine suitability for irrigation, wildlife, recreation and aquatic life. The imagery should be of great utility for managing water quality as soon as water quality standards for color and turbidity are established in estuaries.

Although the Rappahannock is renowned for its rich resources of oysters and fish, the ecology of these organisms is poorly known in terms of water color or light energy. Their growth and reproduction is known mainly from surface observations and laboratory controls of temperature, salinity and oxygen. Since these parameters were not sensed by Skylab cameras it is difficult to directly relate the parameters sensed to the parameters affecting ecology. Mortalities

of oysters in the Rappahannock are mainly caused by excess freshwater of floods or by oxygen depletion. Red tides and sediment loads are important locally, but were not known to cause mortalities at the time of photography.

10. OPERATIONAL FEASIBILITY OF RESULTS AND APPLICATION TO WIDE AREAS

Real-time imagery is required for managing the rapidly changing qualities of coastal waters. Coverage taken at an earlier date (3 to 4 months) may be very useful as baseline information for comparing later coverage, but it is often obsolete for on-the-scene decisions.

Unlike major ocean areas, study of coastal regions requires temporal coverage on the order of minutes or hours. Therefore, most coastal applications, especially circulatory studies, are imaged best by aircraft or geostationary satellites. The combined effects of tide, cloud cover and sun angle limit the opportunities for Skylab-like imagery to only a few opportunities every 3 to 4 months. More static features as bottom topography and shorelines may well be monitored more frequently. To assess current movement consistently requires intense coverage 6 to 8 times during a tidal cycle of 12 ½ hours.

The operational feasibility of this study depended more on orbiting schedules and cloud conditions than on the occurrence of natural phenomena and need for management decisions. Skylab schedules did not permit repetitive coverage of time-dependent features in the test site.

Since aircraft overflights permit communication between ground-truth observers, coordination between observations and imagery is

strengthened. Communication also permits coverage of special features and transient events.

The acquisition of surface observations provides adequate control for charting color water types from the imagery, but the charts are valid only for the instant of photography. This is because water color and turbidity are constantly changing. This fact must be taken into account if surface truty-film density relationships are to be used in other estuaries or remote areas of the world. The relationships developed are believed to be good for a single water mass or water type. Nonetheless, natural phenomena like the turbidity maximum and red tides are common to other estuaries of the world and are recorded in other Skylab imagery. Water color boundaries of the 4 types described also are displayed and permit an interpretation of secondary circulation in remote estuaries.

11. CONCLUSIONS

1. Analysis of water color in the Rappahannock test site demonstrates utility of Skylab imagery for mapping water types that relate to transparency, turbidity and suspended sediment load. Analysis by an Optronics-WALDIPS system yielded the best water color charts.

2. Water color features, e.g. turbidity maxima and red tides can be detected and mapped in red and green band imagery or in natural color photography.

3. By using suspended material as a tracer of water movement, small-scale mixing patterns and local tidal currents are discerned. Large-scale color patterns indirectly reflect the bottom topography which is a source of suspended material. For another part they record a broad seaward decreasing gradient of suspended material from the river to the Bay.

4. Field and imagery studies revealed four types of water color boundaries which relate to convergence zones of secondary currents or to shear boundaries between different water types.

5. Skylab imagery is superior to aerial photography and surface observations for mapping water color. The high vantage point of space cameras provides near-orthographic views that are well exposed and evenly lighted. The full field of color in the imagery allows closer delineation of color boundaries than surface observations.

6. By providing a means for readily charting water color, Skylab imagery is of potential use for managing estuarine water quality. The imagery is a valuable contribution to the study of coastal processes.

11.1 REFERENCES CITED

Burgess, F. J., James W. P., 1971. Airphoto analysis of ocean outfall dispersion: Water Poll. Control Research Series No. 16070 ENS, 288 p.

Ciray, C., 1967. On Secondary Currents. Proc. 12th Congr. of the Intern. Assoc. for Hydraulic Res., Color. State Univ. V. 1, p 408-412.

Conrod, A., Kelly, M. and Boersma, A., 1968. Aerial photography for shallow water studies on the west edge of the Bahama Banks: Exper. Astronaut. Lab., M.I.T. Rept. RE-42 esp. p. 16-17.

Ewing, G.C., 1971. The color of the sea. In Oceans from Space, P.C. Badgley et. al. p. 46-49.

Keller, M., 1963. Tidal current surveys by photogrammetric methods. Photogrammetric: Engin. v. 29, p. 824-832.

Ichiye, T. and Plutchak, N.B., 1966. Photodensitometric measurements of dye concentration in the Ocean. Limnol. and Oceanography 2. p. 364-370.

Nelson, B.W , 1960. Clay mineralogy of the bottom sediments, Rappahannock River, Va. 7th Nat. Confr. Clay Minerals, p. 135-147.

Nelson, B.W., 1959. Transportation of colloidal sediment in the freshwater-marine transition zone. First Internat'l. Oceanogr. Congr. preprints, abstr. p. 640-641.

Nichols, M., 1971. "Ground truth" data for NASA Mission 144, VIMS data report. 22 p.

Nichols, M., 1973. Development of the Turbidity Maximum in a coastal plain estuary. Contr. Rept. AROD, 47 p.

Piech, R.R. and Walker, J.E., 1971. Aerial color analyses of water quality. A.S.C.E. Journal of Surveying & Mapping. SU2, p. 185-197.

Potter et. al., 1974. Summary of flight performance of the Skylab Earth Resources Esperiment Package, U.S. Govt. Printing Office 671-192, p. 1-44.

Ross, D., 1971. Color enhancement for ocean cartography: In Oceans from Space, P.C. Badgley et. al. editor, p. 50-63.

Strandberg, C. H., 1967. Comparative Analysis: Section 6, In Aerial Discovery Manual: John Wiley, New York, p. 61-65.

Vanoni, V. A., 1946. Transportation of Suspended Sediment by Water. Am. Soc. Civil Engin. Trans. V. 11, paper No. 2267, p. 67-132.

Waldichuk, M., 1966. Currents from aerial photography in coastal pollution studies: 3rd Intern. Conf. Water Pollution Res., Sec. III, Paper No. 13, 22 pp.

APPENDIX 12.1 Surface observations and data for southern Chesapeake Bay, May 31, 1973.

STAT. No.	TIME EST	DEPTH m	LAT.	LONG.	TEMP °C	SALIN. ‰	SED CONC mg/l	OPTICAL RATIO	SECCHI DISC m	SUSP'D COLOR	CHLOR "A" ug/l	PHYTO-PLANK cells/l	DISC DEPTH 1/Dm
1	10.9	0.0	37°48.7'N	76°44.7'W	[illegible]	[illegible]	10.55	+0.43	---	7.5Y/4	7.0	5.60	
2	11.1	0.0	37°49.1'N	76°44.2'W	24.9	9.04	30.59	+1.00	---	2.5Y/6	10.9	3.23	
3	11.2	0.0	37°49.6'N	76°43.9'W	24.1	8.04	7.83	+0.25	0.85	5Y/4	13.4	2.17	1.18
4	11.2	3.0	37°49.6'N	76°43.9'W	----	8.74		+0.94	---	2.5Y/6	8.3	----	
5	11.2	6.0	37°49.6"N	76°43.9'W	----	10.48	20.59	+0.80	---	2.5Y/4	10.2	----	
6	11.3	0.0	37°49.6'N	76°43.5'W	24.1	9.88	20.00	+0.88	0.65	2.5Y/4	16.3	1.01	1.54
7	11.4	0.0	37°50.1'N	76°43.4'W	24.2	9.24	25.63	+0.92	0.55	2.5Y/4	12.9	1.30	1.82
8	11.7	0.0	37°51.4'N	76°45.4'N	25.7	7.21	6.52	+0.18	0.85	5Y/4	8.0	2.04	1.18
9	11.8	0.0	37°53.6'N	76°46.9'W	25.8	5.94	6.59	+0.16	0.95	7.5Y/4	12.9	4.69	1.05
10	11.9	0.0	37°55.1'N	76°49.2'W	26.2	4.43	2.99	-0.02	0.95	7.5Y/4	5.9	2.34	1.05
11	12.0	0.0	37°55.9'N	76°51.1'W	25.9	3.12	5.82	+0.18	1.00	2.5Y/6	5.7	2.31	1.0
12	12.0	3.0	37°55.9'N	76°51.1'W	----	3.13	15.85	+0.62	----	2.5Y/4	11.9	----	
13	12.1	4.5	37°55.9'N	76°51.1'W	----	3.25	60.27	>1.0	----	2.5Y/6	10.8	----	
14	12.2	0.0	37°55.9'N	76°49.2'W	26.3	4.42	3.98	+0.22	0.90	7.5Y/6	10.2	2.04	1.11
15	12.4	0.0	37°53.6'N	76°46.9'W	26.1	6.70	5.76	+0.22	0.75	7.5Y/4	6.3	3.10	1.33
16	12.4	3.0	37°53.6'N	76°46.9'W	----	6.85	57.38	+0.56	----	7.5Y/6	36.6	----	
17	12.5	7.0	37°53.6'N	76°46.9'W	----	8.53	58.33	>1.0	----	2.5Y/6	20.6	----	
18	12.6	0.0	37°51.4'N	76°45.4'W	26.4	8.00	18.47	+0.18	0.95	5Y/4	10.4	3.67	1.05
19	12.8	0.0	37°50.1'N	76°43.4'W	26.0	9.52	27.65	+0.82	0.70	5Y/4	10.4	1.72	1.43
20	12.8	0.0	37°49.6'N	76°43.5'W	25.9	10.11	29.95	+0.72	0.75	5Y/4	8.2	0.80	1.33
21	12.9	0.0	37 49.6'N	76°43.9'W	26.3	9.24	36.04	+0.27	1.1	7.5Y/4	14.3	4.72	.91
22	12.9	3.0	37°49.6'N	76°43.9'W		9.47	30.32	+0.38	----	5Y/4	11.1	----	
23	12.9	6.0	37°49.6'N	76°43.9'W		10.56	27.06	+0.45	----	2.5y/4	6.0	----	
24	12.9	B+1	37°49.6'N	76 43.9'W		12.16	70.08	>1.0	----	2.5Y/4	7.5	----	
25	13.0	0.0	37°49.1'N	76°44.2'W	26.2	8.85	30.67	+0.40	0.70	5Y/6	6.3	2.28	1.43
26	13.1	0.0	37°48.7'N	76°44.7'W	25.5	8.68	28.48	+0.32	0.75	5Y/4	8.7	3.55	1.33
27	13.3	0.0	37°51.4'N	76°45.4'W	26.7	8.35	25.93	+0.15	0.85	7.5Y/4	7.4	4.32	1.18

Appendix 12.1 cont'd.

STAT. No.	TIME EST	DEPTH m	LAT.	LONG.	TEMP °C	SALIN. ‰	SED CONC mg/l	OPTICAL RATIO	SECCHI DISC m	SUSP'D COLOR	CHLOR "A"	PHYTO-PLANK cells/l	DISC DEPTH 1/D.m
28	13.4	0.0	37°53.6'N	76°46.9'W	26.3	7.47	30.85	+0.32	0.80	5Y/4	8.8	2.95	1.25
29	13.4	3.0	37°53.6'N	76°46.9'W	----	7.78	47.97	+0.82	----	2.5Y/6	11.9	----	
30	13.5	B+1	37°53.6'N	76°46.9'W	----	9.06	78.48	>1.0	----	2.5Y/6	12.9	----	
31	13.6	0.0	37°55.1'N	76°49.2'W	26.2	6.19	37.79	+0.32	0.95	5Y/4	15.4	1.82	1.05
32	13.8	0.0	37°55.8'N	76°51.2'W	26.1	3.74	38.04	+0.36	0.80	5Y/4	18.9	1.20	1.25
33	13.8	0.0	37°55.9'N	76°51.1'W	26.1	3.62	32.21	+0.22	0.85	5Y/4	7.1	2.60	1.18
34	13.8	3.0	37°55.9'N	76°51.1'W	----	4.52	49.22	+0.45	----	5Y/4	14.4	----	
35	13.9	B+1	37°55.9'N	76°51.1'W	----	5.31	108.94	>1.0	----	2.5Y/6	12.5	----	
49	13.9	0.0	37°56.2'N	76°50.8'W	26.2	5.12	36.72	+0.32	0.60	5Y/4	15.9	2.28	1.66
50	14.0	0.0	37°56.3'N	76°50.6'W	26.2	4.89	35.33	+0.45	0.80	5Y/4	12.5	----	1.25
51	14.1	0.0	37°55.1'N	76°49.2'W	26.1	5.86	37.42	+0.41	0.75	5Y/4	4.7	----	1.33
52	14.2	0.0	37°53.6'N	76°46.9'W	26.3	7.58	31.44	+0.67	0.70	5Y/6	24.2	----	1.43
53	14.2	3.0	37°53.6'N	76°46.9'W	----	7.84	44.62	+0.50	----	5Y/4	16.5	----	
54	14.3	B+1	37°53.6'N	76°46.9'W	----	9.00	60.56	+0.52	----	2.5Y/4	20.0	----	
55	14.4	0.0	37°51.4'N	76°45.4'W	26.8	8.60	40.23	+0.57	0.62	7.5Y/6	43.5	----	1.61

APPENDIX 12.2 Surface observations and data for the Rappahannock Estuary, Sept. 12, 1973.

STAT. No.	TIME EST	DEPTH m	LAT.	LONG.	TEMP °C	SALIN. ‰	SED CONC mg/l	OPTICAL RATIO	SECCHI DISC m	SUSP'D COLOR	CHLOR "A"	PHYTO-PLANK cells/l	DISC DEPTH 1/0m
R1	10.9	0.0	36°57.1'N	76°51.1'W	25.5	1.66	32.43	+0.47	0.96	5Y/4	6.8	12.06	1.04
R2	11.1	0.0	37°58.8'N	76°52.9'W	25.6	0.80	27.17	+0.56	1.00	5Y/4	5.4	2.25	1.00
R3	11.2	0.0	38°00.2'N	76°54.4'W	26.0	0.38	34.88	+0.62	0.82	5Y/6	broken	3.18	1.22
R4	11.3	0.0	38°03.2'N	76°55.2'W	26.5	0.07	33.57	+0.70	0.77	5Y/6	22.8	9.64	1.30
R5	11.3	0.0	38°04.9'N	76°57.1'W	26.5	0.06	30.22	+0.69	0.73	7.5Y/6	16.0	8.00	1.37
R6	11.4	0.0	38°05.8'N	76°59.5'W	26.4	0.06	32.02	+0.90	0.73	5Y/6	15.5	6.20	1.37
R7	11.5	0.0	38°06.3'N	77°02.4'W	26.4	0.06	54.63	>1.0	0.50	7.5Y/6	24.5	15.68	2.00
R8	11.6	0.0	38°08.8'N	77°03.3'W	25.5	0.06	37.82	>1.0	0.45	7.5Y/6	19.5	17.20	2.22
RA	11.7	0.0	38°06.3'N	77°02.4'W	26.4	0.06	54.35	>1.0	----	5Y/6	24.5	12.15	
RB	11.8	0.0	38°05.9'N	77°00.7'W	26.4	0.08	69.90	>1.0	0.52	5Y/6	39.1	21.88	1.92
R1	12.0	0.0	36°57.1'N	76°51.1'W	26.1	3.13	33.81	+0.42	0.88	5Y/4	7.1	1.07	1.14
R2	13.0	0.0	37°58.8'N	76°52.9'W	26.7	1.19	30.22	+0.43	1.00	5Y/4	6.4	3.14	1.00
R3	13.1	0.0	38°00.2'N	76°54.4'W	26.7	0.51	23.73	+0.44	0.92	5Y/4	5.7	1.48	1.09
R4	13.2	0.0	38°03.2'N	76°55.2'W	27.1	0.10	26.22	+0.57	1.07	7.5Y/6	18.1	11.19	.93
R5	13.3	0.0	38°04.9'N	76°57.1'W	27.4	0.06	27.85	+0.60	0.72	7.5Y/6	9.3	12.07	1.39
R6	13.4	0.0	38°05.8'N	76°59.5'W	27.3	0.06	26.47	+0.65	0.69	7.5Y/6	22.7	28.02	1.45
R7	13.4	0.0	38°06.3'N	77°02.4'W	26.4	0.05	34.48	>1.0	0.63	7.5Y/6	20.0	31.74	1.59
R8	13.5	0.0	38°08.8'N	77°03.3'W	26.4	0.06	31.65	>1.0	0.52	7.5Y/6	14.3	28.97	1.92
R9	13.6	0.0	38°09.3'N	77°07.3'W	25.5	0.06	45.32	----	0.55	7.5Y/6	25.5	33.83	1.82
RC	13.8	0.0	38°00.2'N	76°54.4'W	26.2	1.00	32.80	----	0.86	5Y/6	7.2	1.95	1.16
R2	13.9	0.0	37°58.5'N	76°51.9'W	25.6	3.02	36.99	----	0.75	5Y/6	7.7	??	1.33

Appendix 12.2 cont'd.

STAT. No.	TIME EST	DEPTH m	LAT.	LONG.	TEMP °C	SALIN. ‰	SED CONC mg/l	OPTICAL RATIO	SECCHI DISC m	SUSP'D COLOR	CHLOR "A"	PHYTO-PLANK cell/l	DISC DEPTH 1/0m
296	11.5	0.0	37°32.1'N	76°18.1'W	24.9	15.19	35.05	+0.30	0.4	7.5Y/4	63.6	2.67	2.5
299	11.6	0.0	37°34.4'N	76°15.5'W	25.4	14.99	26.44	+0.21	1.0	7.5Y/4	45.5	2.48	1.0
297	11.7	0.0	37°34.5'N	76°16.2'W	25.2	15.28	26.59	+0.22	1.1	7.5Y/4	10.8	1.96	.91
298	11.8	0.0	37°35.6'N	76°21.4'W	25.5	13.99	23.42	+0.06	1.0	7.5Y/4	22.4	2.96	1.0
301	11.8	0.0	37°35.6'N	76°21.4'W	----	14.12	28.90	+0.30	---	7.5Y/4	24.0	----	
300	12.0	0.0	37°35.9'N	76°20.9'W	----	14.06	-----	+0.08	---	------	34.7	----	
302	12.0	0.0	37°37.7'N	76°28.2'W	25.7	12.85	21.83	-0.25	1.3	7.5Y/4	10.2		.77
303	12.2	0.0	37°40.0'N	76°33.1'W	25.9	12.60	13.76	-0.28	1.2	10Y/4	9.3	2.72	.83
305	12.3	0.0	37°43.7'N	76°34.7'W	25.8	11.93	13.83	-0.20	1.2	10Y/4	5.5	2.44	.83
306	12.5	0.0	37°45.2'N	76°37.1'W	25.7	10.76	16.34	+0.25	0.8	7.5Y/4	7.2	3.66	1.25
307	12.5	0.0	37°48.1'N	76°41.7'W	25.5	10.56	17.86	+0.10	0.9	7.5Y/4	8.4	3.60	1.11
304	12.5	0.0	37°48.2'N	76°41.8'W	25.8	10.03	18.99	+0.10	0.9	7.5Y/4	21.0	2.93	1.11
260	13.0	0.0	37°33.6'N	76°10.6'W	25.5	16.94	6.02	-0.28	1.3	7.5Y/4	21.5	2.14	.77
263	13.0	0.0	37°33.7'N	76°10.8'W	25.5	16.52	3.45	-0.23	1.2	10Y/2	17.1	1.44	.83
261	13.2	0.0	37°33.7'N	76°15.6'W	25.5	15.67	2.45	-0.25	1.5	10Y/2	5.0	2.56	.67
269	13.3	0.0	37°37.8'N	76°15.6'W	25.5	15.55	6.31	-0.17	1.2	7.5Y/4	16.1	0.67	.83
266	13.4	0.0	37°33.9'N	76°16.3'W	25.5	14.50	19.32	+0.13	0.8	5Y/4	49.5	3.36	1.25
264	13.5	0.0	37°33.8'N	76°15.9'W	25.5	15.19	8.86	+0.11	1.0	7.5Y/4	22.9	2.88	1.0
262	13.5	0.0	37°34.1'N	76°15.9'W	25.5	14.60	10.60	+0.02	0.9	7.5Y/6	34.7	2.95	1.11
265	13.6	0.0	37°35.9'N	76°22.3'W	----	13.73	12.22	+0.10	0.8	7.5Y/6	38.1	2.68	1.25
268	13.6	0.0	37°35.9'N	76°22.2'W	25.6	13.78	8.47	0.00	1.0	7.5Y/4	22.4	2.22	1.0
271	13.7	0.0	37°36.9'N	76°31.7'W	25.6	12.54	4.39	-0.00	1.1	10Y/4	10.3	2.29	.91
284	13.9	0.0	37°43.2'N	76°35.3'W	25.6	12.23	11.05	-----	0.6	7.5Y/4	16.0	2.08	1.67
285	14.0	0.0	37°43.2'N	76°35.1'W	25.5	12.12	3.22	-0.13	1.3	10Y/4	22.2	2.15	.77
291	14.2	0.0	37°46.2'N	76°39.4'W	26.6	10.97	10.05	-0.35	0.6	7.5Y/4	10.3	1.80	1.67
294	14.3	0.0	37°46.4'N	76°39.1'W	27.0	11.22	5.58	0.00	0.9	7.5Y/4	24.5	2.25	1.11

APPENDIX 12.3 Film density values for Skylab 3
Rappahannock River Estuary, Sept. 12, 1973.

		Joyce - Lobel					Optronics		
Sta. Code	Time	N.C.	C.I.R.	Red	Green	Red;Green	Red	Green	Red;Green
		absolute densities					relative densities		
296	11.5	.62	.34	.28	.08	.08	116	95	20
299	11.6	.64	.30	.31	.21		118	98	24
297	11.7	.64	.35	.32	.21	.11	123	98	26
298	11.3	.63	.36	.38	.21	.17	124	97	28
300	12.0	.65	.36	.35	.25		123	99	26
302	12.0	.60	.36	.42	.27	.15	125	96	26
303	12.2	.61	.41	.30	.23	.07	111	87	17
305	12.3	.60	.39	.31	.20	.11	110	90	17
306	12.5	.55	.36	.24	.16	.09	92	85	8
307	12.5	.51	.33	.22	.16	.09	90	81	2
304	12.5	.51	.35	.23	.21	.08	93	84	4
260	13.0	.72	.39	.35	.20	.15	126	104	22
263	13.0	.68	.38	.35	.19	.16	129	105	26
261	13.2	.69	.36	.34	.21	.13	122	99	29
269	13.3	.69	.37	.37	.23	.14	121	101	20
266	13.4	.53	.35	.29	.22	.07	117	96	19
264	13.5	.56	.34	.27	.17	.10	116	103	16
262	13.5		.32	.27	.19	.08	119	99	19
265	13.6	.69	.36	.37	.27	.10	124	96	28
268	13.6	.67	.37	.34	.24	.10	120	98	25
271	13.7	.62	.46	.31	.23	.08	111	91	20
284	13.9	.50	.33	.78	.14	.14	93	85	6
285	14.0	.54	.34	.23	.18	.05	102	89	13
291	14.2	.50	.39	.23	.15	.08	93	86	8
294	14.3	.53	.37	.26	.18	.08	99	88	15
8	11.7		.34	.17	.11		81	84	-2
11	12.0		.38	.14	.10		73	86	0
14	12.2		.34	.15	.09		87	83	2
15	12.4		.30	.15	.09		81	83	0
18	12.6		.31	.17	.09				
83	11.1		.33	.10	.09				
84	11.2		.30	.07	.06				

APPENDIX 12.4 Surface observations and data for the Rappahannock Estuary, June 13-14, 1974

STAT. No.	TIME EST	DEPTH m	LAT.	LONG.	TEMP °C	SALIN. ‰	SED CONC mg/l	OPTICAL RATIO	SECCHI DISC m	SUSP'D COLOR	WATER COLOR % Reflect. 500	600	700	SUN SCALE	MEAN SIZE μ	DISC DEPTH 1/0m
298	1050	0	37°43.8'	76°23.0'		11.687	5.6	- .28	2.0	10y/4	.08	.12	.14	30	7.4	0.5
302	1130	0	37°42.1'	76°28.7'		10.913	6.0	- .18	1.7	7.5y/4	.16	.26	.22	100	8.0	0.6
303	1225	0	37°40.3'	76°33.1'		10.274	3.0	- .13	1.7	10y/4	.48	.60	.64	100	6.3	0.6
305	1245	0	37°43.4'	76°34.5'		9.466	6.5	- .16	1.6	10y/4	.43	.61	.60	100	5.4	0.6
306	1306	0	37°45.7'	76°36.8'		8.291	8.0	+ .27	1.0	7.5y/6	.38	.53	.45	100	4.4	1.0
307	1330	0	37°46.4'	76°39.8'		7.658	7.0	+ .05	1.1	5y/4	.30	.46	.21	100	4.4	0.9
213	1350	0	37°48.7'	76°42.8'		6.116	14.5	+ .55	0.7	7.5y/4	.28	.42	.21	100	4.1	1.4
252	1450	0	37°49.6'	76°44.0'		5.205	14.0	+ .42	0.6	7.5y/4	.20	.26	.20	100	4.5	1.7
188	1510	0	37°51.4'	76°45.4'		3.[illegible]	10.5	+ .37	0.6	5y/4	.20	.27	.24	100	4.5	1.7
9	1525	0	37°53.7'	76°46.1'		3.114	14.5	+ .59	0.5	5y/4	.20	.26	.19	100	5.1	2.0
10	1600	0	37°55.0'	76°49.3'		1.795	16.0	+ .68	0.5	5y/4	.21	.24	.16	100	5.8	2.0
33	1050	0	37°55.9'	76°51.1'		3.555	12.5	+ .53	0.7	5y/4	.20	.26	.22	100	5.4	1.4
R1	1112	0	37°57.9'	76°51.6'		2.175	9.5	+ .40	0.6	7.5y/4	.21	.25	.20	100	5.4	1.7
RC	1140	0	38°00.4'	76°54.4'		.282	15.0	+ .62	0.5	5y/4	.23	.22	.20	100	5.2	2.0
R4	1203	0	38°02.9'	76°55.1'		.082	18.0	+ .78	0.5	5y/4	.26	.30	.24	100	---	2.0
R6	1245	0	38°05.1'	76°58.5'		.123	13.5	+ .75	0.5	7.5y/4	.51	.66	.43	100	5.9	2.0
R7	1330	0	38°05.1'	77°01.4'		.055	15.5	+ .55	0.5	7.5y/4	.16	.22	.20	100	7.2	2.0

VIRGINIA INSTITUTE OF MARINE SCIENCE

Gloucester Point, Virginia 23062

SKYLAB MSS vs. PHOTOGRAPHY FOR ESTUARINE WATER COLOR CLASSIFICATION PART II

Final Report for NASA Contract NAS 6-2327

Skylab EREP Number 602647(517)

Virginia Institute of Marine Science

William J. Hargis, Director

David Oberholtzer, Ph.D.
NASA-Wallops Flight Center
Technical Monitor

Report Prepared By
Hayden H. Gordon
Maynard M. Nichols
Va. Inst. of Marine Science

TABLE OF CONTENTS

ACKNOWLEDGEMENTS

The authors wish to express their gratitude to personnel at LARS, especially to Mr. F.E. Goodrick, for many helpful suggestions pertaining to the computer classification. We appreciate the use of the computer terminal at NASA Wallops Flight Center and that at NASA Langley Research Center.

A critical review by Dr. J.D. Oberholtzer of NASA Wallops and several excellent typescripts by Cindy Otey are gratefully acknowledged.

INTRODUCTION

On September 12, 1973 at 12:09 EST, the Skylab III satellite passed over the Chesapeake Bay and sensed energy containing information about a large section of the estuary. On the same day scientists from the Virginia Institute of Marine Science simultaneously gathered data in the Rappahannock River, a tributary of the Bay, to determine the physical characteristics of the surface water. Although the satellite contained many sensors in the Earth Resources Experiment Package (EREP), of most interest were those sensing reflected energy in the visual and near infrared spectral region, and thermally emitted radiation. The photographic equipment consisted of a bank of 6 boresighted cameras with 6-inch (152 mm) focal length matched lenses (S190A), and one high resolution camera with an 18-inch (457 mm) focal length lens (S190B). The S190A sensors were loaded with black and while film filtered to record energy in the green, red, and two reflective infrared bands, color film, and color infrared film. The S190B camera used natural color film.

The imagery was analyzed by densitometry, by pattern analysis, and by comparison of photo density and ground truth. Spectral characteristics of the scenes were derived from selected individual bands of filtered B & W film as well as from color separations of color and color infrared film. Procedural details and results are presented in a final report for NASA contract NAS6-2327, "Southern Chesapeake Bay Water Color and Circulation Analysis", 1975.

Remote sensing of the Rappahannock test site from Skylab also included multiband coverage from a multispectral scanner (S192) operating in 13 narrower regions of the EM spectrum from visual, through reflective infrared, to the thermal infrared. The output in digital form not only enabled better spectral resolution than photography, but allowed the determination of water "type" signatures by making use of simultaneous multiband, registered data and classification algorithms. The LARS (Laboratory for Applications of Remote Sensing) computer classification system located at Purdue University in Indiana was used because two LARS terminals were available at nearby NASA centers.

Because estuarine water continually changes color with the tide from place to place at any given instant, an unsupervised computer classification was run whereby the "system" decided the proper number of spectrally distinct classes and the distribution of each class in the scene. A philosophy of overclassification and recombination was used in order to characterize the data and to allow close examination of spectral attributes.

To compare the classification derived from narrow band multispectral data with the broad band photography, a classification was performed using color film from the S190B camera, digitized with an automatic scanning microdensitometer. Choice of color film included blue band (.4-.5 μm) spectral information although with considerable loss of the land-water discrimination capability of the near-infrared.

COVERAGE AND SENSOR OPERATION

The area covered by the S190B frame and the MSS S192 scanner over the test site is shown in Figure 1. The Earth Terrain Camera (S190B) covers its outlined area at one instant in time, whereas the MSS scans conically line by line and uses the forward motion of the satellite to make a continuous record of information. Data from the MSS, which was recorded on magnetic tape, was initially reformatted to remove curved scan lines thus making a LARS compatible data set with new scan lines normal to the satellite ground track. In the process the calibration at the end of each original scan line was lost. Color film (Kodak SO-242) loaded in the Earth Terrain Camera had a demonstrated ground resolution of approximately 13 meters (40 feet), and spectral coverage of .4-.7 μm over a square area 109 km (59 n. mi.) on a side. The MSS spectral coverage is shown in Table I. The instantaneous field of view (IFOV) on the ground was a 79 m (260 feet) square and thus is the limiting factor on resolution. The EREP Sensor Performance Evaluation Final Report (1975) indicates essentially nominal operation of the MSS on SL III with the exception of bands 1, 13, and 14 which are discussed in the report.

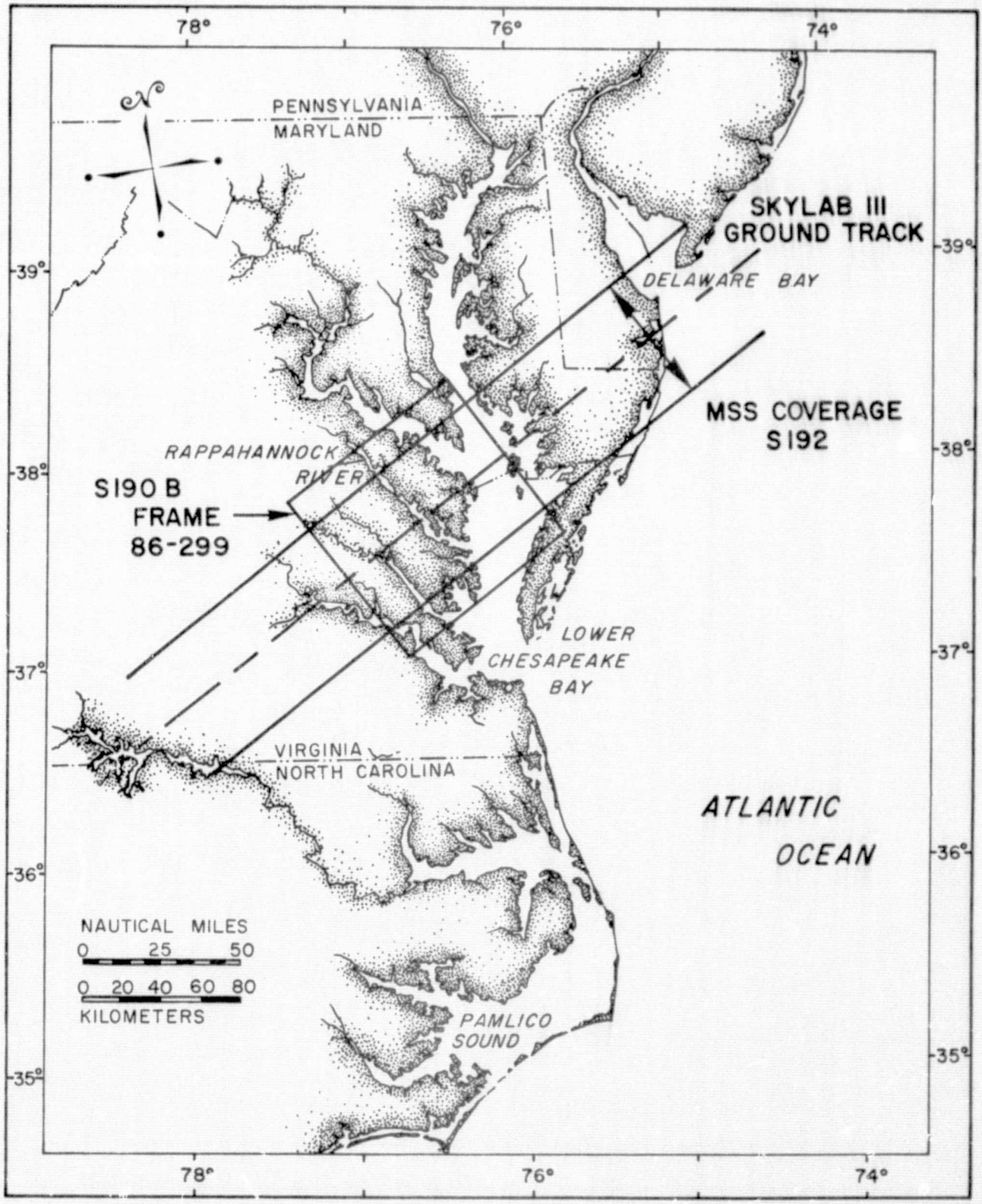

Figure 1. Location of the Rappahannock Estuary test site in the Chesapeake Bay region. Lines show Skylab III ground track and coverage area of MSS (S192) and S190B.

TABLE I

MSS SPECTRAL RESPONSE

Band	Wavelength Band*(μm)	Color Response
1	.42 - .45	Blue[2]
2	.45 - .50	Blue[2]
3	.50 - .55	Green[2]
4	.54 - .60	Green - Red[2]
5	.60 - .65	Red[2]
6	.65 - .73	Red (to approx. .68)[2]
7	.77 - .89	Reflective Infrared
8	.93 - 1.05	Reflective Infrared
9	1.03 - 1.19	Reflective Infrared
10	1.15 - 1.28	Reflective Infrared
11	1.55 - 1.73	Reflective Infrared
12	2.10 - 2.34	Reflective Infrared
13/14[1]	10.07 - 12.68	Thermal Infrared

* Based on band width at ½ power points

[1] Redundant data with slightly different calibration

[2] Color film emulsion layer affected

The Rappahannock Estuary

The Rappahannock Estuary is one of nine major estuarine tributaries to Chesapeake Bay. Like the Potomac and the James Estuaries, it is narrowly funnel-shaped and relatively shallow, less than 5 meters deep on the average except for the axial channel which is 8 to 23 meters deep. A submerged sill at the mouth, 9 meters deep, partly deters inflowing water from the Bay so that the estuary is dominated by the river.

The Rappahannock offered several advantages for study of EREP data. Its configuration is relatively straight and bottom geometry is simple. Water properties, namely salinity and suspended sediment concentrations, gradually change seaward along the estuary length as part of a broad gradient. Local tributaries that drain into the estuary supply freshened water from different sources. However, the estuary is relatively undisturbed by major engineering works and it is relatively free from pollution except for the duck farm effluent near Urbanna which is largely contained in ponds. The estuary is renowned for its oyster production. The chief advantage of this estuary as a test site is that its turbid waters and circulation are well known from previous field studies (Nelson, 1959, 1960; and Nichols, 1972) as well as from numerous NASA photographic overflights since 1968 (e.g. Nichols, 1971). Such information provided substantial baseline control and a predictive understanding of use for analyzing the surface truth. Figure 1 shows the Rappahannock Estuary in its geographic setting

of the Chesapeake region. Figure 2 shows the Rappahannock River in more detail, and includes distance upstream for later reference.

The chief movement of water in the estuary is produced by the tide. Waves are important on shoals during short periods of high wind. The tide range is 70 cm on the average and currents vary from nearly zero at slack water to more than 30 cm per sec at maximum current over a period of 3 hours. Such currents cause intensive mixing of fresh and salty water. Velocities are capable of scouring soft bottom muds and supporting particulate material in suspension more than 50 percent of the time.

The mean tidal current diminishes with distance seaward from 35 cm per second in middle reaches to 14 cm per sec near the mouth. This trend follows the seaward increase in cross-sectional areas as the estuary deepens and widens toward the mouth. But in the upper estuary mean velocities are relatively uniform along the estuary channel from 30-35 cm per sec. Consequently, the transporting capacity of the current is also relatively constant through the upper estuary between 48 and 40 km above the mouth. Because the time of slack waters varies along the estuary length the current speed at any one time, such as captured by an instantaneous photograph, also varies. When the current is slack at the mouth it is maximal in the upper estuary near Tappahannock.

River inflow averages 45 m^3 per sec on the average at Fredericksburg. At the time of EREP photography in early June 1973 a small freshet of about 336 m^3 per sec flowed through the estuary,

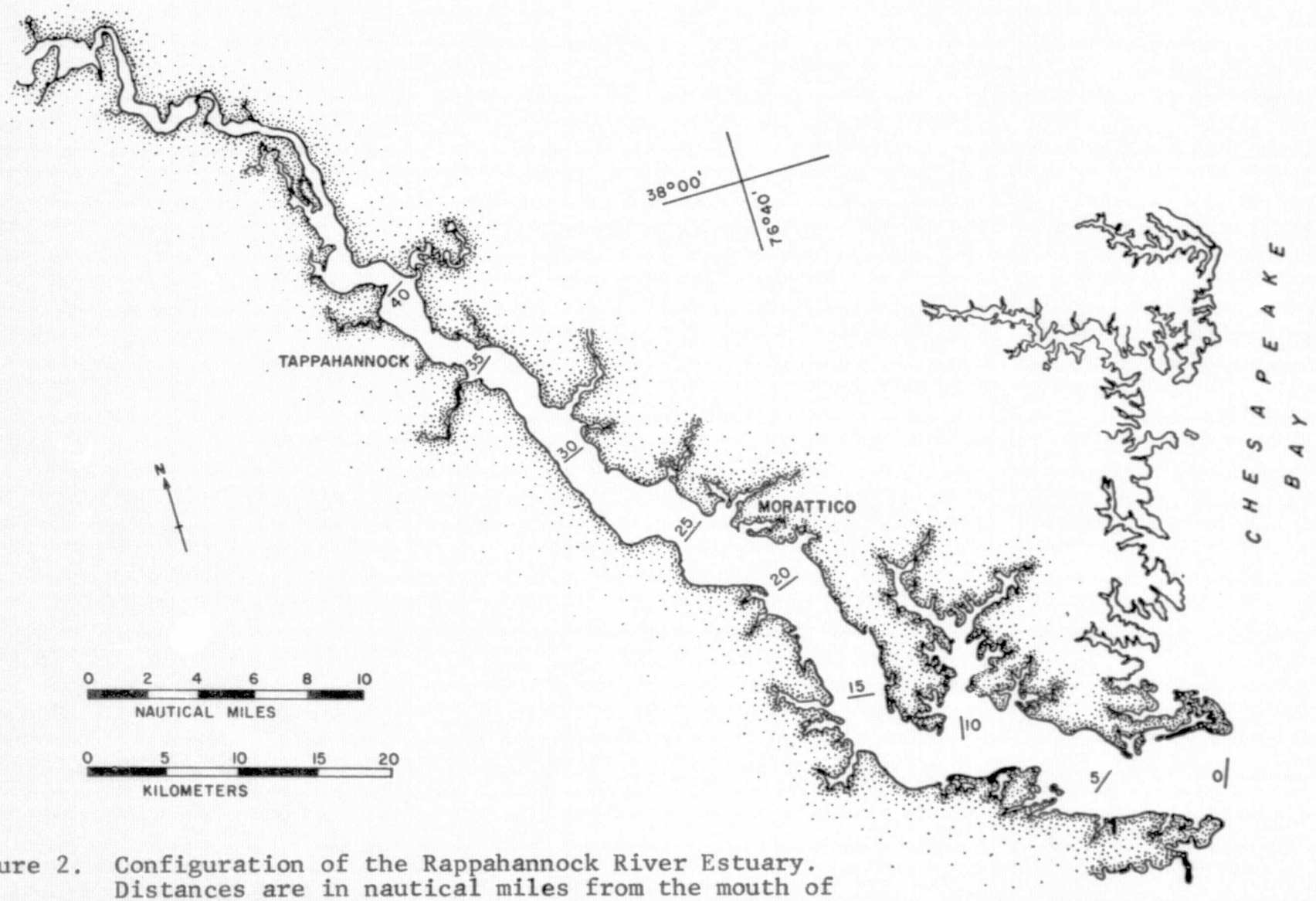

Figure 2. Configuration of the Rappahannock River Estuary. Distances are in nautical miles from the mouth of the river.

whereas at the time of photography Sept. 1973, inflow was very low, less than 14 m^3 per sec. Consequently, the sediment load at this time was supplied mainly from the floor and shores of the estuary proper rather than from the river, as was the case in early June.

Concentrations of suspended material typically vary with tidal current speed at one point over one-half a tidal cycle. The concentrations rise and fall with the strength of the current whereby concentrations are higher near maximum current than near slack water. The variations are most pronounced near the bottom but they also occur near the surface, especially over the shoals. Only about 10 to 20 percent of the load remains in suspension at slack water; whereas the rest is alternately resuspended from the bottom and settled out.

Superimposed on the back and forth motion of the tide there is a small net or residual current generated by density differences between fresh and salty water. Speeds are only 2 to 4 cm per sec but over many tidal cycles the current is significant in transporting material in suspension over the long term. Thus, material suspended in the lower layer below about 6 meters is gradually carried landward whereas material in the upper layer and in fresh water reaches, is carried seaward.

Estuary water is partly-mixed most of the time. Vertical mixing of salt and fresh water is incomplete throughout the salt

intrusion and therefore the transition from fresh to salty water is relatively broad. The Rappahannock lacks a sharp interface and turbid front characteristic of salt wedge systems except during short periods of extreme flooding. However, a partly-mixed system like the Rappahannock is the most common type in the Chesapeake region and along the U.S. East Coast.

In summary, the Rappahannock Estuary test site has relatively mild hydrographic conditions of tide and river inflow. Its geometry is relatively simple consisting of an axial channel bordered by submerged shoals; its shoreline is relatively straight. Rapid changes in tidal currents produce marked changes in suspended material with time. The estuary is undisturbed by major engineering works and is relatively free of pollution.

C-2

Data Processing - MSS

The first step in the processing sequence was to print a computer graymap of all 13 spectral channels covering the Rappahannock Estuary and adjacent land areas to detect any bad scan lines or anomalies which could cause problems in later classification. Since the scanner used 8 bit A/D encoding particular attention was paid to saturation values of 255 which might indicate clouds or a dropped scan line. The 40 mile section of the river and adjacent land area, contained in a minimum size rectangle, consisted of approximately 500,000 pixels per channel. To achieve a 40% reduction in classification area (i.e., reduce the amount of land) the river was divided into 4 subsections.

The next processing step was to cluster the points into spectral groupings. The cluster function implements an unsupervised classification algorithm to assign each data point into a predefined number of groups called clusters. The program initially calculates a point in feature space (an n-dimensional space where n is the number of spectral components or MSS channels) for each cluster center and assigns all points to the nearest cluster. A mean is then calculated for each cluster which becomes the new cluster center. The points are again reassigned to the nearest center, and a new mean is calculated. The process is iterated until the cluster centers cease to move when a new mean is calculated. Since the computer will cluster 20,000 points at a time, and the number of points in our data set was on the order of

200,000 pixels x 14 spectral vectors it was necessary to reduce the size of the set. Instead of selecting every 140th point it was decided to run cluster three times on subsets (using every 45th point) to insure enough points from the river to adequately represent water. For each of the three sections 15 clusters were chosen to represent land, clouds and water (the three most distinct scene elements). The number 15 is suggested by experience as adequate to over-cluster the scene with the idea of recombining clusters at a later step to form spectrally separable classes. Since the reflectance of water drops sharply in the near infrared, a ratio of cluster means in red band and a near IR band (channel 6/7) can be used to select water clusters (Figure 3). Considering the three sections of data clustered, a total of nine clusters were assigned for water. Clusters representing clouds were selected by looking for uniformly high radiance (large cluster mean) in all spectral channels.

Output from each section of the data set clustered, when combined, gives a total of 45 clusters. Each run of cluster produced a deck of cards representing the mean and variance for each of the 15 clusters in all 14 spectral bands. The three decks of cards were merged (using computer program MERGESTATISTICS) into one composite deck containing 44 clusters (one cluster containing 2 data points was deleted). Separability information from the CLUSTER processor suggested that some of the 15 groups in each section should be regrouped. Clusters representing clouds and

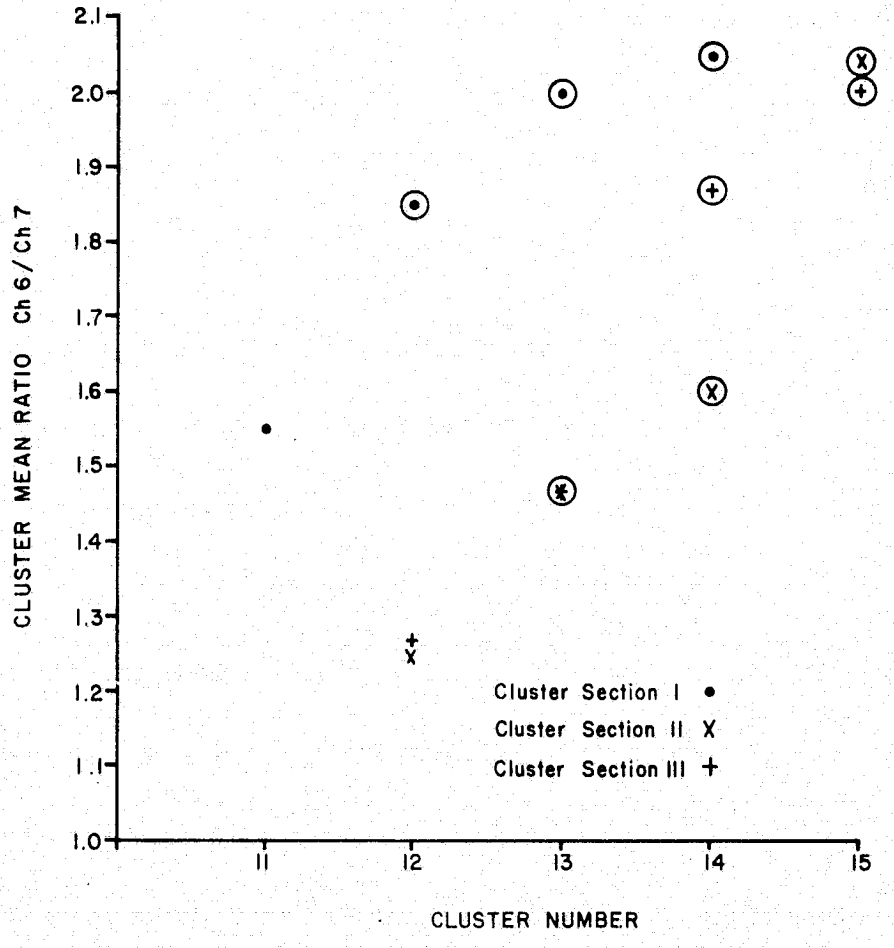

Figure 3. Ratio of cluster means in far red channel (6) and near infrared channel (7). Points circled are most likely to represent water clusters.

and various types of land were combined to form a lesser number of groups more distinct in spectral space. Clusters which represented water were not altered since it was desired to keep the greatest number for later examination. As expected no more than three water clusters were found in any of the three cluster sections since water is in general less spectrally separable from itself than is land. This heavily weights a classification in favor of land. The actual combination of the statistics to form the reduced number of clusters was not made until several more processing steps were completed.

The LARS computer program SEPARABILITY is used to determine the best combination of spectral channels (number and spectral coverage) for the classification. The function is implemented by using the mean vectors and covariance matrices for the clusters to calculate the divergence for all cluster pairs for each set of channels. Divergence is a measure of the distance between cluster densities. In order to reduce the effect of very widely separated cluster pairs, transformed divergence is used to achieve a saturating effect by placing an upper limit on the actual divergence value. The function is also used to determine which clusters are marginally separable and should be combined into a single class. The SEPARABILITY function:

1. calculate average divergence (D_{AV}) - cluster pairwise divergence averaged - for all combinations of n channels taken m at a time and prints results ordered on D_{AV}.

2. Prints a list of those clusters for which the pairwise divergence is less than a user defined value.

This information is used to choose the best combination of spectral channels to separate clusters of prime interest in spectral space, and to decide on a combination of clusters into a class structure best representing the scene being classified. The first pass through SEPARABILITY, with 26 clusters from the entire river, indicated 5 classes to represent land areas, 3 classes for clouds, 9 classes for water, and 4 classes called "other" bordering between land and water in spectral space (due to an intermediate red/near IR reflectance ratio).

Using the 21 classes and 6 of the 14 spectral vectors (1, 3, 4, 6, 8, 13) a classification of the river was performed. The program uses the class means and covariance matrices, and the data from each point classified, to calculate the probability that the point belongs to each of the classes. It then assigns the point to the most probable class and writes the classification (together with a value indicating the associated probability) on an output file. This classification was used as a first pass to delineate water areas and get a general feel for the scene. The classification was weighted toward land and cloud classes since their separability is greater both among themselves and with water. Interclass separability for water is generally lower and the tendency will be to combine water classes before combining other classes. This will result in a scene well classified for land,

but not adequately classified for water. Hence the decision was made to select only areas of interest--the Rappahannock River and adjacent Chesapeake Bay--to form a new data set for reclustering. To accomplish this 45 test areas were outlined using the first classification map to include as much of the River (shore to shore) and Bay as possible with rectangular shapes. Each area, called a test field, was chosen to include only water (based on the first classification) and to approach the shoreline as nearly parallel as possible. Ability to outline an irregular shape would have greatly simplified the procedure, and would have enhanced the sampling of nearshore points. The data set consisted of approximately 100,000 points, each representing one 260 foot square pixel.

Reclustering of the data set containing only water pixels was performed on a sampling of every 50th point in all 13 spectral channels (14 spectral vectors). As before the number of points in the data set was reduced to achieve a computer core load. This subset comprised a uniform sample of all pixels of interest in the scene representing water areas. Again 15 clusters were chosen to over divide the scene with combination into a fewer number of classes done subsequent to separability analysis.

Statistics from 15 clusters were used with the SEPARABILITY function to examine the divergence between cluster pairs in spectral space for combinations of spectral channels. The program was run with a selection of 10 channels: the entire visible spectrum (channels 1-6), two reflective infrared (channels 7, 8), and the thermal infrared (channels 13, 14). The best combinations of 10

channels taken 8, 6, 5, 4 and 3 at a time were printed, both in order of the average divergence (D_{AV}) between all cluster pairs (106 combinations) and in order of the minimum divergence between the least separable pair. There may be many different combinations of channels to examine (e.g., 252 for 10 spectral channels taken 5 at a time) and the program will typically list the best 30. Properties of the divergence are such that adding more spectral vectors will cause the new divergence value to be greater than or equal to the old. Hence a greater number of MSS channels will increase separability of classes (which may increase classification accuracy), but will also rapidly increase the amount of computer time necessary to complete a classification. A tradeoff is needed to find the minimum number of spectral vectors which will still allow adequate separation of significant classes. Testing and extensive experience by personnel at LARS show that increases in classification accuracy decrease rapidly when more than 5 spectral vectors are used (Wu et al., 1974). A plot of D_{AV} against the number of spectral vectors for water (Fig. 4) indicates that 5 channels will yield a divergence value greater than 50% of the way between the divergence for 3 and 8 channels. With the number of MSS channels chosen the next step is to combine clusters with low divergence into single classes. This process is generally accomplished by setting a divergence lower limit and combining those cluster pairs which fall below this limit. Research at LARS (Swain, King, 1973) has shown that a divergence of

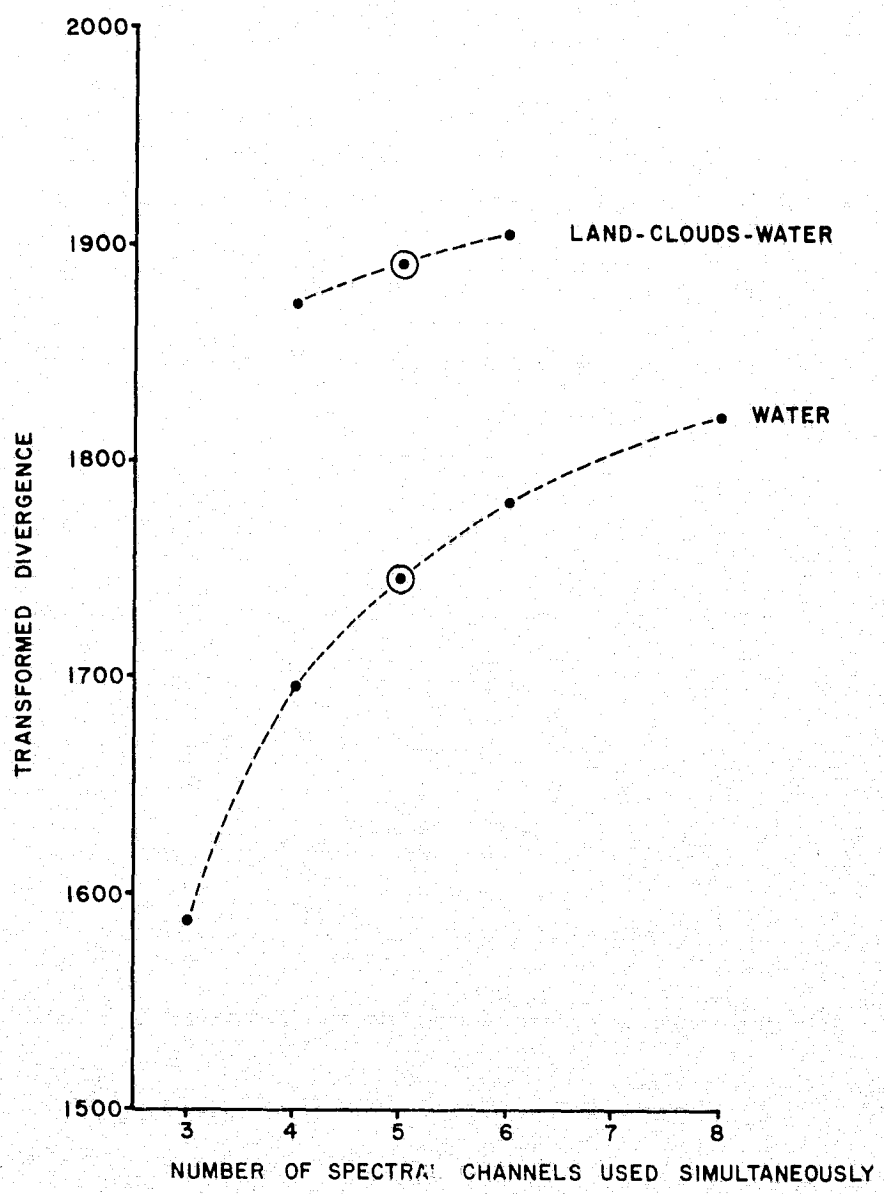

Figure 4. Average transformed divergence between water clusters only and all clusters in scene as a function of spectral channels used.

1500 will generally achieve a 90% classification accuracy in a supervised classification. The problem in the case of the tidal estuary as examined in this paper necessitates an unsupervised classification with no accuracy determination possible. Furthermore, the average divergence for water intercluster combinations is 1744 versus 1959 for land intercluster divergence and 1999 for divergence between land and water (based on a saturation maximum value of 2000). Relaxing the water pairwise divergence value by 200 to 1300 for the recombination criteria would lower classification accuracy to approximately 85% and appears reasonable in light of the lower average water intercluster divergence. However, it was not always possible to combine cluster pairs into groups of three or four without encountering divergence values greater than 1300, even though the group average might be less than 1300. In one instance it was advantageous to combine two clusters with a divergence of 1364 since neighboring clusters in spectral space were near the saturation limit of 2000. A close study of all reasonable combinations of water clusters with low divergence indicated a reduction from 15 clusters to 9 classes. It is emphasized that this combination does not represent a case of black and white in making a clear cut choice, but rather the best of several possible combinations to realize a representative class structure. Figure 5 shows the combination used and the average divergence between the combined clusters.

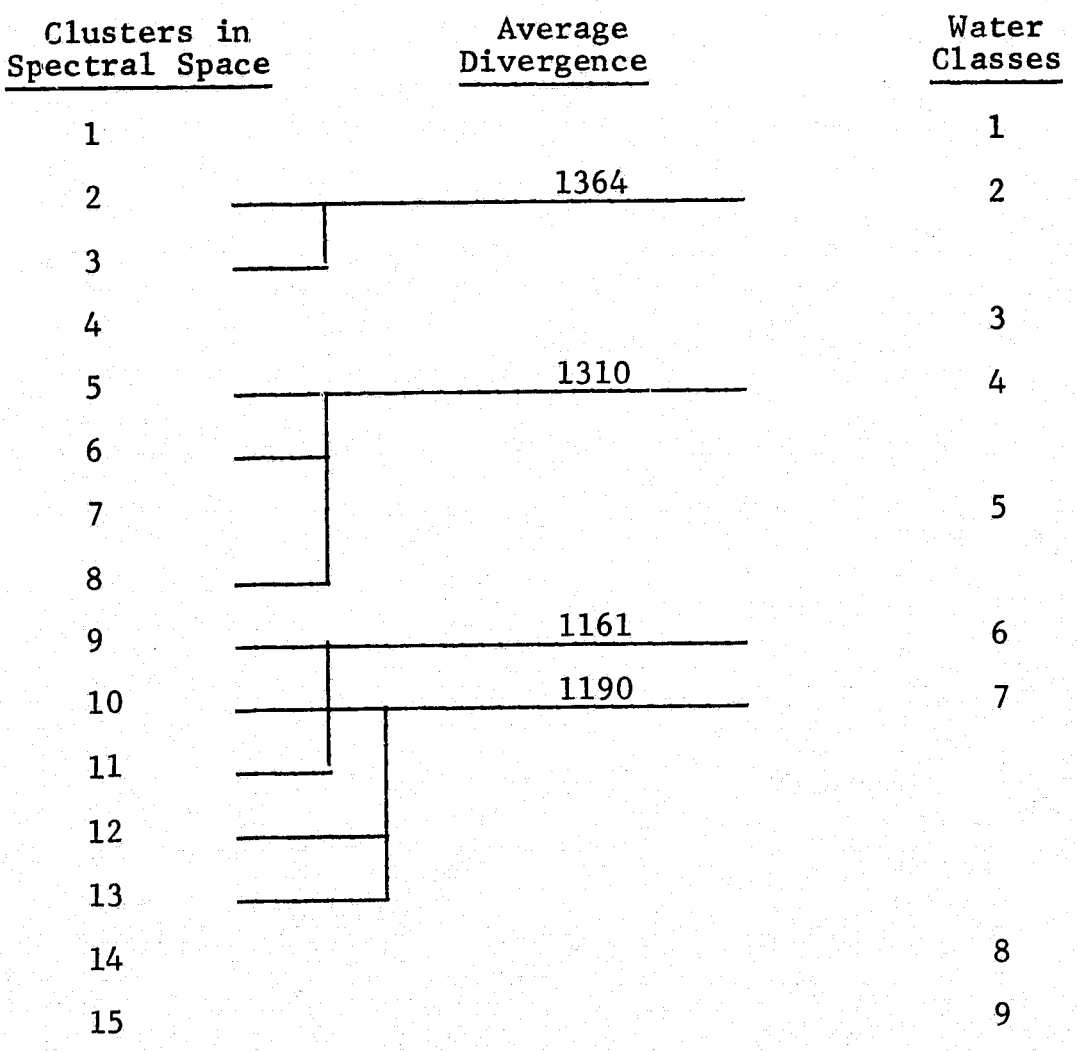

Figure 5. Combination of Water Clusters into Water Classes.

At this point in the processing sequence there existed two statistics decks from the two passes through the cluster processor: one deck with 15 water clusters, and one deck with 44 clusters for land, clouds, other, and water. It is important to note that although the separability processor has been used to arrive at a class structure by combining clusters, the actual manipulation with the statistics parameters is done in another program. To form a combined set of statistics more representative of the scene for classification the two statistics decks were merged to form one composite set of punched statistics with 27 classes. All of the 15 water clusters were retained (even though SEPARABILITY indicated reduction to 9 classes) to maintain maximum flexibility for the classification. The number of clusters of land, clouds, and other was reduced to 12 classes and the original 9 water clusters (from the first run of CLUSTER) were eliminated.

A final run of SEPARABILITY was made before classification with the new combined statistics to choose the best channels based on both land and water divergence calculations. Greatest average separability was achieved with channels 1, 5, 6, 8, 13 at 1907. All combinations of five spectral vectors with divergence greater than 1900 had channels 1, 8, 13 in common. Combinations of the other visual channels seemed to make little difference in the average separability. The final run of SEPARABILITY indicated some further class combinations which could be made. The five classes of "land" were reduced to four, three classes of "clouds" to two, and four classes of "other" to two classes.

Using the combined statistics for 12 land-cloud-other classes and 15 water classes a classification of the entire section of the Rappahannock River covered by the MSS was performed. The statistical reduction from 12 to 8 classes of land-clouds-other was made in the CLASSIFYPOINTS algorithm just prior to the point by point classification of the river and adjacent land areas. This does not alter the input statistics deck with 27 classes, but does take into account combinations indicated by SEPARABILITY. Classification was performed using all 15 water clusters with the idea of reducing the number to 9 by employing common symbols in computer classification maps.

With the classification completed the function PRINTRESULTS is used to obtain a graphical and tabular display of the computer derived classes. An important parameter to be chosen before printing is the threshold value which will eliminate those points with a low probability associated with the class to which they were assigned. A 1% thresholding was used; that is, those points not having a 99% probability of falling into one of the land, water or cloud classes were not classified.

A classification map of the river was printed using every line and every other column, and symbols for water combined to form the 9 classes indicated by separability information (Figure 5). By using alternate columns the resulting map is similar to a 1 x 1 ERTS rendition since the Skylab MSS data set was stretched by a factor of two to accommodate differences in sample rate among the

spectral channels (Earth Resources Data Format Control Book, Vol. 1). The line printer used to make the maps prints 10 characters/inch and 8 lines/inch, resulting in a 20% distortion in the computer generated classification maps.

Presentation of Results - MSS

Results of the classification were analyzed in two ways: the frequency of water classes was plotted as a function of distance from the mouth of the river, and single class maps were printed to examine spatial distribution of each type of water in the river.

The frequency of the nine classes of water within the field of view of the MSS was determined by returning to the 45 test fields used to originally define the "water only" data set. In each of these test fields the PRINTRESULTS function lists the composition by number of points and percentage for all classes. This includes not only water classes, but land, clouds, other and threshold. In order to relate the class frequencies to distance along the river an overlay was made from National Ocean Survey (Department of Commerce) Nautical Charts and scaled as nearly as possible to the distorted classification map (with test fields outlined). The test fields were then grouped into one to six mile (average 2 mile) units and percentage class composition calculated for the new units. A tabular account of this information is included as Appendix A. The data were plotted against distance upstream as presented in Figure 6 for the 9 water classes. A continuous curve was drawn through the points as an aid in comparing the different classes, and in no way suggests a functional relationship. A striking feature of the data, at first glance and after closer examination, is the division of the 9 classes into

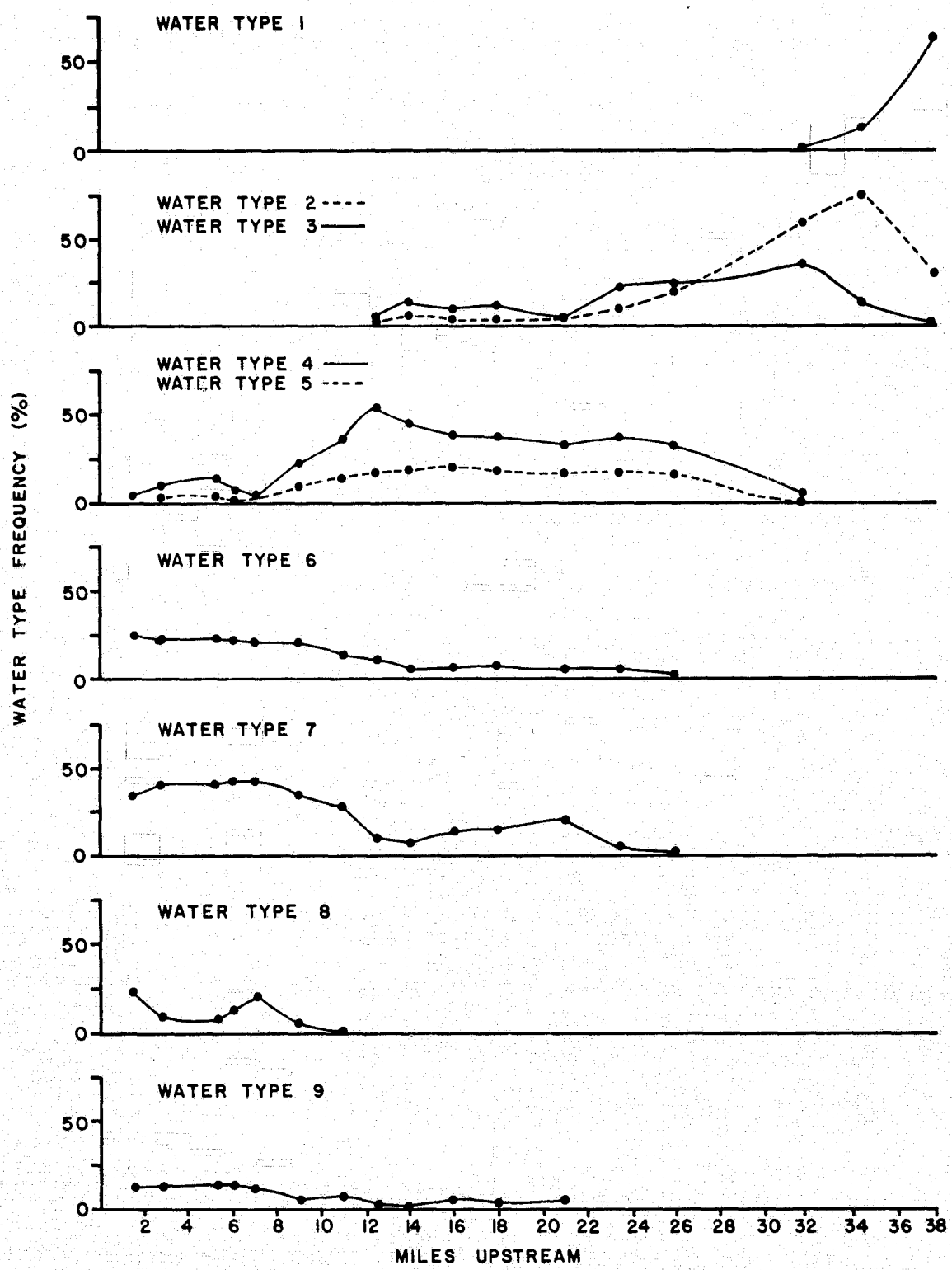

Figure 6. Distribution of water types along the length of the Rappahannock River - 9 classes of water - MSS classification channels 1, 4, 6, 8, 13.

4 by geographic region within the river. The first of these 4 new classes is composed of old classes 6-9 and extends from the mouth of the river to mile 12. An arbitrary cut-off of 10% has been set as the point at which a class is no longer significantly contributing to the water types in a section of the river. In using this criterion care is exercised to observe whether such classes are distributed contiguously, and thus may have physical meaning as a local water type. The second new class is composed of old classes 4 and 5 and overlaps the first class, beginning at mile 8 and ending at mile 28. The third class comprises previous classes 2 and 3 and stretches from mile 22 to mile 36, overlapping its downstream neighbor. The last class remains distinctly separate both geographically and in spectral space as well. There is a significant increase in class 7 where classes 4 and 5 are dominant (new class 2) which may represent a relict feature from the immediately previous flood tide. This occurs in a region where the course of the river undergoes a major change in direction and the channel becomes markedly shallower. Water from downriver (types 6 and 7) appears to stay confined to the channel in the relative center of the river on the upstream side of the bend and persists for approximately 8 miles.

In order to examine the two dimensional distribution of water types in the river a series of classification maps were printed using only one water symbol at a time. This resulted in nine maps of the river and greatly facilitated recognizing surface patterns. A careful examination of water types 4, 5, 6, 7, 8, and

9 revealed a banding phenomenon exhibited by the regular grouping of water class symbols. In some areas the banding appeared to carry through land into adjacent water bodies, and took on the shape of conical scan lines. A check back to the photographic images of the 5 bands used in the classification confirmed a suspended noise problem in the thermal band (13). The EREP Sensor Performance Report (MSC-05528, Vol III) documents a low frequency noise affecting the thermal bands more than other bands. Although an algorithm was to be used to remove the noise, a classification of a section of our data set exhibiting the worst thermal variation, using only channel 13 revealed the same scan patterns originally noticed in the water classes, and very apparent in the photographic S192 screening imagery. Apparently the nine classes of water represent an "overclassification" of the river based on noise in the thermal band, and a new classification using 5 spectral vectors excluding bands 13 or 14 is suggested. SEPARABILITY was rerun using 9 water classes and 8 classes of land, clouds, and other. A subset of 5 channels (1, 3, 4, 6, 8) selected from 10 gave the greatest divergence, 1869, compared with 1907 in the previous classification (using channel 13). Figure 7 shows some of the possible water class groupings and the associated interclass divergence both with and without channel 13. Water classes 4 and 5 which were moderately separable in spectral space with the thermal band included are now virtually indistinguishable ($D_{AV} = 365$). The averaged divergence for classes 6, 7, 8 and 9 has been reduced from 1404 to 554. The most marked change is in class 9 which

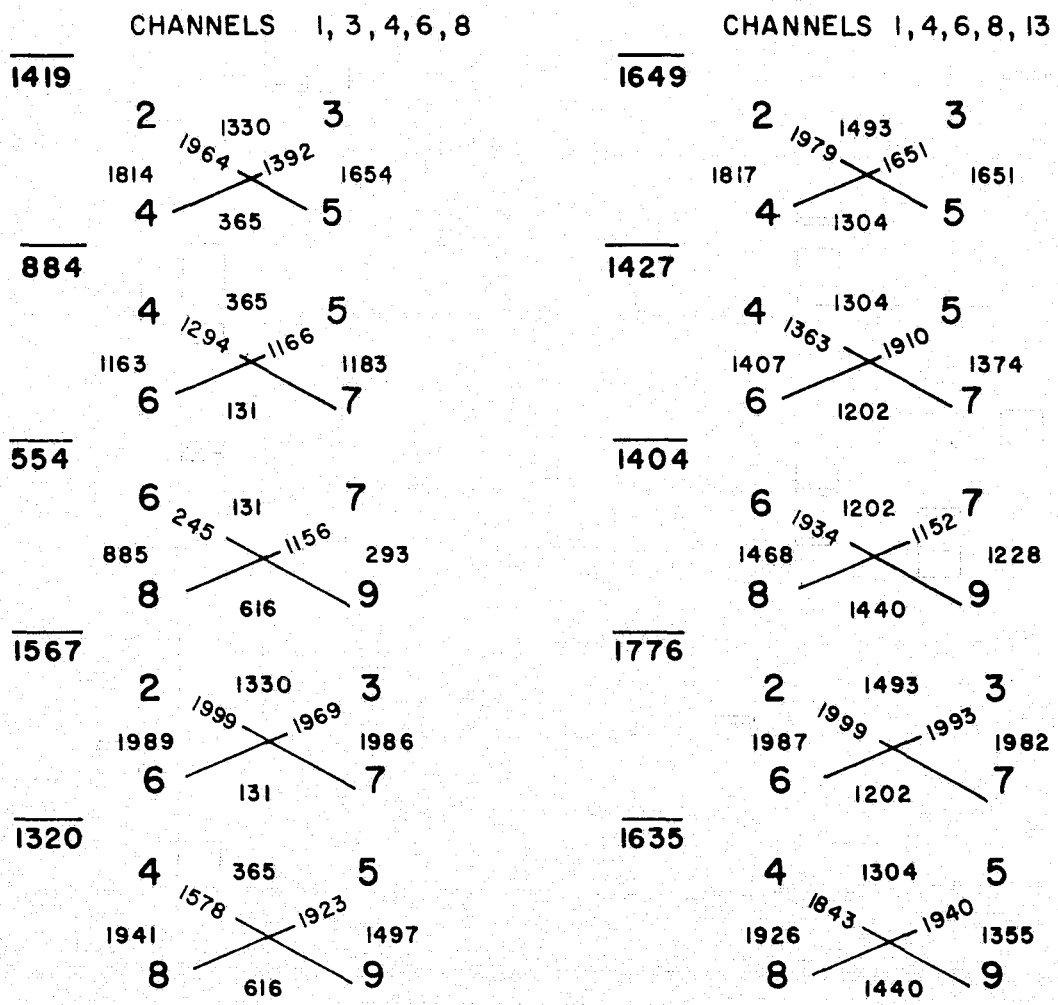

Figure 7. Pairwise divergence between 8 of the 9 water classes, with and without thermal channel (13). Average divergence for each grouping of four classes shown in upper left.

exhibited the worst banding, and in the absence of band 13 is extremely close to classes 6, 7 and 8. Classes 4 and 5 are somewhat close to class 7, but well separated from 8 and 9. Classes 2 and 3 in the upper river are spectrally distinct from any classes in the middle or lower reaches of the estuary. A new grouping of the 9 classes into 4 (1, 2 + 3, 4 + 5, 6+7 + 8+9) was made and the entire Rappahannock River reclassified (CLASSIFYPOINTS). Table II lists the mean and standard deviation of the classes for each channel. The grouping of water classes in spectral space is the same as the geographic grouping suggested in Figure 6, class frequency vs distance upstream. Using information from the new classification (4 water classes, 8 land, clouds, other classes) a new frequency plot was made as shown in Figure 8. Note that the occurrance of the 4 classes is the same as predicted by the geographic combination of 9 water classes into 4. A classification map is presented in Figures 9 through 12 for the entire River. Water classes 1-4 are depicted with appropriate numerical symbols, clouds with C, and land and other with special symbols (see legend). A tabular accounting of percent water frequency is given in Appendix B.

TABLE II

Water Class	Ch 1 Mean/S.D.	Ch 3 Mean/S.D.	Ch 4 Mean/S.D.	Ch 6 Mean/S.D.	Ch 8 Mean/S.D.
1	255/0.1	114/13	61/8	77/10	37/9
2	164/9	126/7	57/6	53/6	27/6
3	150/5	116/4	47/4	44/55	22/5
4	140/5	111/4	41/4	39/4	17/5

Mean and standard deviation not normalized between channels.
Low radiance = 0, high radiance = 255.

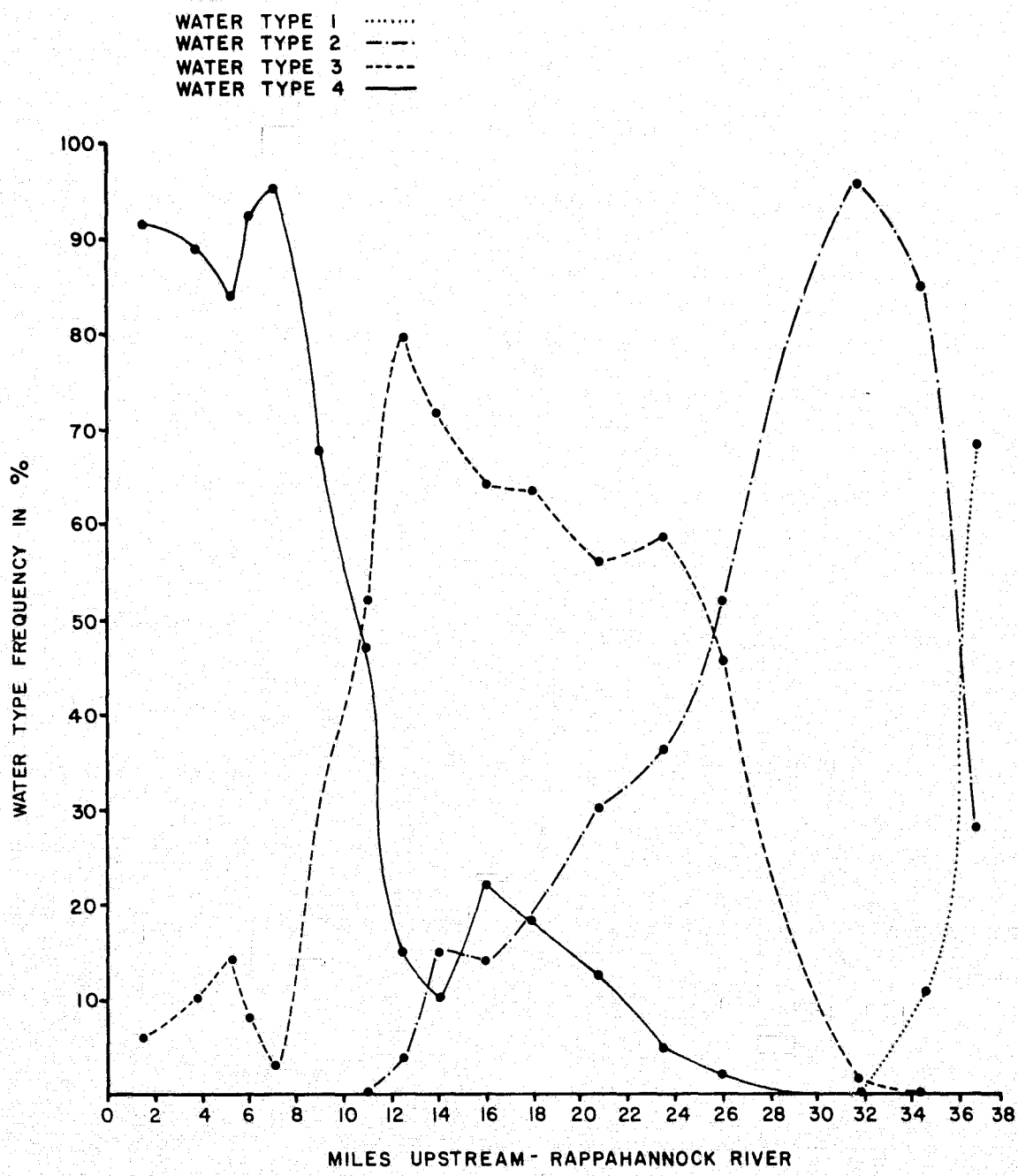

Figure 8. Distribution of water types along the length of the Rappahannock River - 4 classes of water - MSS classification channels 1, 3, 4, 6, 8.

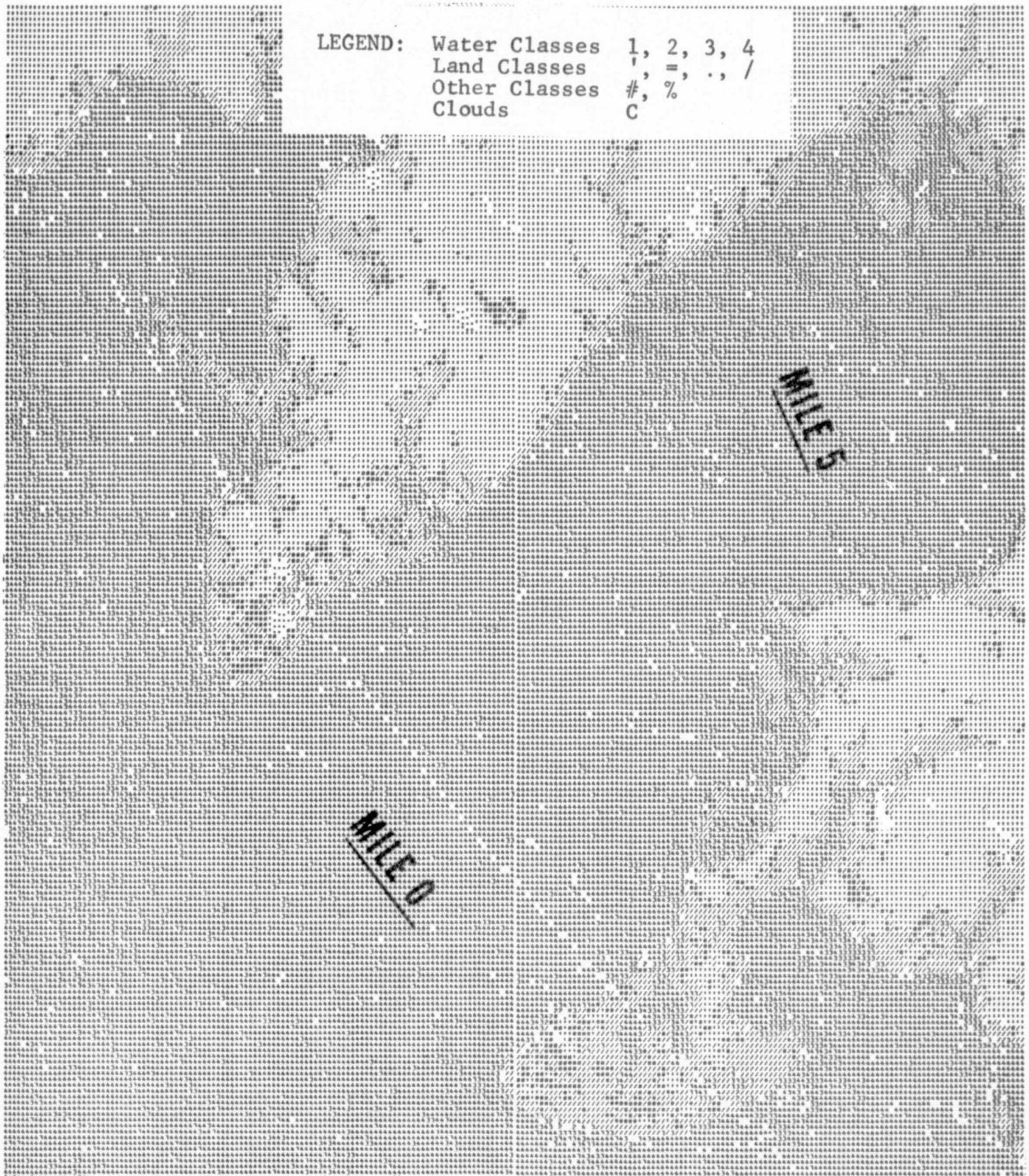

Figure 9. Classification map, Rappahannock River, Mile 0-7.

Figure 10. Classification map, Rappahannock River, Mile 7-18.

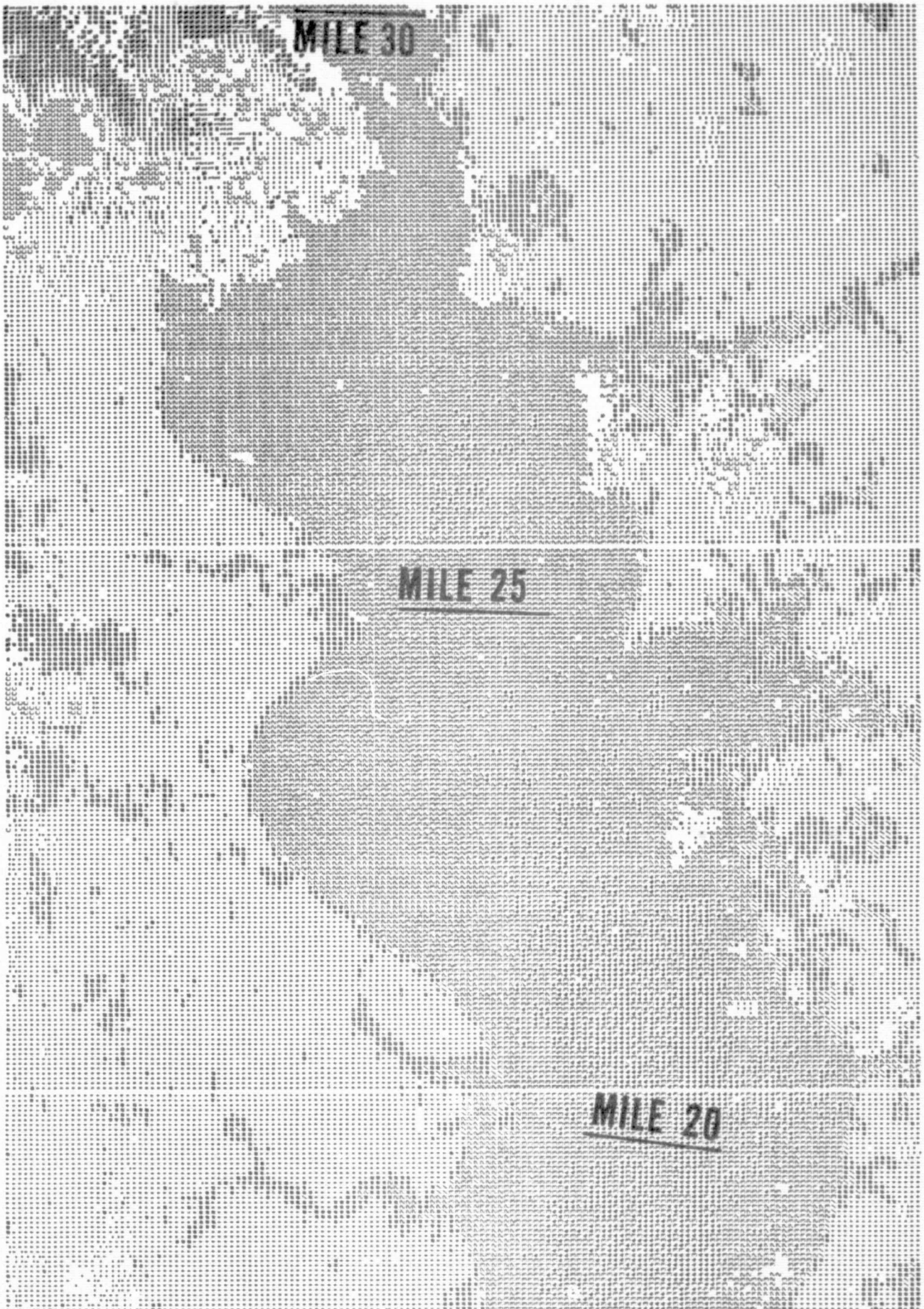

Figure 11. Classification map, Rappahannock River, Mile 18-30.

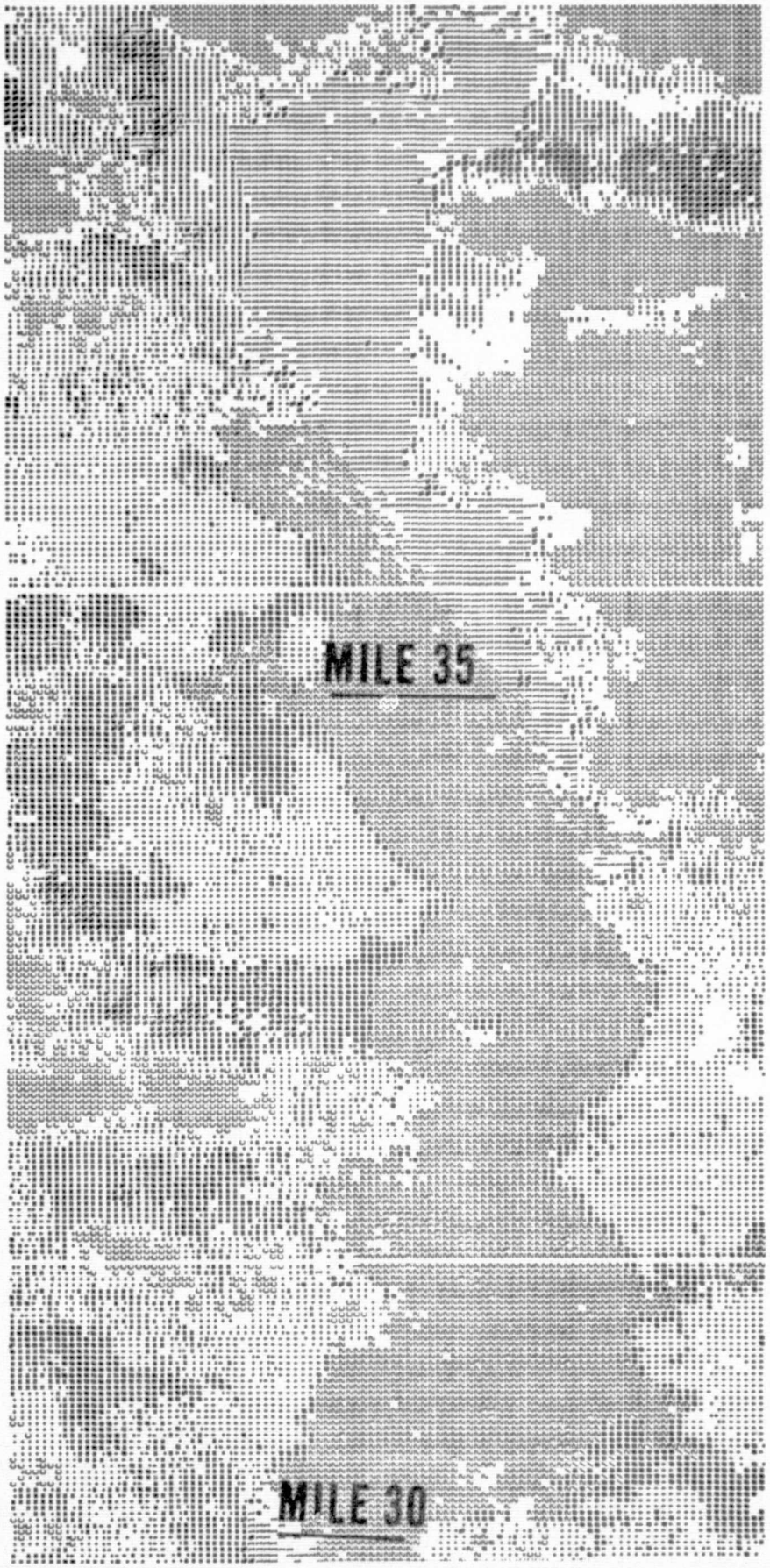

Figure 12. Classification map, Rappahannock River, Mile 30-39.

Classification of Color Imagery from S190B

Using color film from the Earth Terrain Camera (S190B) taken simultaneously with the S192 data a classification of the Rappahannock River was made. In order to get LARS compatible digital data an Optronics scanning microdensitometer was employed with filters to separate the data into three distinct records: red band (.58-.69 μm), green band (.50-.58 μm), and blue band (.40-.50 μm). An aperture of 50 μm was used to simulate, as nearly as possible, the MSS instantaneous field of view (IFOV). A single band graymap was used to choose areas of the river, clouds, and land for clustering. The task was exceedingly difficult since the river and land have similar signature (densities) in all of the three bands. Only from a good prior knowledge of the scene, and marked cloud patterns, was it possible to make any distinction at all. One large area typical of land, and one of clouds were chosen and clustered into 15 classes. Water data were selected from 13 test fields and also clustered into 15 classes. Both data sets were merged and SEPARABILITY run to arrive at a class structure. The result was 5 water classes, 4 land classes, 2 cloud classes, and 5 classes of other (combinations of clusters from land and water data sets). Using these 16 classes a classification of the Rappahannock estuary was made, and the PRINTRESULTS function used. The 13 test fields were grouped by miles upstream and a frequency vs distance plot made. Without the reflective infrared available to separate land and water there was significant confusion in the classification, and no definite land-water boundary. Considering

the 13 test fields selected only from the river 72% of the class symbols are "other", 27% are "water", and 1% "land". The distribution of 4 of the 5 water classes (one class with 30 symbols was eliminated) is presented as Figure 12. There are definite similarities between two of the water classes derived from photography and the MSS. The class predominating in the lower estuary (beginning at mile 0) shows a primary and secondary increase in frequency at the same general area of the river when comparing Figures 8 and 13. The next class upriver has very nearly the same shape in both cases, but slightly more spread on the MSS frequency curve. The two classes in the uppermost reaches of the river (delineated by the end of MSS coverage) do not correspond closely comparing the scanner and the film. However, if the S190B classes are added (see -.....-, Fig. 13) there is a marked frequency increase near mile 33 in both S190B and the MSS. There is no corresponding spectrally distinct class derived from the color film which resembles the MSS class 1, predominate after mile 36. This would seem to indicate that water classification in the lower estuary is from the visual portion of the electromagnetic spectrum, while in the upper estuary the reflective infrared may have significant information.

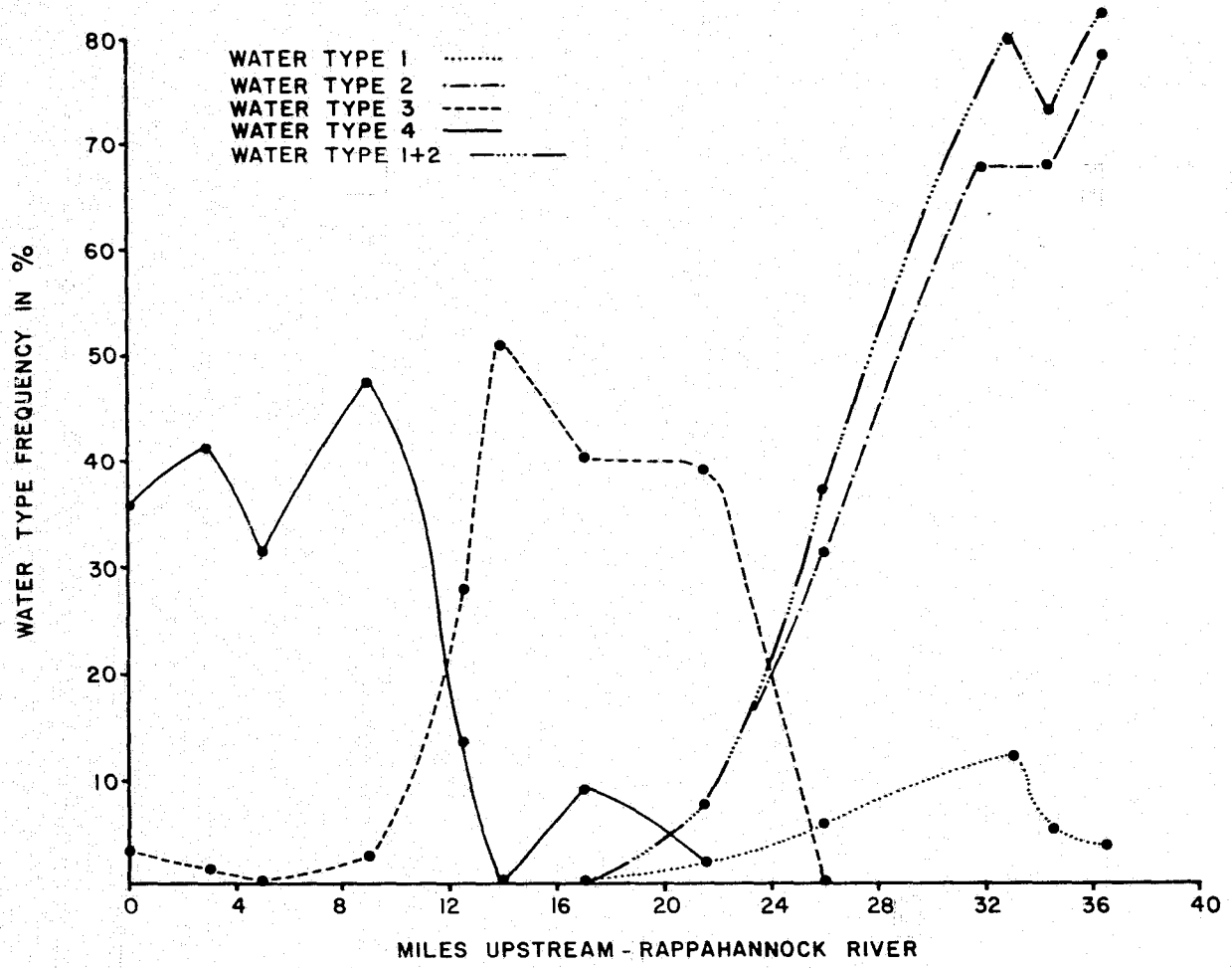

Figure 13. Distribution of water types along the length of the Rappahannock River - 4 classes of water - color film (S190B) classification.

CONCLUSION

The computer classification performed in an unsupervised manner assumes no a priori knowledge of the ground scene, and relies on the spectral separation of clusters in feature space to arrive at a reasonable class structure. Whether or not the class structure is meaningful is determined by correlation with specific scene parameters measured independently, or with observed conditions averaged over a period of time. Many ground truth samples were taken on the day of the Skylab overpass in the Rappahannock River and adjacent portion of the Chesapeake Bay. Since the measurements were not as synoptic as the photography, but made over a period of hours, they can be used only for a broad outline of the range of parameters, and to identify general trends. Table III lists the most important information from samples taken within 30 minutes of the satellite overpass. Comparison of specific measurements with one another and with film density is found in the final report for Skylab contract NAS6-2327 (Hargis, 1975). The photography shows an increase in radiance in all bands proceeding up the river which corresponds to an increase in MSS signal. Surface suspended solids were high in the lower estuary (large particle size), dropped sharply in the middle reaches near maximum flood current (mile 30-37), and increased in the upper estuary with smaller particles. The water in the estuary was relatively isothermal, increasing 1°C over the 40 mile length. This indicates why the thermal infrared MSS band (13) was not ultimately useful in the classification. By contrast salinity increased with distance

TABLE III

Mile	Water Class	Depth (m)	Tide Stage	Time (EST)	T. Surf. (°C)	Salin. ($^{o}/_{oo}$)	Sed. Conc. (mg/1)	Chlor. "A" (μg/1)
0	4	0	Slack	11.7	25.2	15.3	26.6	10.8
4	4	0	Slack	11.8	25.5	14.0	23.4	22.4
10	3,4	0	Late Fl.	12.0	25.7	12.8	21.8	10.2
15	3,4	0	Late Fl.	12.2	25.9	12.6	13.8	9.3
18	3,4	0	Late Fl.	12.3	25.8	11.9	13.8	5.5
21	3,4	0	Late Fl.	12.5	25.7	10.8	16.3	7.2
25	3	0	Late Fl.	12.5	23.5	10.6	17.9	8.4
25	3	0	Late Fl.	12.5	25.8	10.0	19.0	21.0
31	2	0	Max Fl.	11.7	25.7	7.2	6.5	8.0
33	2	0	Max Fl.	11.8	25.8	5.9	6.6	12.9
33	2	0	Late Fl.	12.4	26.1	6.7	5.8	6.3
35	2	0	Max Fl.	11.9	26.2	4.4	3.0	5.9
35	2	0	Late Fl.	12.3	26.3	4.4	4.0	10.2
37	1	0	Late Fl.	12.1	25.9	3.1	5.8	5.7
37	1	3.0	Late Fl.	12.1	-	3.1	15.8	11.9
37	1	4.5	Late Fl.	12.1	-	3.2	60.3	10.8

seaward from 1‰ above Tappahannock to more than 15‰ off the estuary mouth, the largest gradient (3-7‰) occurring between mile 23 and 37. The photography visually shows many color boundaries indicative of fine-scale structure and mixing patterns of tidal currents that are active in the upper estuarine layer. When a computer classification is performed the result both from photography and from the MSS is broader, and water types more uniform.

There is good general agreement between the classification of water types when comparing frequency distributions derived from the MSS and the color photography in the lower and middle estuary. It is felt that the photography could offer much the same information as the MSS if the ability to discern land and water were incorporated. Color infrared film, of course, offers this capability but at the loss of information in blue band which seems to have been used to advantage in both classifications.

The MSS water type 1 in the upper estuary, which has no correspondence on the color film, is thought to have been caused by atmospheric conditions and poor spatial frequency response of band 1. Pitts et al. (1974) have shown that atmospheric water vapor can change the signature on Landsat classifications. It is possible that the IR band 8, which is being used to differentiate land and water, is recording a sharp increase in atmospheric water over the river (which has a small IR return) giving rise to a pseudo water class. This is being reinforced by the documented

poor spatial frequency response of band 1 (MSC-05546) which has the effect of smearing clouds adjacent to the river across the river in the uppermost reaches recorded by the MSS. To eliminate band 1, however, would have a detrimental effect on the classification.

Three of the four types of water in the Rappahannock Estuary have good separability in spectral space and are thought to be valid physical divisions within the river. The fact that there is no direct correlation with ground measurements simply reinforces the time dependance of the surface truth-remote sensing system. Since the water types are broad and uniform in spatial extent they may be more representative of groupings which indicate water quality than are water color boundaries evident in single band analysis or derived from mapping color or color infrared film.

REFERENCES

Hargis, W. 1975. Southern Chesapeake Bay water color and circulation analysis. VIMS Final Rept. for NASA contract NAS6-2327.

Nelson, B.W. 1960. Clay mineralogy of the bottom sediments, Rappahannock River, Va. 7th Nat. Confr. Clay Minerals, p. 135-147.

Nelson, B.W. 1959. Transportation of colloidal sediment in the freshwater-marine transition zone. First Internat'l. Oceanogr. Congr. preprints, abstr. p. 640-641.

Nichols, M. 1971. "Ground truth" data for NASA Mission 144, VIMS data report. 22 p.

Nichols, M. 1973. Development of the turbidity maximum in a coastal plain estuary. Contr. Rept. AROD, 17 p.

Pitts, David E., William E. McAllum, and Alyce E. Dillinger. 1974. The effect of atmospheric water vapor on automated classification of ERTS data. Proc. 9th Intern. Symp. on Remote Sensing of Environment, 483 p.

Skylab Program Earth Resources Experiment, Package Sensor Performance Evaluation, Final Report, Vol. III (S192), MSC-05546.

Swain, P.H. and R.C. King. 1973. Two effective feature selection criteria for multispectral remote sensing. LARS Information Note 042673.

Wu, C.L., D.A. Landgrebe, and P.H. Swain. The decision tree approach to classification. LARS Information Note 090174.

APPENDIX A

PERCENT WATER FREQUENCY VS. LOCATION IN RAPPAHANNOCK RIVER

9 WATER CLASSES

Test Field #	Test Area Start Mile	Center Mile	Stop Mile	% Water 1	% Water 2	% Water 3	% Water 4	% Water 5	% Water 6	% Water 7	% Water 8	% Water 9	# Samples
5a- 9	0	1.5	2.5				3.5		25.1	34.0	23.5	12.2	5,616
10-14	2.5	3.8	5.0				9.4	2.7	22.3	40.5	8.2	12.3	2,866
15	5.0	5.2	5.5				12.2	2.6	22.3	40.5	7.4	14.2	1,078
16	5.5	6.0	6.3				6.1	1.0	23.2	42.7	12.1	13.0	1,342
17	6.3	7.0	8.0				3.3		20.9	42.1	21.1	11.1	1,482
18-20	8.0	9.0	10.0				22.8	8.6	21.4	35.5	4.9	5.6	2,875
21-22	10.0	11.0	12.0				35.4	11.9	14.5	27.8		7.0	3,252
25	12.0	12.5	13.0		1.8	3.8	53.1	16.6	9.9	10.2		2.3	1,122
26-27	13.0	14.0	15.0		5.8	13.7	45.2	18.2	6.1	8.2		1.0	1,850
28-31	15.0	16.0	17.5		4.5	9.4	38.2	20.1	6.7	14.8		5.0	3,415
32	17.5	18.0	18.2		3.9	12.2	38.3	18.6	8.3	14.8		3.6	880
33-36	18.2	20.8	23.0		4.7	6.0	32.3	16.7	6.0	19.9	1.0	6.7	5,249
37	23.0	23.5	24.0		10.3	22.9	37.2	17.1	4.7	5.1		1.6	1,876
38-40	24.0	26.0	28.2		21.1	24.3	33.0	15.0	2.4	2.6			4,277
41-42	29.2	31.8	33.5		58.0	34.7	4.4						1,740
43-44	34.0	34.5	35.2	10.9	73.9	13.3							809
45	35.2	36.7	38.5	67.9	29.5	1.3							616
												Total	40,345

APPENDIX B

PERCENT WATER FREQUENCY VS. LOCATION IN RAPPAHANNOCK RIVER

4 WATER CLASSES

Test Field #	Test Area Start Mile	Center Mile	Stop Mile	% Water 1	% Water 2	% Water 3	% Water 4	# Samples
6- 9	0	1.5	2.5			5.7	91.5	3,809
10-14	2.5	3.8	5.0			10.1	89.0	2,866
15	5.0	5.2	5.5			14.1	84.3	1,078
16	5.5	6.0	6.3			8.3	90.2	1,342
17	6.3	7.0	8.0			3.0	95.7	1,482
18-20	8.0	9.0	10.0			31.1	67.8	2,875
21-22	10.0	11.0	12.0			51.6	47.1	3,252
25	12.0	12.5	13.0		4.2	79.3	15.4	1,122
26-27	13.0	14.0	15.0		15.4	72.4	10.5	1,850
28-31	15.0	16.0	17.5		14.1	64.0	21.5	3,415
32	17.5	18.0	18.2		18.3	63.6	17.7	880
33-36	18.2	20.8	23.0		12.6	55.8	29.9	5,249
37	23.0	23.5	24.0		35.9	58.7	4.7	1,876
38-40	24.0	26.0	28.2		52.0	45.4	1.9	4,277
41-42	29.2	31.8	33.5		95.7	1.5		1,740
43-44	34.0	34.5	35.2	10.7	85.0			809
45	35.2	36.7	38.5	67.8	28.2			616
							Total	38,538